Order Number 9506205

Spectroscopic and chromatographic investigation of derivatized cyclodextrins

Gahm, Kyung-Hyun, Ph.D.

University of Hawaii, 1994

U·M·I
300 N. Zeeb Rd.
Ann Arbor, MI 48106

SPECTROSCOPIC AND CHROMATOGRAPHIC INVESTIGATION OF DERIVATIZED CYCLODEXTRINS

A DISSERTATION SUBMITTED TO THE GRADUATE DIVISION OF THE UNIVERSITY OF HAWAII IN PARTIAL FULFILLMENT OF THE REQUIREMENTS FOR THE DEGREE OF

DOCTOR OF PHILOSOPHY

IN

CHEMISTRY

AUGUST 1994

By

Kyung-Hyun Gahm

Dissertation Committee:

Apryll M. Stalcup, Chairman
Bradley S. Davidson
Karl Seff
Robert S.H. Liu
Marguerite Volini

ACKNOWLEDGEMENTS

I wish to appreciate most sincerely to my supervisor Professor A. M. Stalcup for her helpful advice and patient supervision throughout the duration of this work as well as financial support. I wish to thank Professors Davidson, Liu, Seff, and Volini for advice and assistance beyond the call of refereeing a dissertation. I wish to thank Dr. Ramamurphy of Tulane University for the consideration of thermodynamic aspects of my study.

I wish to acknowledge the assistance and valuable discussions with Dr. Niemczura, supervisor of the NMR facility in the Department of Chemistry. He is responsible for the computer modeling in Discover of Biosym Technologies. Interpretation of computer modeling result is solely my responsibility. I wish to thank Wesley Y. Yoshida for teaching me how to use the 300 MHz GE NMR and the software for the 500 MHz GE NMR. He was always easy to approach and to discuss my problems. I wish to thank Mike Burger for obtaining FAB spectra. I must thank Karen Williams for valuable discussions and willingness to listen.

I wish to thank for my mother and mother-in-law for encouragement me to finish my degree spiritually as well as monetarily. Finally, I wish to extend special thanks to my

wife Eun-Sil and my two sons, Dong-Yeup and Dennis Dong-Min for their patience over this pressured period.

ABSTRACT

Regioselective reactions of 1-(1-naphthyl)ethyl isocyanate (NEIC) with β-cyclodextrin (β-CD) were studied with and without NaH activation of β-CD in N,N-dimethylformamide (DMF) and pyridine. All six possible monosubstituted CD products were separated by HPLC and characterized by ^{1}H NMR. The primary substitution product predominates when the reaction is carried out under reflux conditions in pyridine without NaH activation. The C-2 substitution product predominates when the reaction is carried out in DMF. Conversion of 2-O-(1-(1-naphthyl)ethylcarbamoyl)-β-CD to 6-O-(1-(1-naphthyl)ethylcarbamoyl)-β-CD was observed when NaH was used to the activate hydroxyl groups of CD.

^{1}H and ^{13}C NMR spectra of 2-O-((R)-1-(1-naphthyl)ethylcarbamoyl)-β-cyclodextrin (RC-2) and 2-O-((S)-1-(1-naphthyl)ethylcarbamoyl)-β-cyclodextrin (SC-2) were obtained in D_2O. NMR spectra indicate at least two conformers existing both in RC-2 (90:10) and SC-2 (61:39) at 25 °C. Complete assignment of ^{1}H and ^{13}C spectra of the major conformer of RC-2 was accomplished using homo- and heteronuclear two dimensional NMR techniques. Correlations observed in 2D NMR (ROESY, HMBC) revealed complete glucose connectivity of RC-2 and SC-2. The inclusion state and

orientation of the naphthyl substituent for both **RC-2** and **SC-2** was derived from the correlations observed between naphthyl and cyclodextrin (**CD**) protons in **ROESY** spectra, as was the various extents of anisotropic effects on the seven glucose units induced by the naphthyl group. The relative populations of the included and excluded orientation of the naphthyl substitutent in **RC-2** and **SC-2** were found to be solvent dependent in methanol/water systems. Computer modeling revealed one stable (included in the cavity) conformer in **RC-2** and two possible excluded conformers in **SC-2**.

Regiospecifically monosubstituted 1-(1-naphthyl)ethyl-carbamoylated β-cyclodextrins (**NEC-β-CDs**) were successfully employed as chiral additives to achieve chiral separation of N-(3,5-dinitrobenzoyl)-phenylglycine (**3,5-DNB-PG**), phenylalanine (**3,5-DNB-PA**), and homophenylalanine (**3,5-DNB-HPA**). The enantioselectivity of the various site-substituted **NEC-β-CDs** in capillary zone electrophoresis (**CZE**) was compared with that of native **β-CD**. Complexation constants of the three **3,5-DNB-** amino acids with **β-CD** were determined from the **CZE** results:**3,5-DNB-L-HPA** (473 $\pm$ 9 M^{-1}), **3,5-DNB-D-HPA** (460 $\pm$ 10 M^{-1}), **3,5-DNB-L-PA** (260 $\pm$ 4 M^{-1}), **3,5-DNB-D-PA** (161 $\pm$ 3 M^{-1}), and **3,5-DNB-PG** (43 $\pm$ 4 M^{-1}).

TABLE OF CONTENTS

page

ACKNOWLEDGMENTS..... iii

ABSTRACT..... v

LIST OF TABLES..... xii

LIST OF FIGURES..... xiv

LIST OF ABBREVIATIONS..... xix

CHAPTERS

1. INTRODUCTION..... 1

1.1 Chiral separations..... 2

1.1.1 HPLC-chiral stationary phases(CSPs) ... 3

1.1.1A Pirkle type CSPs..... 3

1.1.1B Protein based CSPs..... 4

1.1.1C Native cyclodextrin-based chiral stationary phases (CD-CSPs)..... 4

1.1.1D Derivatized cyclodextrin-based chiral stationary phases..... 8

1.1.2 Chiral separations using capillary zone electrophoresis (CZE)..... 11

1.1.2A Theory of CZE..... 15

1.1.2B Theoretical aspects of chiral separation in CZE..... 17

1.2 Studying interactions between CD and guest molecules by non-chromatographic means..... 21

1.2.1 NMR..... 22

1.2.2 UV-VIS and fluorescence..... 23

1.3 The scope of this research..... 24

2. SYNTHESIS OF MONOSUBSTITUTED NAPHTHYLETHYL-CARBAMOYLATED CYCLODEXTRINS..... 26

2.1 Introduction..... 26

2.2 Experimental..... 28

2.2.1 Chemicals..... 28

2.2.2 Chromatographic conditions..... 29

2.2.3 NMR and Mass spectrometry..... 29

2.2.4 Elemental analysis..... 30

2.2.5 Synthesis of C-18 functionalized silica..... 30

2.2.6 Synthesis of 2-O-((S)-1-(1-naphthyl)-ethylcarbamoyl)-β-CD (SC-2)..... 30

2.2.7 Synthesis of 3-O-((S)-1-(1-naphthyl)-ethylcarbamoyl)-β-CD (SC-3)..... 32

2.2.8 Synthesis of 6-O-((S)-1-(1-naphthyl)-ethylcarbamoyl)-β-CD (SC-6)..... 33

2.2.9 Synthesis of 2-O-((R)-1-(1-naphthyl)-ethylcarbamoyl)-β-CD (RC-2)..... 34

2.2.10 Synthesis of 3-O-((R)-1-(1-naphthyl)-ethylcarbamoyl)-β-CD (RC-3)..... 35

2.2.11 Synthesis of 6-O-((R)-1-(1-naphthyl)-ethylcarbamoyl)-β-CD (RC-6)..... 36

2.2.12 Role of solvent..... 37

2.2.13 Role of base..... 37

2.3 Results..... 38

2.3.1 Identification of the regioisomers..... 38

2.3.2 Role of solvent..... 45

2.3.3 Role of base..... 45

2.4 Discussion..... 49

2.4.1 NMR..... 49

2.4.2 Synthesis..... 52

3. ^{1}H AND ^{13}C NMR STUDY OF 2-O-1-(1-NAPTHTYL)ETHYL-CARBAMOYLATED CYCLODEXTRINS..... 58

3.1 Introduction..... 58

3.2 Experimental..... 61

3.2.1 Materials..... 61

3.2.2 NMR spectroscopy..... 61

3.2.3 Computer modeling..... 63

3.3 Results and Discussion..... 63

3.3.1 Assignment of ^{1}H and ^{13}C resonances of of native β-CD..... 63

3.3.2 Assignment of ^{1}H and ^{13}C resonances of RC-2 and SC-2..... 68

3.3.2A RC-2: ^{1}H Assignments..... 73

3.3.2B RC-2: ^{13}C Assignments..... 76

3.3.2C SC-2..... 79

3.3.3 Connectivity of glucoses..... 81

3.3.4 Conformational analysis..... 87
3.3.4A RC-2..... 87
3.3.4B SC-2..... 99
3.3.4C The differences in the conformations of RC-2 and SC-2..... 106
3.3.5 Molecular modeling..... 110
3.4 The effect of solvent polarity on the populations of in- or excluded conformers.. 114
3.5 Chiral recognition of RC-2 and SC-2 toward several 3,5-dinitrobenzoylated amino acids. 118

4. STUDY OF NAPHTHYLETHYLCARBAMOYLATED β-CYCLODEXTRINS BY CAPILLARY ZONE ELECTROPHORESIS (CZE)..... 122
4.1 Introduction..... 122
4.2 Experimental..... 123
4.2.1 Chemicals..... 123
4.2.2 Synthesis of 3,5-DNB-HPA and PA..... 124
4.2.3 Electrophoretic conditions..... 124
4.3 Results and discussion..... 125
4.3.1 Theory: calculation of complexation constant..... 125
4.3.2 β-CD as a chiral mobile phase additive (CMA)..... 128
4.3.3 NEC-β-CDs..... 138
4.3.3A NEC-β-CDs as CMA..... 140

4.3.3B SC-2 as a CMA..... 143

4.3.3C SC-6 as a CMA..... 144

4.3.3D RC-2..... 144

4.3.3E RC-6..... 145

4.3.4 Relative strength of binding of NEC-β-CDs toward AAs..... 146

4.3.5 The origin of enhanced enantio-selectivity..... 150

4.4 Conclusion..... 150

5. CONCLUSIONS AND SUGGESTIONS FOR FURTHER EXPERIMENTS..... 152

5.1 Conclusions..... 152

5.2 Suggestions for further experiments..... 154

REFERENCES..... 157

LIST OF TABLES

Table		Page
1.1	Physical properties of cyclodextrins.....	7
2.1	^{1}H chemical shifts of readily identified protons of the derivatized glucose unit of mono-substituted NEC-β-CDs in deuterated methanol.....	44
2.2	Distribution of regioisomers under various reaction conditions.....	46
3.1	^{1}H and ^{13}C NMR data of β-CD in D_2O.....	67
3.2	^{1}H chemical shifts of β-CD and SCSs of RC-2 in D_2O.....	88
3.3	^{13}C chemical shifts of β-CD and SCSs of RC-2 in D_2O.....	89
3.4	^{1}H chemical shifts of β-CD and SCSs of SC-2 in D_2O.....	90
3.5	^{13}C chemical shifts of β-CD and SCSs of SC-2 in D_2O.....	91
3.6	^{1}H and ^{13}C chemical shifts non-carbohydrate unit..	92
3.7	Equilibrium dependence of included and excluded conformer of RC-2 in various volume fractions of methanol in methanol/water system.....	116
3.8	Equilibrium dependence of included and excluded conformer of SC-2 in various volume fractions of methanol in methanol/water system.....	117
4.1	CZE data of separation of 3,5-DNB-HPA, PA, and PG using β-CD.....	131

4.2 Association constants between 3,5-DNB-HPA, PA, and PG with β-CD and line fitting data..... 135

4.3 CZE data of separation of 3,5-DNB-HPA, PA, and PG using various monosubstituted NEC-β-CDs..... 142

4.4 CZE data of NEC-β-CDs and β-CD using amino acids as electrolyte additives 149

LIST OF FIGURES

Figure		Page
1.1	Structures of cyclodextrins	6
1.2	Schematic diagram of NEC-β-CD-CSPs	10
1.3	Basic configuration of a capillary electrophoresis system	13
2.1	HPLC chromatograms of the separation of monosubstituted NEC-β-CDs	39
2.2	Structure of NEC-β-CDs and the numbering system of protons and carbon atoms of the products	40
2.3	Partial 500 MHz ^1H spectra of SC-2(a), SC-3(b), and SC-6(c) in CD_3OD	41
2.4	Partial 500 MHz ^1H spectra of RC-2(a), RC-3(b), and RC-6(c) in CD_3OD	42
2.5	Product distribution for the reaction between S-NEIC and β-CD in pyridine (reflux)	47
2.6	Product distribution for the reaction between S-NEIC and β-CD in DMF (reflux)	48
2.7	Product distribution for the reaction between S-NEIC and β-CD in DMF (NaH activation, ambient temperature)	50
2.8	Product distribution for the reaction between S-NEIC and β-CD in pyridine (NaH activation)	51
2.9	Reaction schemes for the synthesis of monosubstituted NEC-β-CDs	53

2.10 Proposed mechanism for the conversion of the C-2 substituted isomer to the C-6 substituted isomer..... 56

3.1 500 MHz ^{1}H and 125 MHz ^{13}C NMR spectra of β-CD taken in D_2O..... 65

3.2 ^{1}H and ^{13}C COSY spectrum of β-CD..... 66

3.3 The numbering system of the proton and carbon atoms and the seven glucoses of RC-2 and SC-2... 69

3.4 The 500 MHz ^{1}H NMR spectra of (a) RC-2 and (b) SC-2 in D_2O..... 70

3.5 The 125 MHz ^{13}C NMR spectra of (a)RC-2 and (b) SC-2 in D_2O..... 71

3.6 The anomeric region of partial ROESY spectrum of SC-2 showing the correlations between the two exchanging conformers..... 72

3.7 The strategy for the assignment of ^{1}H and ^{13}C resonances of RC-2 and SC-2..... 74

3.8 Partial ^{1}H-^{1}H COSY spectrum of RC-2 in D_2O showing the correlations of anomeric protons and H-2s..... 75

3.9 Partial HMQC spectrum of RC-2 showing the correlations between H-1s and C-1s..... 77

3.10 Partial HMBC spectrum of RC-2 showing the correlations between H-4s and C-6s..... 78

3.11 Partial HMBC spectrum of RC-2 showing the correlation between H-2A and C-13′ of carbamate indicating the derivatization site..... 80

3.12 Partial ROESY spectrum of RC-2 showing the correlation between H-1 in one glucose and H-4 in neighboring glucose..... 82
3.13 Partial ROESY spectrum of SC-2 showing the correlation between H-1 in one glucose and H-4 in neighboring glucose..... 83
3.14 Partial HMBC spectrum of RC-2 showing the correlation between H-4 in one glucose and C-1 in neighboring glucose..... 84
3.15 Partial HMBC spectrum of SC-2 showing the correlation between H-4 in one glucose and C-1 in neighboring glucose..... 85
3.16 Partial HMBC spectrum of RC-2 showing the correlation between H-1 in one glucose and C-4 in neighboring glucose..... 86
3.17 The structure of glucose A of RC-2..... 94
3.18 The schematic diagram showing several possible inclusion modes..... 95
3.19 Partial ROESY spectrum of RC-2 showing the correlations between naphthyl protons and carbohydrate protons..... 98
3.20 The schematic diagram illustrating possible geometry of RC-2 deduced from the NMR experiments..... 100
3.21 Series of ^{1}H NMR spectra of SC-2 showing the effect of solvent polarity on the populations of

in- or excluded conformers..... 102
3.22 The schematic diagrams of SC-2 deduced from the NMR experiment..... 104
3.23 Partial ROESY spectrum of SC-2 showing the correlations between naphthyl protons and carbohydrate protons..... 105
3.24 Proposed structure of RC-2 including carbamate linkage and possible hydrogen bonding between carbamate and carbohydrate..... 108
3.25 Proposed structure of SC-2 including carbamate linkage and possible hydrogen bonding between carbamate and carbohydrate..... 109
3.26 Computer generated stereographic views of RC-2... 111
3.27 Computer generated stereographic views of SC-2... 113
3.28 Series of ^{1}H NMR spectra of RC-2 in the various volume fraction of methanol in water..... 115
3.29 Linear correlations between ln K vs. volume % of methanol for RC-2 and SC-2..... 119
3.30 The structures of the 3,5-DNB- derivatives of HPA, PA, and PG..... 120
3.31 The partial NMR spectra of protons of 3,5-DNB group of racemic 3,5-DNB-PG(a), and complexed with SC-2(b) and with RC-2(c)..... 121
4.1 Vector diagram for the migration behavior of a negatively charged analyte in a buffer with β-CD as CMA..... 127

4.2 Electropherograms of 3,5-DNB-HPA, PA, and PG (a) without CD and (b) with CD..... 130

4.3 Graph demonstrating the dependence of migration times of analytes upon [CD]..... 133

4.4 Plot of $(t_{ep,f} - t_{ep})/(t_{ep} - t_{ep,c})$ vs [CD]..... 134

4.5 Dependence of enantioresolution of HPA and PA on [CD]..... 136

4.6 HPLC separation of 3,5-dinitrobenzoic acid, HPA, PA, and PG..... 139

4.7 Electropherograms of 3,5-DNB-AAs using various NEC-β-CDs as chiral selectors..... 141

4.8 Electropherograms of the separations of NEC-CDs including β-CD using 3,5-DNB-PA as an additive..... 147

LIST OF ABBREVIATIONS

AAs	= Amino Acids
AGP	= α_1-acid glycoprotein
BSA	= Bovine Serum Albumin
α-CD	= α-Cyclodextrin (6 glucose units)
β-CD	= β-Cyclodextrin (7 glucose units)
γ-CD	= γ-Cyclodextrin (8 glucose units)
COSY	= ^1H - ^1H Correlation spectroscopy
CSP	= Chiral stationary phase
CZE	= Capillary Zone Electrophoresis
DANS-AAs	= Dansylated Amino Acids
DMF	= N,N-Dimethylformamide
DMSO	= Dimethylsulfoxide
3,5-DNB-AA	= 3,5-Dinitrobenzoyl Amino Acid
3,5-DNB-Cl	= 3,5-Dinitrobenzoyl chloride
3,5-DNB-HPA	= N-(3,5-Dinitrobenzoyl)-homophenylalanine
3,5-DNB-PA	= N-(3,5-Dinitrobenzoyl)-phenylalanine
3,5-DNB-PG	= N-(3,5-dinitrobenzoyl)-phenylglycine
EI-MS	= Electron impact mass spectrometry
EOF	= Electroosmotic Flow
FAB-MS	= Fast atom bombardment mass spectrometry
HMBC	= ^1H - ^{13}C Heteronuclear multiple bond correlation spectroscopy

HMQC	= ^{1}H - ^{13}C Heteronuclear multiple quantum coherence spectroscopy
HPA	= Homophenylalanine
HPLC	= High pressure liquid chromatography
MHz	= Megahertz
NEC	= 1-(1-naphthyl)ethylcarbamoyl group
NEC-CD CSP	= 1-(1-naphthyl)ethylcarbamoylated cyclodextrin chiral stationary phase
2-O-R-β-CD (=RC-2)	= 2-O-((R)-1-(1-naphthyl)ethyl-carbamoyl)-β-CD
3-O-R-β-CD (=RC-3)	= 3-O-((R)-1-(1-naphthyl)ethyl-carbamoyl)-β-CD
6-O-R-β-CD (=RC-6)	= 6-O-((R)-1-(1-naphthyl)ethyl-carbamoyl)-β-CD
PA	= Phenylalanine
PG	= Phenylglycine
R-NEIC	= (R)-1-(1-naphthyl)ethyl isocyanate
2-O-S-β-CD (SC-2)	= 2-O-((S)-1-(1-naphthyl)ethyl-carbamoyl)-β-CD
3-O-S-β-CD (SC-3)	= 3-O-((S)-1-(1-naphthyl)ethyl-carbamoyl)-β-CD
6-O-S-β-CD (SC-6)	= 6-O-((S)-1-(1-naphthyl)ethyl-carbamoyl)-β-CD
S-NEIC	= (S)-1-(1-naphthyl)ethyl isocyanate
NMR	= Nuclear resonance spectroscopy
NOE	= Nuclear Overhauser enhancement

ROESY	= Rotating frame nuclear Overhauser spectroscopy under spin locking
TOCSY	= ^{1}H - ^{1}H Total correlation spectroscopy
UV	= Ultraviolet spectroscopy

CHAPTER 1

INTRODUCTION

Chirality is a part of Nature's characteristics. For a long time, humans have recognized chirality whether it was called chirality or not. One of the most frequently encountered chiral objects is a human body which contains many elements of chirality. For example, the right and left hands are same in the number and arrangment of fingers and yet the left glove does not fit well on the right hand and the right glove does not fit well on the left hand. However, it is sometimes difficult to fully comprehend the nature of chirality. Like the shape of human body, many molecules comprising the human body are chiral compounds. Amino acids, which are the building materials of proteins, occur primarily as the L form. Ribose, an essential constituent of DNA or RNA, occurs as the D form. In most cases, Nature selected only one form of two possible enantiomers.

Because most life forms, including human, utilize highly stereoselective metabolic and communication pathways at the molecular level, it is necessary to study chirality to better understand these stereoselective life processes. The emergence of chirality has most impacted pharmaceutical

sciences. Just as the right glove fits better on the right hand, one of two possible forms of a racemic drug may be more suitable to treat diseases.

1.1 Chiral separations

The separation of chiral compounds is currently one of the most active and challenging subjects in analytical science because it is a leading issue in pharmaceutical sciences. A recent survey indicated that 88% of all synthetic chiral drugs were marketed as the racemic mixtures.[1] Because many different stereoisomers show different physiological activities, chiral separations are fundamental to research on the relationship between drug chirality and its bioactivity.[2,3,4,5,6]

There are several ways to achieve chiral separations including crystallization, various forms of chromatography,[7,8] and capillary zone electrophoresis (CZE).[9,10] Chiral separation by crystallization may be achieved after conversion of enantiomers to diastereomers, which have different chemical and physical characteristics. By employing chiral mobile phase additives or chiral stationary phases, separation of enantiomers may also be done by chromatography. Among several chromatographic methods, High Performance Liquid Chromatography (HPLC) has been the most

widely used separation method for enantiomeric separation, especially with the development of new chiral stationary phases (CSPs).

1.1.1 HPLC-chiral stationary phases (CSPs)

There are a number of successful CSPs, including Pirkle type,[11] protein based,[12] and cyclodextrin based chiral stationary phases (CD-CSPs).[13]

1.1.1A Pirkle type CSPs

Pirkle type CSPs were obtained by the attachment of an optically active moiety to silica gel. The enantio-recognition mechanism involves hydrogen bonding, dipolar, and charge transfer interactions, and steric hindrance.[14] Attachment of 3,5-dinitrobenzoyl (3,5-DNB) phenylglycine (PG) and later leucine as well as other amino acids to the silica gel provided π-electron acceptor sites to resolve enantiomers with aromatic π-electron donor functional groups.[15,16,17] Later, Pirkle introduced N-aryl-α-amino acid chiral stationary phases based on the reciprocity concept.[18] These phases are π-electron donors designed to separate 3,5-DNB derivatives (π-acceptor) of amino acids, amines, alcohols, thiols, and so on.[19]

1.1.1B Protein based CSPs

The highly selective interactions between proteins and substrates have been utilized for affinity chromatography.[20] Availability and immobilization of proteins on the silica gel made it possible to use proteins as CSPs. One of the first applications of protein based CSPs was based on Bovine Serum Albumin (BSA) bonded to silica.[21] BSA is a globular protein of molecular weight of 66210 and consists of 581 amino acids with 17 disulfide bridges. These phases were successfully applied to separate aromatic amino acids, amino acid derivatives, aromatic sulfides, coumarin derivatives, and benzoin derivatives. In addition to BSA, α_1-acid glycoprotein (AGP)[22] and ovomucoid[23] were also successfully employed as CSPs. AGP is a protein present in human plasma with molecular weight of 41000. Ovomucoid is another acid glycoprotein which comprises approximately 10 % of egg white content.

1.1.1C Native cyclodextrin-based chiral stataionary phases (CD-CSPs)

Cyclodextrins (CDs) are cyclic oligosaccharides consisting of 6, 7, or 8 glucopyranose units, usually referred to as α-, β-, or γ-cyclodextrins, respectively. All glucose units are connected through α-(1,4) linkages to

form a doughnut-like ring.[24] The structures of CDs are shown in Figure 1.1. The molecule is slightly tapered with the hydroxyl groups of C-2 and C-3 lying on the larger rim and the CH_2OH groups on the smaller rim. The cavity sizes and physical properties of CDs are listed in Table 1.1.[24] The sides of the ring consist of pyranose units with the width of a single pyranose unit. A CD has a polar, hydrophilic outside and a relatively nonpolar lipophilic inside. These two distinct regions make CDs unique for complex formation.

The ability of CDs to form inclusion complexes with various guest molecules has long been recognized[24,25] and led to attempts to use CDs in chromatography.[26,27] Because the cavity of CD is chiral, CD was expected to distinguish enantiomers in complex formation. Stability constants of two different diastereomers formed by inclusion complexation should be different. The controlling factor for inclusion was thought to be the relative sizes of the CD cavity and a guest molecule. CD-CSPs have several advantages over other chiral phases. Because cavity sizes of CDs are different, one can separate a variety of different size enantiomers by selecting the appropriate CD. Additional flexibility of CD-CSPs can be easily obtained through the derivatization of the native CD-CSPs.

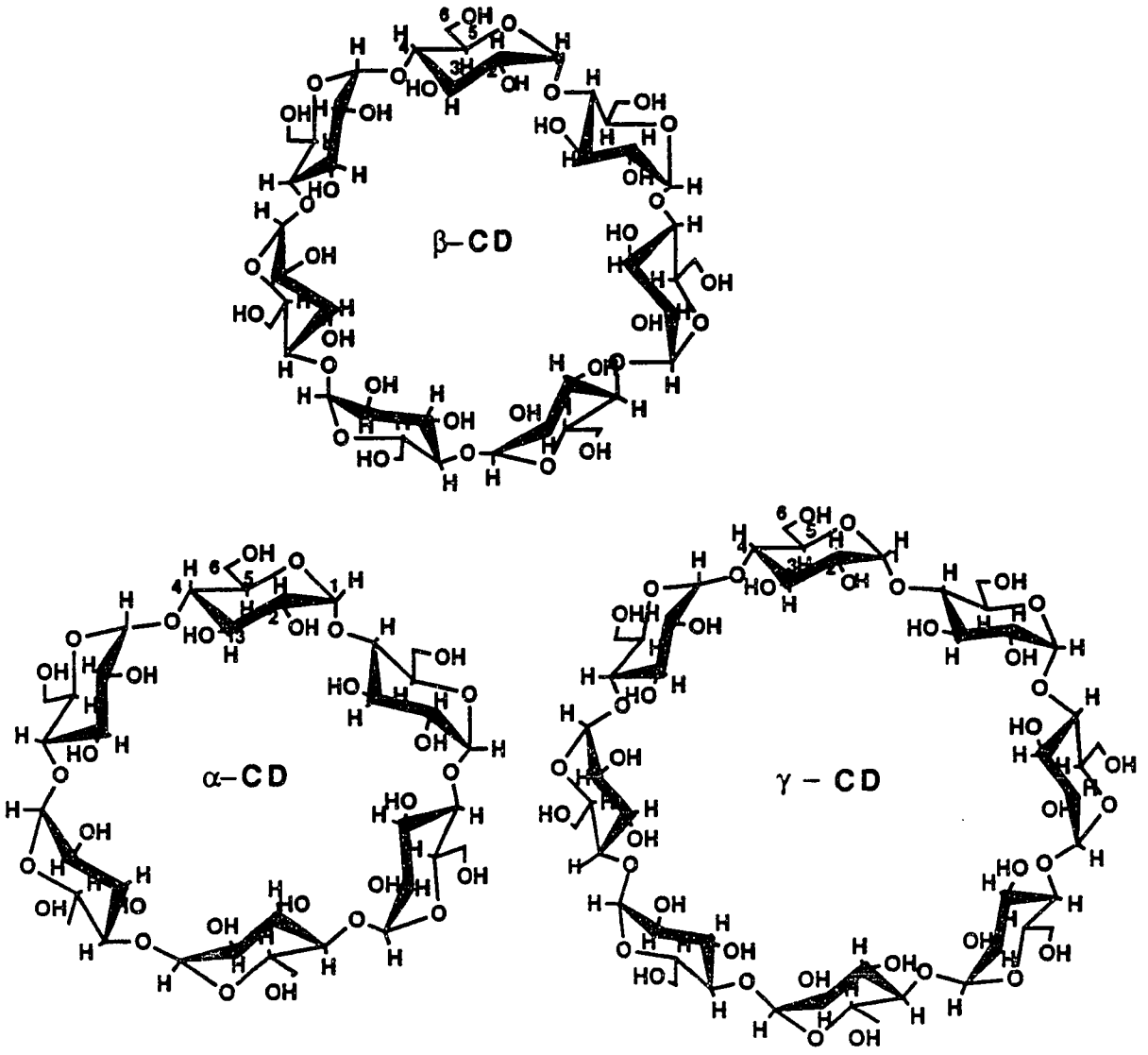

Figure 1.1 Structures of Cyclodextrins.

Table 1. 1 Physical properties of cyclodextrins

CDs	# of glucose residue	M.W.	water solubility (M)	specific rotation $[\alpha_D]^{25}$	Internal diameter (Å)	External diameter (Å)	Depth of cavity (Å)
α-CD	6	973	0.114	150.5	5.7	13.7	7.8
β-CD	7	1135	0.016	162.5	7.8	15.3	7.8
γ-CD	8	1297	0.179	177.4	9.5	16.9	7.8
δ-CD	9	1459	very soluble	191			

Attachment of CDs on silica gel has been attempted through amine or amide linkages.[28,29] However, the amine and amide linkages are not hydrolytically stable, which limits the use of hydro-organic mobile phases, and the amount of CD actually attached to the silica gel was often too low. In the 1980's, CD was successfully immobilized on silica gel through specific non-hydrolytic silane linkages.[27] These CD-CSPs are hydrolytically stable and used mainly in the reversed phase mode. The chromatographic data for hundreds of compounds separated on these columns are well publicized.[30] In a reversed phase mode, the interaction between the hydrophobic cavity of CD and hydrophobic parts of analytes are thought to be the main mechanism for the chiral selectivities.

1.1.1D Derivatized cyclodextrin-based chiral stationary phases

The polarity of the CD based stationary phases can be easily modified by solid phase derivatization with an appropriate derivatizing reagent. Several derivatized CD-CSPs have been synthesized. The CDs were multiply substituted by propylene oxide,[31] acetic anhydride, 2,6-dimethylphenyl isocyanate, p-toluoyl chloride, and (R)- or (S)-1-(1-naphthyl)ethyl isocyanate (NEIC) etc.[32,33,34] Derivatization of CDs alters their physicochemical

characteristics as well as their complexation mechanisms. Contrary to the native **CD-CSPs**, the chiral separation mechanism on the derivatized **CD-CSPs** is thought to be not solely dependent upon inclusion complexation.

Among several derivatized **CD-CSPs**, the naphthylethyl-carbamoylated **β-CD** chiral stationary phases (**NEC-β-CD-CSPs**) were used both in reversed and normal phase modes because of their stability and unique resolution capability in both modes.[35,36,37] The schematic diagram illustrating **NEC-β-CD-CSPs** is shown in Figure 1.2. The introduction of π-π and additional hydrogen bonding sites as well as residual **CD** hydroxyls makes these phases unique in enantioselectivity.

In the normal phase mode, these phases successfully resolved a wide variety of 3,5-dinitrobenzoyl (**3,5-DNB**) derivatives of alcohols, amines, amino alcohols, and carboxylic acids.[37] In hydro-organic solvents, it behaves similarly to native **CD-CSPs**.[36] However, these phases successfully resolved some enantiomers which were not separated on a native **CD** column.[36,38]

The elution order for 3,5-DNB-phenylglycine (**3,5-DNB-PG**) and **3,5-DNB**-tyrosine was reversed by changing the chirality of the pendant **NEC** groups on **NEC-β-CD-CSPs**.[37] On

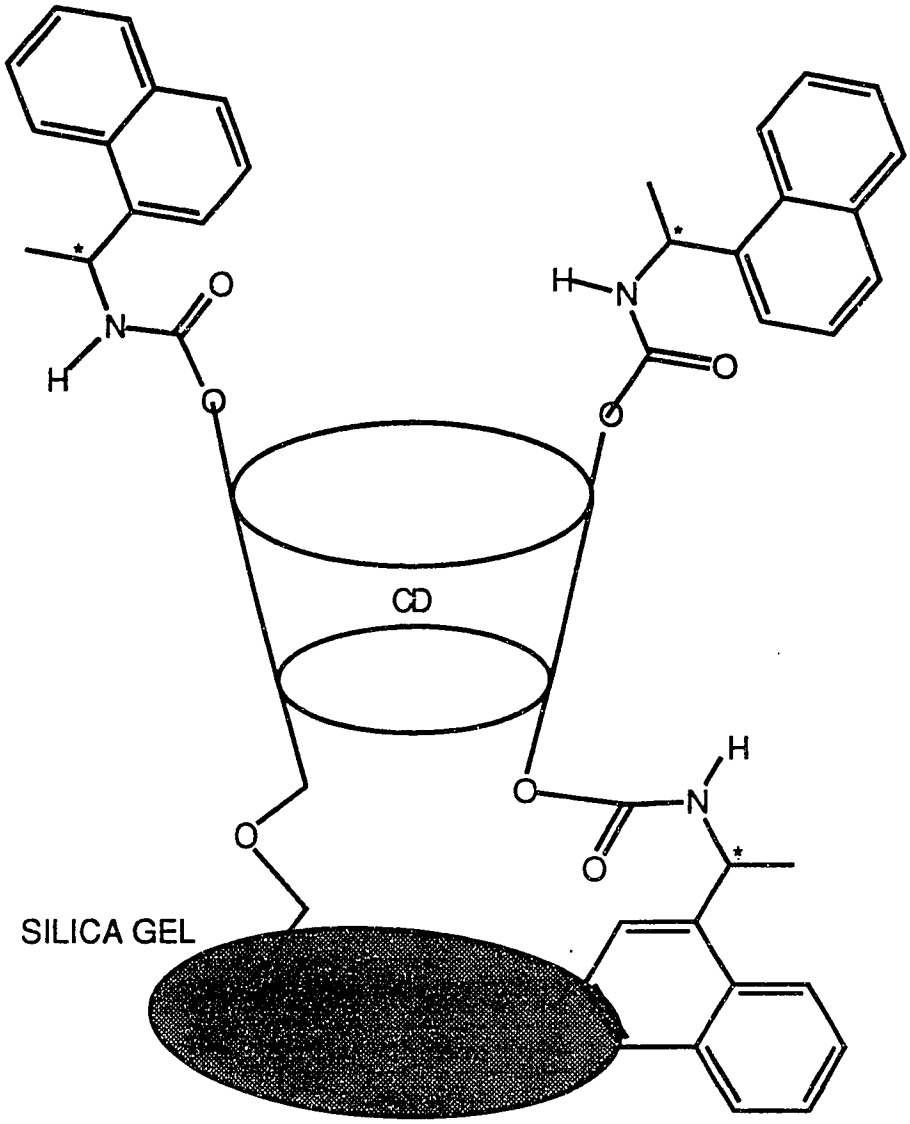

Figure 1.2 Schematic diagram of naphthylethyl-carbamoylated cyclodextrin chiral stationary phase.

the other hand, the elution order for 3,5-DNB-phenylalanine (3,5-DNB-PA) and 3,5-DNB-homophenylalanine (3,5-DNB-HPA) was independent of the chirality of the NEC groups. Further, the elution order of 3,5-DNB-HPA from S-NEC-β-CD-CSP was opposite that obtained from S-NEC-γ-CD-CSPs.[33]

Recently, a systematic study on the resolution of several derivatized amino acids (AAs) on several different CD-CSPs in the reversed phase mode indicated that 3,5-DNB-AAs were resolved better on the (R)- or (S)-NEC-β-CD column than native β-CD-CSP.[39] The proposed mechanism of chiral recognition of the NEC-β-CD-CSPs involved inclusion complexation with β-CD, π-π interaction with the naphthyl moiety, interactions with remaining secondary alcohols at the CD-mouth, and steric hindrance.

1.1.2 Chiral separations using capillary zone electrophoresis (CZE)

Capillary zone electrophoresis (CZE) has been demonstrated as a powerful separation device which can separate charged molecules under the influence of a high electrical field in a fused-silica capillary of small inner diameter (typically 20-200 μm I.D.) filled with buffer.[40,41] Its high resolution capability and lower

sample loading relative to **HPLC** makes it ideal for the separation of minute amounts of components in complex biological mixtures. The basic configuration of a capillary electrophoresis system is shown in Figure 1.3.

Separations in **CZE** have been reported for peptides,[42] **AAs**,[43] proteins,[44] DNA,[45] catecholamines[46,47] and various organic molecules. Many chiral separations have been demonstrated by the complexation of analytes with chiral Cu(II)-aspartame complex, or Cu(II)-L-histidine complex.[48,49] The first chiral separation in **CZE** was done by the addition of optically active Cu(II)-L-histidine to resolve dansylated amino acids (**DANS-AAs**).[49] Diastereomeric ternary complex formation between Cu(II)-histidine and the amino acids was explained as the basis for the achieved chiral separation. The more strongly bound enantiomers migrate faster because of the positive charge of Cu(II)-histidine complex. The same group also reported the successful use of Cu(II)-aspartame complex electrolyte to achieve chiral resolution of **DANS-AAs**.[48]

The addition of chiral surfactants (micelles) to the electrolyte enabled chiral separation of both neutral and charged molecules in the same electropherogram.[50,51] Micelles increase the solubility of neutral molecules in buffer solution as well as alters migration rates of

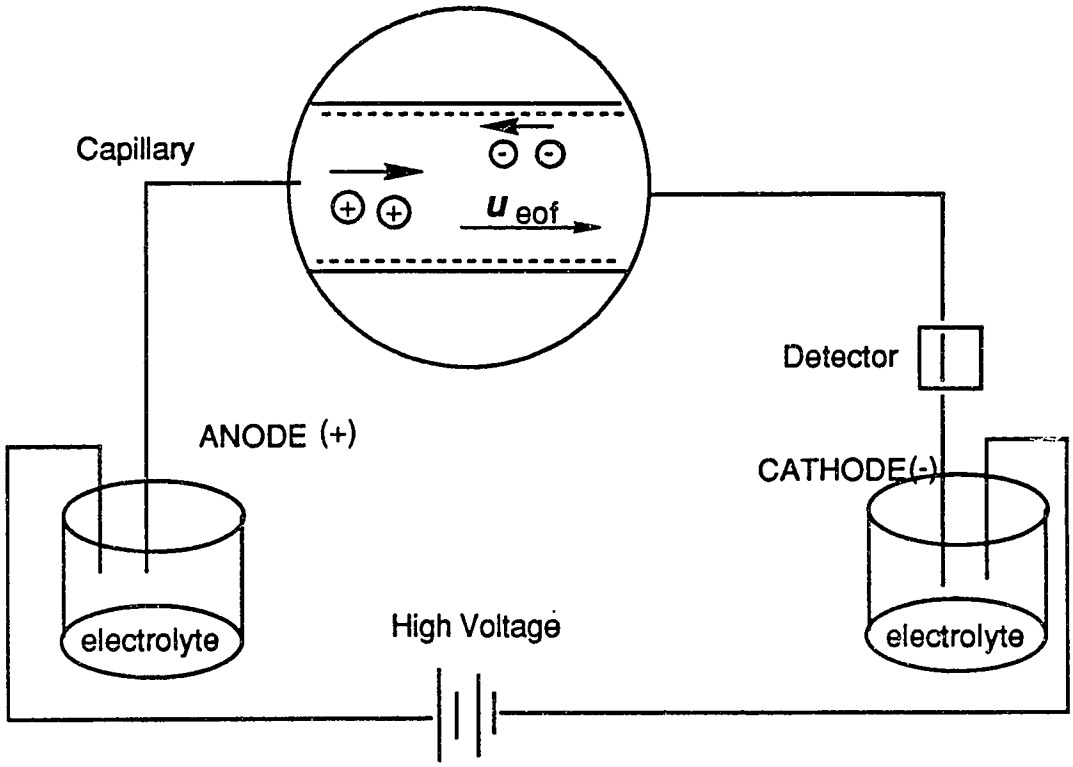

Figure 1.3 Basic configuration of a capillary electrophoresis system.

chiral analytes. Chiral separation could be possible on the basis of differential partitioning into charged micelles regardless of the charges of the two enantiomers. Chiral micellar systems using sodium N-dodecanoyl-L-valinate in borate-phosphates buffer made the chiral resolution of 3,5-DNB- derivatives of amino acid isopropyl esters possible.[52] Bile salts, which are formed from bile acid, were successfully used as micelle-like long chain alkyl-type surfactants to achieve chiral separation.[53]

Native and derivatized CDs, with proven chiral resolution capabilities in HPLC have also been used for chiral resolution in CZE.[54,55,56,57,58,59,60] Among many possible derivatized CDs, methylated CDs have been the most widely applied. By employing CDs as supporting chiral modifiers, migration rates are affected. Decreased chiral resolution and reversal of migration order of enantiomers were observed for the separation of DANS-AAs when methylated CDs were used instead of native CD in CZE.[61] Native CD, 2,6-dimethyl-β-CD and 2,3,6-trimethyl-β-CD were studied for the chiral resolution of sympathomimetic drugs.[62] Among the CDs studied, 2,6-dimethyl-β-CD exhibited the best chiral resolution implying the most effective complexation with these drugs.

1.1.2A Theory of CZE

The schematic diagram illustating migration behaviour of a charged particle in a homogenous buffer solution under the constant field gradient is shown in Figure 1.3. The migration velocity (v) of a charged particle is given by (1.1)

$$v\ (cm/\text{sec}) = \mu\ E = \mu\ (\frac{V}{L_t}) \qquad (1.1)$$

where E: electric field gradient, V: potential across the capillary, μ: the electrophoretic mobility, and L_t: length of capillary. The electrophoretic mobility ($cm^2/(V \times sec)$) represents the distance a solute migrates in a given time period under the constant field gradient. The migration time (t), analogous to retention time in chromatography, is the time it takes a solute to move from the injector site of the capillary to the detection window as given in (1.2).

$$t = \frac{L_d}{v} = \frac{L_d}{\mu\ E} = \frac{L_d\ L_t}{\mu\ V} \qquad (1.2)$$

where L_d is the length of capillary from the injector site to the detector. Assuming molecular diffusion is the only

reason for band broadening, the spatial variance (σ^2_1) at a given time t is given in (1.3)

$$\sigma_1^2 = 2\ D \times t \tag{1.3}$$

where D is the molecular diffusion coefficient of the solute. Substitution of (1.2) into (1.3) yields,

$$\sigma_1^2 = 2\ D \times \frac{L_d\ L_t}{\mu\ V} \tag{1.4}$$

The chromatographic definition of separation efficiency can be borrowed to express the separation efficiency in electrophoresis. The number of theoretical plates, N, is defined as

$$N = \frac{L_t^2}{\sigma_1^2} \tag{1.5}$$

Substitution of (1.4) into (1.5) assuming post-capillary detection ($L_d = L_t$) yields,

$$N = \frac{\mu V}{2 D} \qquad (1.6)$$

equation (1.6), as first derived by Jorgenson et al.,[40] suggests that the separation efficiency in CZE is independent of the length of the capillary and directly proportional to the applied potential.

1.1.2B Theoretical aspects of chiral separation in CZE

As indicated previously, in CZE, the addition of a chiral mobile phase additive is a common method for the resolution of chiral compounds. The addition of complexing agents to the supporting electrolyte, affected the migration rates of analytes. This migration change led to the calculation of complexation constants between chiral analytes and chiral selectors.[63,64]

The retention of analytes in CZE was well characterized by Guttman et al.,[65] and later Wren et al.[66,67] Recently, Rawjee et al.[68] studied the role of pH and the concentration of a chiral selector on the chiral selectivity. As described by Guttman et al.,[65] the electrophoretic mobility (μ) of a solute can be represented by a

weighted sum of mobility in the free state (μ_f) and that in the complexed state (μ_c) as shown in (1.7)

$$\mu = R\,\mu_f + (1 - R)\,\mu_c \tag{1.7}$$

where R is the fraction of solute in free state and is equal to c_f/c_t; c_f = concentration of an uncomplexed analyte, A, and c_t = total concentration of A. R can be related to complexation constant K by

$$A + CD \rightleftharpoons A{\bullet}CD \tag{1.8}$$

$$K = \frac{[A{\bullet}CD]}{[A]\ [CD]} = \frac{[c_t - c_f]}{[CD]\ [c_f]} = \frac{(1-R)}{[CD]\ R} \tag{1.9}$$

Therefore,

$$K\,[CD]\,R = 1 - R \tag{1.10}$$

and,

$$R = \frac{c_f}{c_t} = \frac{1}{1 + K\,[CD]} \tag{1.11}$$

$$1 - R = \frac{K\ [CD]}{1 + K\ [CD]} \qquad (1.12)$$

Substitution of (1.11) and (1.12) to (1.7) yields the general mobility expression shown in (1.13),

$$\mu = \frac{\mu_f}{1 + K[CD]} + \frac{K\ [CD]\ \mu_c}{1 + K[CD]} = \frac{\mu_f + K[CD]\,\mu_c}{1 + K[CD]} \qquad (1.13)$$

The association constant can be calculated from (1.13) by plotting mobility vs. [CD]. The complexed state mobility must be estimated from extrapolation to the infinite concentration of CD.

The difference in the electrophoretic mobility of chiral analytes may be expressed as

$$\Delta\mu = \frac{\mu_{1,f} + K[CD]\,\mu_{1,c}}{1 + K_1\mu\,[CD]} - \frac{\mu_{2,f} + K[CD]\,\mu_{2,c}}{1 + K_2\mu\,[CD]} \qquad (1.14)$$

where 1 and 2 represent two enantiomers migrating earlier and later, respectively. Rearragement of (1.14) yields (1.15) for the clear expression for the chiral separation, as first derived by Wren et al.,[66]

$$\Delta\mu = \frac{[CD]\,(\mu_{1,f} - \mu_{1,c})\,(K_2 - K_1)}{1 + [CD]\,(K_1 + K_2) + K_1K_2\,[CD]^2} \qquad (1.15)$$

where $\mu_{1,f}$ and $\mu_{1,c}$ were assumed to be the same as $\mu_{2,f}$ and $\mu_{2,c}$, respectively. From eq. (1.15), it is clear that if $K_1 = K_2$ or $\mu_{1,f} = \mu_{1,c}$, there will be no chiral separation. It is also notable that [CD] should not be zero or very large to obtain different in mobilities for the two enantiomers. Between these two extremes of [CD], it is possible to achieve chiral separation. The optimum concentration of CD can be found by differentiation of (1.15), i.e., $d\Delta\mu/d[CD] = 0$. The condition occurs when

$$[CD] = \frac{1}{\sqrt{K_1K_2}} \qquad (1.16)$$

In reality, the manipulation of migration data for the calculation of complexation constant is complicated because of the existence of electroosmotic flow (**EOF**). The silanol groups of the fused silica capillary can be ionized, resulting in a negatively charged wall which attracts positively charged ions from the buffer. This attraction of positively charged ions creates an electrical double layer.

The positively charged double layer migrates toward the cathode under the electric field, carrying water along. The result is a net flow of buffer solution toward the cathode. It is common to observe even negatively charged ions migrating toward cathode. At higher pH, the **EOF** gets higher because of more extensive ionization of the silanol groups. Therefore, this net flow must be compensated for in the calculation of the complexation constant from the migration data.

1.2 Studying interactions between CD and guest molecules by non-chromatographic means

In chromatography, to achieve chiral separations, two enantiomers should have somewhat different interactions with a stationary phase and thus, the complex formation constants should be different. Even though one can deduce chiral interaction mechanisms by analyzing the chromatographic data, the information obtained is not complete. However, the information obtained in chromatography may be complemented by other spectroscopic means.

For instance, the interactions between an analyte and cyclodextrin may be studied by nuclear magnetic resonance (NMR),[69] UV/VIS absorption,[70,71] fluorescence,[72,73] etc.

1.2.1 NMR

A large number of NMR studies have been done to determine the enantiomeric purity using either chiral derivatizing agents or chiral solvating agents.[74] Derivatization of chiral compounds with optically pure derivatizing agents yields discrete diastereomers which may have different NMR signals. In contrast to chiral derivatizing agents, chiral solvating agents form reversible diastereomeric complexes which are in fast exchange on the NMR time scale.

Inclusion complex formation between native CDs and guest molecules have been extensively studied. Inclusion of aromatic compounds in the native CD cavity usually induces a net upfield shift of the CD protons H-3, and H-5, located in the cavity.[75,76] However, the resultant NMR spectrum provides only averaged CD NMR signals (only one set of a single glucose unit) because the reversible inclusion complexation between CD and a guest molecule is fast on the NMR time scale and the included moiety has some rotational freedom within the cavity. The time averaged NMR signals yield only limited information about any distortion of the CD torus induced by the guest molecule.[75,76]

Because of the chirality of CD cavity, complexation with enantiomers results in diastereomeric complexes. If the two diastereomers should have different chemical shifts, the CD may act as a NMR chiral shift reagent. Many NMR studies of CDs have been done to determine enantiomeric purity of pharmaceutically important compounds. Greatbanks and Pickford[77] observed diastereomeric pairs between β-CD and propranolol in deuterated water at 400 MHz. When they used α-CD, they could not observe this phenomenon and concluded that the cavity of the α-CD is too small to fit the naphthalene moiety of propranolol. The chemical shift differences of the diastereomeric pairs were observed in the naphthalene and alkyl protons of propranolol as well as CD protons. Through nOe experiments, the naphthyl group of the molecule was found to enter the cavity. Not only aromatic compounds but also an aliphatic compound such as α-pinene, was shown to form diasteromeric complexes with CDs.[78]

1.2.2 UV-VIS and fluorescence

It is well known that complexation by CD alters the UV and fluorescence spectra of many guest molecules. Bender et al.[71] observed that the presence of CD induces almost identical changes in the UV spectra of aqueous p-t-butylphenol as are observed for p-t-butylphenol in dioxane.

Marquez et al.[79] found that the addition of β-CD to the aqueous solution of warfarin enhances fluorescent intensity. They concluded that warfarin occupies the CD cavity and is protected from the probable quencher, water.

1.3 The scope of this research

Chiral selectivity of a new chiral column is obviously dependent upon interactions between the CSPs and enantiomeric analytes. Therefore, understanding these interactions is fundamental for the modification of the CSPs and further development of new chiral stationary phases.

Among the several derivatized CD based chiral stationary phases, the NEC-β-CD-CSPs may be the best model for the study because these CSPs are hydrolytically stable and show chiral selectivities in both normal and reversed phase modes.[35,36,37] The introduction of π-π donor and additional hydrogen bonding sites by the aromatic and carbamate substituents as well as residual CD hydroxyl sites are all thought to contribute to their uncommon enantio-selectivity. However, several issues about these CSPs remain unanswered: the sites of substitution, the orientation of the substituent and its role in chiral recognition under different mobile phase conditions, and the integrity of toroidal configuration of the CD upon

derivatization. Given that the average degree of substitution varies from 3 to 8 and the substitution sites are not known, the chiral recognition mechanism of these phases is not clear.[33,34] To better understand the substitution sites of this chiral stationary phase, monosubstituted naphthylethylcarbamoylated β-CDs were synthesized under several different conditions. Among three possible regioisomerically monosubstituted products, C-2 hydroxyl substitution product was used for the study of conformational change of the NEC group under the various solvent conditions by NMR spectroscopy because modification of the more opened secondary hydroxyl side of CDs is thought to be more important than the narrow primary side for chiral distinction.[80]

Finally, to understand the effect of substitution sites in chiral resolution, various site substitution products were employed as chiral resolving agents toward homologues of 3,5-DNB-HPA, -PA, and -PG in capillary electrophoresis or NMR spectroscopy. The chiral resolution toward these three amino acids in CZE was compared to those from HPLC using CD-CSPs.

CHAPTER 2

SYNTHESIS OF MONOSUBSTITUTED NAPHTHYLETHYLCARBAMOYLATED CYCLODEXTRINS

2.1 Introduction

Derivatized cyclodextrins[81] (CDs) have been extensively studied to obtain better enzyme models,[82,83] molecular recognition models,[84,85,86] and to achieve chiral separations in chromatography.[13]

Regioselective derivatization of the various hydroxyl groups of CDs is not an easy task. The derivatization reaction usually results in multiple substitution without regioselectivity. By the use of a solid base (NaOH, and KOH) and methyl sulfoxide with methyl iodide permethylation of carbohydrates was possible.[87] Selective derivatizations of primary or secondary hydroxyl groups of CDs such as acylation, sulfonylation, or silylation have been reported.[88,89,90,91,92] Selective sulfonation of hydroxyl groups was studied under three different reaction conditions. The reaction of CDs with tosyl chloride in pyridine for 5 h resulted in mono-tosylation at the C-6 hydroxyl group. The same reaction in aqueous buffer with pH 13 for 1 h resulted in primary substitution. The reaction was also carried out in a mixture of DMF and aqueous buffer

(pH 10) at 60 °C for 1 h and resulted in C-2 hydroxyl substitution.[91] Under the DMF-buffer condition, tosylation may also proceed with host-guest complex formation between the CD and the 3-nitrophenyltosylate. Protection of all primary hydroxyl groups prior to the regioselective modification of the secondary hydroxyl site was studied. Protection of all primary hydroxyl groups of β-CD or γ-CD, was possible with t-butyldimethylsilyl chloride either in DMF with imidazole or in pyridine.[93] The silylation reaction in pyridine was found to be more selective towards the primary hydroxyl groups than with imidazole in DMF.

A convenient method of derivatizing C-2 hydroxyl groups of CD was demonstrated using NaH for selective deprotonation, resulting in alkoxides which could undergo various nucleophilic substitutions.[94] The regioselectivity of this process is thought to arise in the deprotonation step of the most acidic hydroxyl group at C-2 and controlled by limiting the amount of NaH consumed. The higher acidity of C-2 hydroxyl group was partly attributed to the hydrogen bonding between C-2 hydroxyl group and C-3 hydroxyl group. The relative reactivities toward methylation of the three different alkoxides produced by excess NaH were reported.[95]

Recently, greater preference for the C-3 substitution over C-2 substitution was observed in the electrophilic

substitution of β-cyclodextrin by carbenes formed from aromatic diazo compounds upon pyrolysis.[96]

In this dissertation work, regioselective reactions of 1-(1-napthyl)ethyl isocyante (**NEIC**) with **β-CD** were studied with and without NaH activation of **β-CD** in N,N-dimethyl-formamide (**DMF**) and pyridine. All six possible monosubstituted **CD** products were separated and characterized by ^{1}H and ^{13}C NMR. Primary substitution product predominates when the reaction was carried out under reflux condition in pyridine without NaH activation. The C-2 substitution product predominates when the reaction was carried out in DMF. Conversion of **2-O-NEC-β-CD** to **6-O-NEC-β-CD** was observed with NaH activation.

2.2 Experimental

2.2.1 Chemicals

β-CD was obtained from Pfanstiehl Laboratories, Inc., (Waukegan, IL). (R)- or (S)-1-(1-naphthyl)ethyl isocyanate (**NEIC**), anhydrous pyridine, **DMF**, sodium hydride (NaH) and deuterated solvents were obtained from Aldrich (Milwaukee, WI). Dimethyloctadecylchlorosilane was obtained from Huls America Inc., (Bristol, PA).

2.2.2 Chromatographic conditions

Product distribution was monitored using a **Shimadzu LC-600** liquid chromatographic system, **SPD-6A UV** detector (282 nm) and a **Rheodyne model 7161** injection valve with a 100 μl sample loop for the **HPLC** separation. Monosubstituted naphthylethylcarbamoylated **β-CD (NEC-β-CDs)** were successfully separated on an **Axxiom ODS 5** micron silica column (4.8 mm x 150 mm). The mobile phase consisted of 75 : 12.5 : 12.5 or 70 : 15 : 15 volume percent of water, methanol and acetonitrile and was degassed before use. A flow rate of 2, 1.5 or 1 ml/min at 18 °C was employed.

2.2.3 NMR and Mass Spectrometry

NMR measurements of all compounds except **SC-3** were carried out in deuterated methanol at ambient temperature (297 K) on a **GE NMR** spectrometer at 500.11 MHz for ^{1}H and 125.76 MHz for ^{13}C. Because of poor solubility of **SC-3** in methanol, 0.5 ml of deuterated dimethylsulfoxide was added to the 0.5 ml of CD_3OD. ^{1}H and ^{13}C chemical shifts were determined relative to the residual methanol peak (3.30 ppm for ^{1}H; 49.0 ppm for ^{13}C). Mass spectra were determined in the positive ion FAB mode.

2.2.4 Elemental analysis

Elemental analyses of monosubstituted products were performed by Galbraith Laboratories, Inc., (Knoxville, TN).

2.2.5 Synthesis of C-18 functionalized silica

C-18 packing material was prepared as follow; silica gel (36.1 g) dried in vacuum was added to 200 ml of anhydrous toluene. Residual water was removed through a Dean Stark trap. Silylating agent (dimethyloctadecyl-chlorosilane, 14.4 g) and 1 ml of pyridine were added to the mixture. After 7 h of refluxing the mixture, the reaction product was filtered through the fritted glass and washed with toluene, methanol, water, methanol, toluene and finally methanol. The product was air dried over night and weighed 44.4 g. The air dried C-18 functionalized silica gel was dried 4 h in vacuum and the final weight was 43.7 g. Therefore, % carbon loading calculated was approximately 13%.

2.2.6 Synthesis of 2-O-((S)-1-(1-naphthyl)ethylcarbamoyl)-β-CD (SC-2)

Anhydrous pyridine (95 ml) was added to 2.30 g (2 mmol) of β-CD dried in vacuum at 110 °C overnight. After

removal of residual water using a **Dean Stark trap**, sodium hydride (0.05 g, 2 mmol) was added to the mixture. The mixture was stirred for 4 h at room temperature under vacuum. After 4 h stirring of the mixture, **S-NEIC** (0.40 g, 2 mmol), dissolved in 5 ml of pyridine, was added to the reaction mixture and the mixture was continuously stirred at room temperature for 4 h. After stirring, the reaction mixture was neutralized by adding several drops of concentrated hydrochloric acid. Chloroform (200 ml) and acetone (600 ml) were added to the mixture. The resultant precipitate was obtained by filtration and subjected to column chromatography (SiO_2, 10:1 -> 2:1 chloroform-methanol, stepwise) (0.93 g, 34% yield).

^{1}H NMR data: δ 8.12 (1H, d, $J_{8',7'}$ 8.5 Hz, H-8'), 7.86 (1H, d, $J_{5',6'}$ 8.0 Hz, H-5'), 7.75 (1H, d, $J_{4',3'}$ 8.5 Hz, H-4'), 7.69 (1H, d, $J_{2',3'}$ 7.0 Hz, H-2'), 7.54 (1H, bt, $J_{7',6'}$, $J_{7',8'}$ 7.5 Hz, H-7'), 7.49-7.44 (2H, m, H-6',3'), 5.58 (1H, q, $J_{11',12'}$ 7.0 Hz, H-11'), 5.01 (1H, bs, H-1), 4.60 (1H, dd, $J_{2,1}$ 3.1 Hz, $J_{2,3}$ 10.8 Hz, H-2), 4.10 (1H, t, $J_{2,3}$, $J_{3,4}$ 9.5 Hz), 1.57 (3H, d, $J_{12',11'}$ 6.5 Hz, H-12'); ^{13}C, δ 157.1, 141.1, 135.4, 132.0, 129.9, 128.6, 127.2, 126.6, 126.6, 124.0, 123.4, 103.9, 103.9, 103.8, 103.6, 101.3, 83.3, 83.1, 83.1, 83.0, 82.9, 75.3, 74.8, 74.2, 74.2, 74.1, 74.0, 73.9, 73.7, 73.4, 71.9, 62.0, 61.8, 61.7, 48.3, 22.5; FABMS (m/z) 1332 ($M + H^+$), 1354 ($M + Na^+$), 1370 ($M + K^+$).

Anal. Calcd for $C_{55}H_{81}O_{36}N \cdot 3H_2O$: C, 47.65; H, 6.33; N, 1.01. Found: C, 47.79; H, 6.64; N, 2.40.

2.2.7 Synthesis of 3-O-((S)-1-(1-naphthyl)ethylcarbamoyl)-β-CD (SC-3)

S-NEIC (0.20 g; 1.0 mmol) was added to a solution of 1.60 g (1.4 mmol) of dried **β-CD** in 100 ml of anhydrous **DMF** and the mixture was refluxed under N_2. After 3 h, the reaction mixture was treated as described for the preparation of **SC-2**. The resultant precipitate was extracted twice with 200 ml of methanol. The methanol extract was concentrated and the residue was dissolved in 70 : 15 : 15 volume percent of water : methanol : acetonitrile. An aliquot of this solution was subjected to C-18 semipreparative HPLC column (**Axxiom ODS** 5 micron, 10 mm x 250 mm) to get a pure product (50 mg, 3% yield).

^{1}H NMR data: δ 8.22 (1H, d, $J_{8',7'}$ 8.5 Hz, H-8'), 7.97 (1H, d, $J_{5',6'}$ 7.0 Hz, H-5'), 7.85 (1H, d, $J_{4',3'}$ 8.5 Hz, H-4'), 7.71 (1H, d, $J_{2',3'}$ 6.5 Hz, H-2'), 7.64-7.53 (3H, m, H-7',6',3'), 5.56 (1H, q, $J_{11',12'}$ 6.5 Hz, H-11'), 5.09 (1H, t, $J_{3,2'}$ $J_{3,4}$ 9.3 Hz, H-3), 1.59 (3H, d, $J_{12',11'}$ 7.0 Hz, H-12'); ^{13}C, δ 158.0, 141.5, 135.3, 131.9, 130.1, 128.6, 127.3, 126.7, 124.2, 123.7, 103.9, 103.7, 103.3, 103.0, 83.3, 83.0,

82.8, 82.8, 82.5, 79.3, 76.6, 74.8, 74.7, 74.5, 74.3, 74.2, 74.1, 73.7, 73.6, 73.6, 73.5, 61.8, 61.7, 61.6, 48.4, 22.6; FABMS (m/z) 1332 ($M + H^+$), 1338 ($M + Li^+$) 1354 ($M + Na^+$), 1370 ($M + K^+$).

Anal. Calcd for $C_{55}H_{81}O_{36}N \cdot 5H_2O$: C, 46.45; H, 6.45; N, 0.98. Found: C, 46.15; H, 6.40; N, 0.99.

2.2.8 Synthesis of 6-O-((S)-1-(1-naphthyl)ethylcarbamoyl)-β-CD (SC-6)

The same procedure as described for the preparation of SC-2 was used except DMF was used instead of pyridine. After 20 days of stirring the reaction mixture was treated as described for the preparation of SC-2 to get a pure product (0.44 g, 16%). The low yield compared to synthesis of SC-2 resulted from nonoptimal chromatographic conditions.

^{1}H NMR data: δ 8.16 (1H, d, $J_{8',7'}$ 8.5 Hz, H-8'), 7.90 (1H, d, $J_{5',6'}$ 8.0 Hz, H-5'), 7.80 (1H, d, $J_{4',3'}$ 8.0 Hz, H-4'), 7.58-7.47 (4H, m, H-2',7',6',3'), 5.60 (1H, q, $J_{11',12'}$ 7.0 Hz, H-11'), 4.41 (1H, d, J_{gem} 11.0 Hz, H-6a), 4.30 (1H, dd, J_{gem} 11.5 Hz, $J_{6b,5}$ 5.3 Hz, H-6b), 1.61 (3H, d, $J_{12',11'}$ 7.0 Hz, H-12'); ^{13}C, δ 158.0, 141.1, 135.4, 132.1, 129.9, 128.7, 127.2, 126.6, 126.5, 124.1, 123.3, 104.1, 103.9, 103.7, 83.5, 83.4, 82.9, 74.8, 74.2, 73.9, 73.7, 71.5, 65.0, 62.1,

61.8, 48.0, 22.3; FABMS (m/z) 1332 ($M + H^+$), 1354 ($M + Na^+$), 1370 ($M + K^+$).

Anal. Calcd for $C_{55}H_{81}O_{36}N \cdot 2H_2O$: C, 48.28; H, 6.26; N, 1.02. Found: C, 48.59; H, 6.27; N, 1.36.

2.2.9 Synthesis of 2-O-((R)-1-(1-naphthyl)ethylcarbamoyl)-β-CD (RC-2)

Anhydrous pyridine (95 ml) was added to 5.76 g (5 mmol) of **β-CD**, which had been dried in vacuum at 110 °C over night. Sodium hydride (0.12 g, 5 mmol) was added and the mixture was stirred for 4 h at room temperature. **R-NEIC** (1 g, 5 mmol), dissolved in 5 ml of pyridine, was added to the reaction mixture and stirring was continued at room temperature for 4 h. The reaction mixture was then neutralized by adding several drops of concentrated hydrochloric acid. The mixture was partitioned between 400 ml of water and 400 ml of chloroform. The aqueous layer was separated and concentrated. Addition of acetone yielded a powder which was subjected to column chromatography (SiO_2, 10:1 -> 2:1 chloroform:methanol, stepwise) to obtain a pure product (1.09 g, 18% yield).

^{1}H NMR data: δ 8.12 (1H, d, $J_{8',7'}$, 8.3 Hz, H-8'), 7.87 (1H, d, $J_{5',6'}$, 8.3 Hz, H-5'), 7.77 (1H, d, $J_{4',3'}$, 8.3 Hz, H-4'), 7.59

(1H, d, $J_{2',3'}$ 7.2 Hz, H-2'), 7.52 (1H, bt, $J_{7',6'}$, $J_{7',8'}$ 7.3 Hz, H-7'), 7.49-7.43 (2H, m, H-6',3'), 5.56 (1H, q, $J_{11',12'}$ 6.7 Hz, H-11'), 5.15 (1H, d, $J_{1,2}$ 3.5 Hz, H-1), 4.54 (1H, dd, $J_{2,1}$ 3.5 Hz, $J_{2,3}$ 10.2 Hz, H-2), 4.05 (1H, bt, $J_{2,3}$, $J_{3,4}$ 9.5 Hz), 1.59 (3H, d, $J_{12',11'}$ 7.2 Hz, H-12'); ^{13}C, δ 157.2, 140.8, 135.4, 132.1, 129.9, 128.8, 127.2, 126.6, 126.5, 124.2, 123.4, 103.9, 103.6, 101.6, 83.5, 83.1, 83.0, 83.0, 82.9, 75.3, 74.8, 74.5, 74.3, 74.2, 73.9, 73.7, 73.5, 73.3, 71.7, 62.2, 62.1, 61.8, 61.8, 61.6, 48.2, 22.3; FABMS (m/z) 1354 ($M + Na^+$), 1370 ($M + K^+$).

Anal. Calcd for $C_{55}H_{81}O_{36}N \cdot 4H_2O$: C, 47.04; H, 6.39; N, 1.00. Found: C, 46.83; H, 6.19; N, 1.49.

2.2.10 Synthesis of 3-O-((R)-1-(1-naphthyl)ethylcarbamoyl)-β-CD (RC-3)

The same procedure as described for the preparation of SC-3 was used except **R-NEIC** was substituted for **S-NEIC**. Overall 50 mg of a pure product (3% yield) was obtained.

^1H NMR data: δ 8.16 (1H, d, $J_{8',7'}$ 9.0 Hz, H-8'), 7.86 (1H, d, $J_{5',6'}$ 8.5 Hz, H-5'), 7.75 (1H, d, $J_{4',3'}$ 8.0 Hz, H-4'), 7.59 (1H, d, $J_{2',3'}$ 7.0 Hz, H-2'), 7.55 (1H, t, $J_{7',8'}$, $J_{7',6'}$ 7.5 Hz, H-7') 7.47 (1H, t, $J_{3',2'}$, $J_{3',4'}$ 7.5 Hz, H-3'), 7.44 (1H, t, $J_{6',7'}$, $J_{6',5'}$, 7.5 Hz, H-6'), 5.59 (1H, q, $J_{11',12'}$ 6.5 Hz, H-

11′), 5.09 (1H, t, $J_{3,2}$, $J_{3,4}$ 9.5 Hz, H-3), 1.60 (3H, d, $J_{12',11'}$ 7.0 Hz, H-12′); ^{13}C, δ 158.6, 141.4, 135.4, 132.1, 129.8, 128.6, 127.2, 126.6, 124.2, 123.3, 103.9, 103.8, 103.5, 103.3, 83.1, 83.1, 83.0, 82.9, 82.8, 82.3, 80.1, 77.0, 74.8, 74.8, 74.7, 74.5, 74.3, 74.2, 73.7, 73.5, 73.0, 62.0, 61.9, 61.8, 61.7, 48.4, 22.4; FABMS (m/z) 1332 ($M + H^+$), 1354 ($M + Na^+$), 1370 ($M + K^+$).

Anal. Calcd for $C_{55}H_{81}O_{36}N \cdot 4H_2O$: C, 47.04; H, 6.39; N, 1.00. Found: C, 47.25; H, 6.29; N, 1.18.

2.2.11 Synthesis of 6-O-((R)-1-(1-naphthyl)ethylcarbamoyl)-β-CD (RC-6)

The same procedure as described for the preparation of **SC-6** was used except **R-NEIC** was used instead of **S-NEIC** (0.445 g, 18% yield).

^1H NMR data: δ 8.15 (1H, d, $J_{8',7'}$ 8.5 Hz, H-8′), 7.87 (1H, d, $J_{5',6'}$ 8.0 Hz, H-5′), 7.77 (1H, d, $J_{4',3'}$ 8.5 Hz, H-4′), 7.55-7.52 (2H, m, H-2′,7′), 7.48 (1H, t, $J_{3',2'}$, $J_{3',4'}$ 7.5 Hz, H-3′) 7.45 (1H, t, $J_{6,7}$, $J_{6,5}$ 7.5 Hz, H-6) 5.55 (1H, q, $J_{11',12'}$ 7.0 Hz, H-11′), 4.37 (1H, d, J_{gem} 12.0 Hz, H-6a), 4.23 (1H, dd, J_{gem} 11.8 Hz, $J_{6b,5}$ 5.5 Hz, H-6b), 1.57 (3H, d, $J_{12',11'}$ 7.0 Hz, H-12′); ^{13}C, δ 158.1, 141.0, 135.5, 132.2, 129.9, 128.8,

127.2, 126.6, 126.5, 124.3, 123.6, 104.1, 103.9, 103.7, 83.5, 83.3, 83.0, 82.9, 74.8, 74.3, 74.0, 74.0, 73.9, 73.7, 73.6, 71.4, 65.2, 62.2, 61.9, 61.8, 61.7, 48.2, 22.2; FABMS (m/z) 1332 ($M + H^+$), 1354 ($M + Na^+$), 1370 ($M + K^+$).

Anal. Calcd for $C_{55}H_{81}O_{36}N \cdot 3H_2O$: C, 47.65; H, 6.33; N, 1.01. Found: C, 47.83; H, 6.47; N, 0.99.

2.2.12 Role of solvent

S-NEIC (0.20 g; 1.0 mmol) was added to a solution of 1.60 g (1.4 mmol) of dried **CD** in 100 ml of anhydrous pyridine (**Exp. 1**) or **DMF** (**Exp. 2**) and subsequently refluxed under N_2. An aliquot (0.50 ml) of the reaction mixture was taken at every 30 minutes, quenched by dissolving 100 ml of 50 : 50 volume percent mixture of methanol and water and analyzed by **HPLC**.

2.2.13 Role of base

Anhydrous **DMF** (95 ml) (**Exp. 3**) or pyridine (95 ml) (**Exp. 4**) was added to 2.30 g (2 mmol) of dried **CD** and 0.046 g (2 mmol) of sodium hydride. The mixture was stirred 4 h at room temperature under vacuum. After 4 h, **S-NEIC** (0.40 g, 2 mmol), dissolved in 5 ml of **DMF** or pyridine, was added to the reaction mixture. The mixture was stirred

continuously at room temperature. An aliquot (0.5 ml) taken at every 30 minutes was quenched and analyzed as mentioned previously. To study the role of NaOH as a base (**Exp. 5**), **SC-2** (100 mg) and NaOH (70 mg) were added to 100 ml of anhydrous DMF and the mixture was stirred continuously at room temperature. Aliquots of the reaction mixture were taken and analyzed by **HPLC**.

2.3 Results

2.3.1 Identification of the regioisomers

(S)-(+)- or (R)-(-)-1-(1-naphthyl)ethyl isocyanate (**S-NEIC** or **R-NEIC**) was reacted with **β-CD** and all six possible monosubstituted products as well as minor amounts of disubstituted products were isolated by HPLC. HPLC chromatograms of the separation of the monosubstituted **NEC-β-CDs** are shown in Figure 2.1. The structure of **CDs** and the numbering system of protons and carbon atoms of the products are in Figure 2.2.

^{1}H NMR spectra of six monosubstituted **NEC-β-CDs** were obtained in CD_3OD and are shown in Figures 2.3 and 2.4. The detailed NMR peaks assignments are given in the section describing the syntheses of individual isomers. The ^{1}H

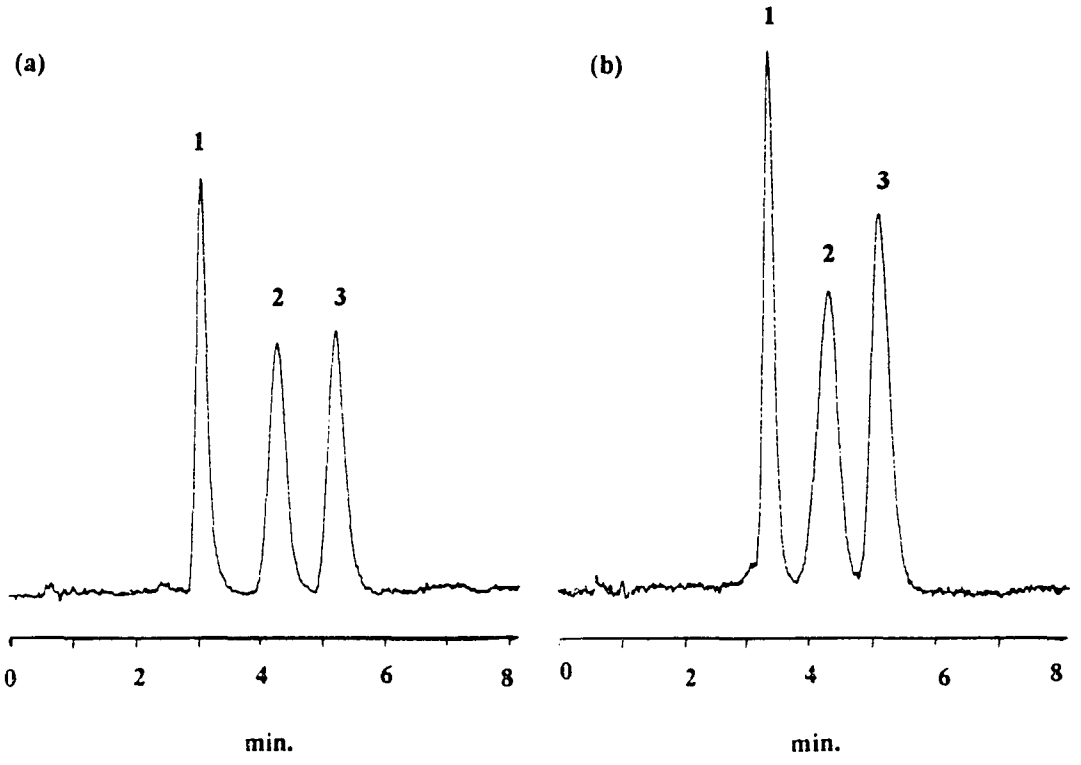

Figure 2.1 HPLC chromatograms of the separation of monosubstituted NEC-β-CDs. (a) 1:SC-3, 2:SC-2, and 3:SC-6 (b) 1:RC-3, 2:RC-2, and 3:RC-6.

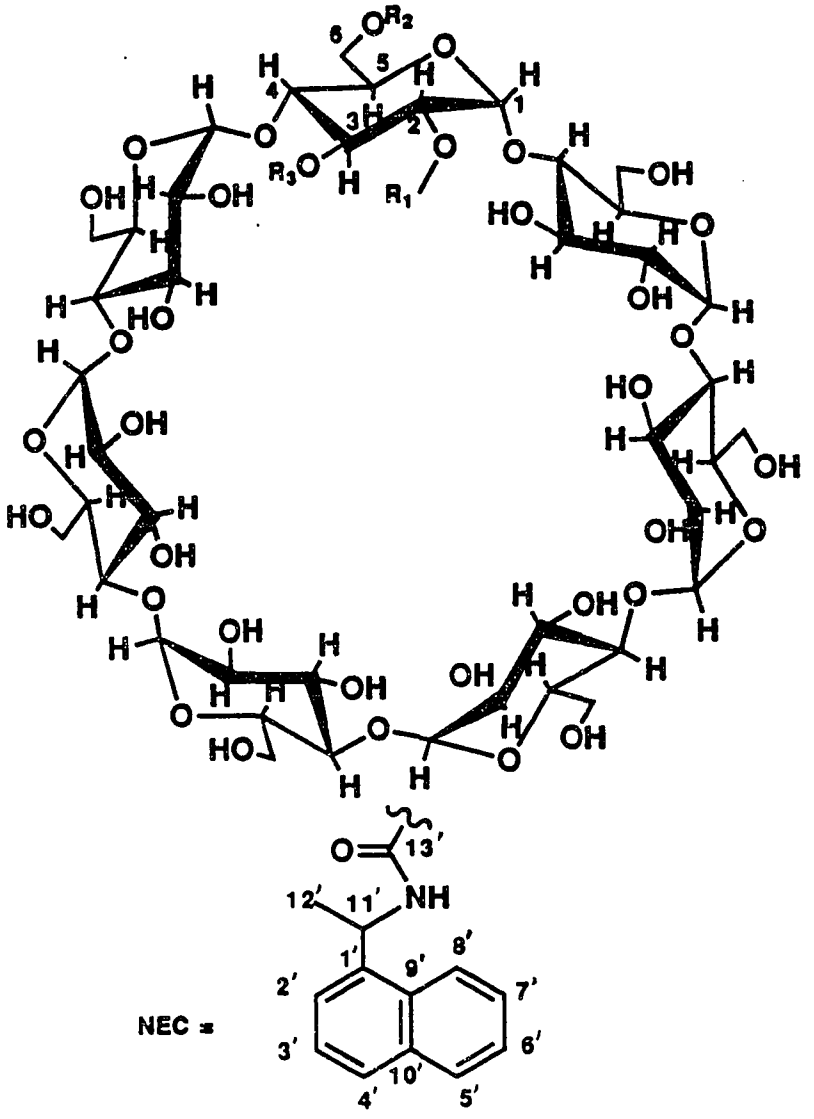

Compound	R_1	R_2	R_3	Configuration of C-11
SC-2	NEC	H	H	S
SC-3	H	H	NEC	S
SC-6	H	NEC	H	S
RC-2	NEC	H	H	R
RC-3	H	H	NEC	R
RC-6	H	NEC	H	R

Figure 2.2 Structure of NEC-β-CDs and the numbering system of protons and carbon atoms of the products.

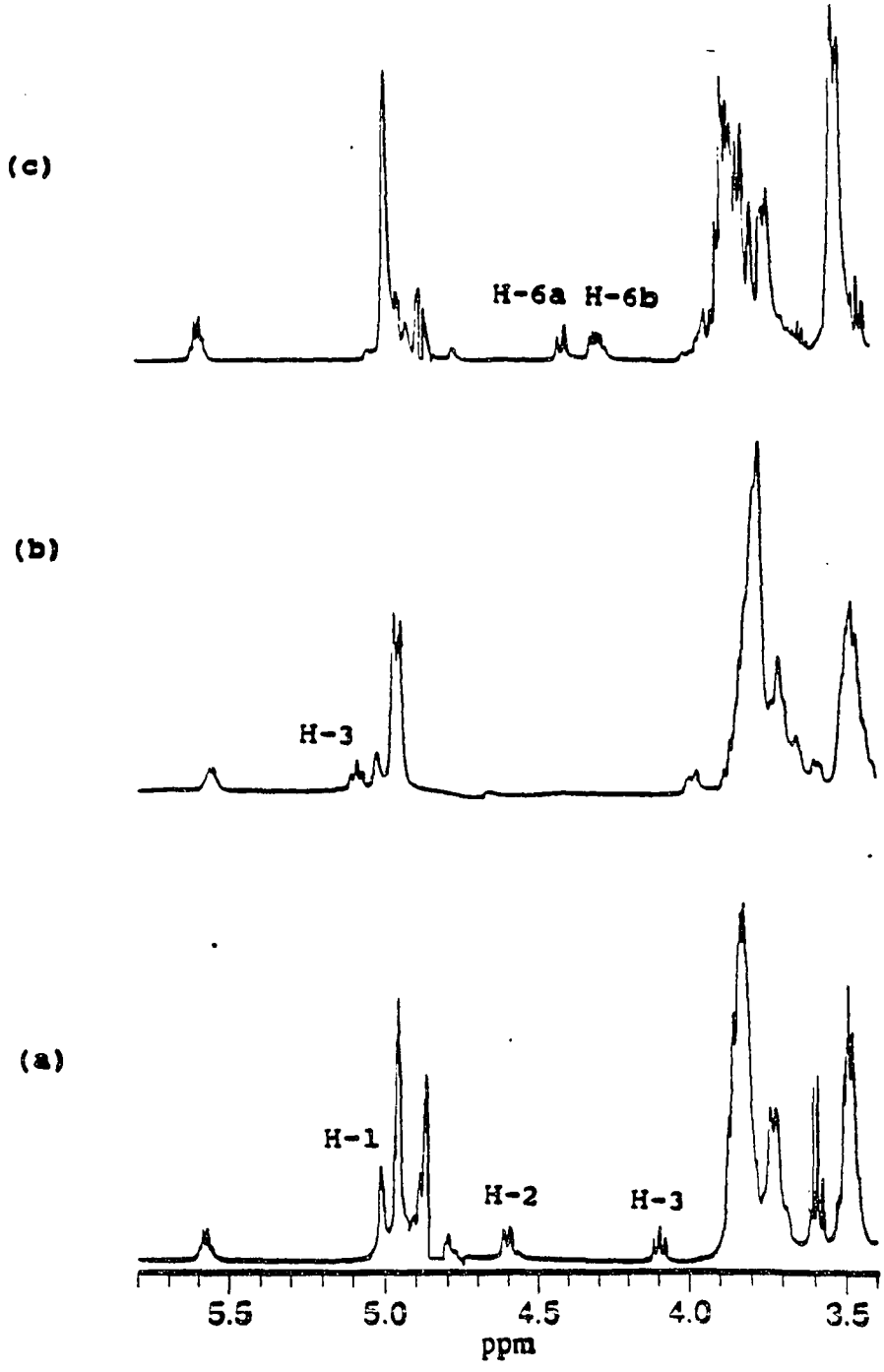

Figure 2.3 Partial 500 MHz NMR ^1H spectra of SC-2(a), SC-3(b), and SC-6(c) in CD_3OD.

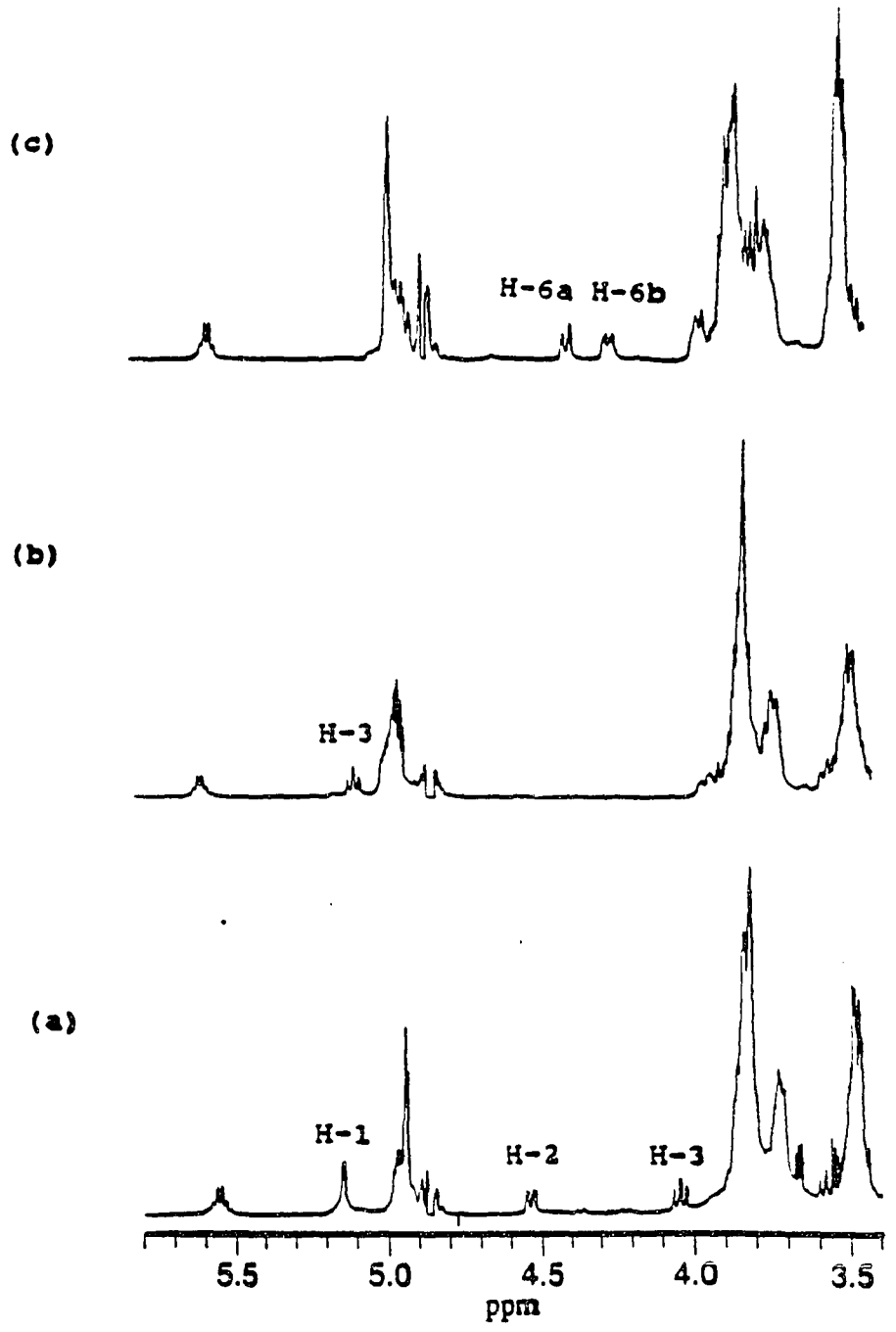

Figure 2.4 Partial 500 MHz NMR ^1H spectra of RC-2(a), RC-3(b), and RC-6(c) in CD_3OD.

chemical shifts of readily identified protons are summarized in Table 2.1. A large downfield shift was observed for the protons α to the site of carbamoylation. This can be attributed to the anisotropic deshielding of the carbonyl group of the carbamate linkage. This shift of adjacent proton resonances away from the main carbohydrate envelope allowed for unambiguous determination of the substitution site. For instance, as shown in the Figure 2.4(a) in the case of **SC-2**, the resonance at δ = 4.60 is a doublet of a doublet with an observed splitting of 3.1 and 10.8 Hz, as a result of coupling to the anomeric and H-3 protons of the derivatized glucose unit of **SC-2**, respectively. Therefore, this peak is unambiguously assigned to H-2 attached to the C-2 derivatized site. The chemical shift of this proton is almost 1.10 ppm downfield compared to those of the underivatized glucose units. Through a ^{1}**H-**^{1}**H COSY** spectrum, the resonances at δ = 5.01 and at δ = 4.10 are assigned to H-1 and H-3 of the derivatized glucose unit, respectively.

Substitution at the 3-O site causes a downfield shift of the C-3 proton of **SC-3** which appears as a triplet at δ = 5.09. The same deshielding phenomena are observed for the H-6 protons of derivatized glucose units of **SC-6**. Multiplets at δ = 4.41 and δ = 4.30 show the typical AB pattern of the H-6 protons. In addition, H-6b couples to H-5 at δ = 3.93, which shows a small β downfield shift.

Table 2.1 The ^1H chemical shifts of readily identified protons of the derivatized glucose unit of monosubstituted NEC-β-CDs in deuterated methanol.

^1H	SC-2	SC-3	SC-6	RC-2	RC-3	RC-6
H-1	5.01			5.15		
H-2	4.60			4.53		
H-3	4.10	5.09		4.05	5.09	
H-6a			4.41			4.37
H-6b			4.30			4.23

Analogously, peak assignments for **RC-2** to **RC-6** could be done as in the case of their epimers, **SC-2** to **SC-6**, respectively.

2.3.2 Role of solvent

Product distributions obtained under reflux conditions in either pyridine (**Exp. 1**) or **DMF** (**Exp. 2**) are listed in Table 2.2. When pyridine was used as a solvent, substitution occurred predominantly at the primary site (ca. 85 %). The combined product yield and the distribution of products was fairly independent of reaction time as shown in Figure 2.5. However, in **DMF**, initial substitution occurred predominantly on the C-2 site (ca. 83 % at 0.5 h reaction time). In addition, the combined yield decreased and the product distribution changed with reaction time as shown in Figure 2.6.

2.3.3 Role of base

Product distributions after activation of the C-2 hydroxyl with stoichiometric amounts of NaH in **DMF** (**Exp. 3**) or in pyridine (**Exp. 4**) with subsequent **S-NEIC** addition are listed in Table 2.2. After 4 or 5 h reaction, there seemed to be no significant increase in the intensity of **SC-2** in both reactions. After stirring the reaction mixture 5 h, the relative percentage of **SC-2** was 88 % and 87 % in Exp. 3

Table 2.2 Distribution of regioisomers under various reaction conditions.

Experiment No.	Solvent used	Reaction condition	Site of Substitution	Relative Percent
1.	pyridine	4 h	2-O	11.3
		Reflux	6-O	84.9
			3-O	4.8
2.	DMF	0.5 h	2-O	83
		Reflux	6-O	< 1
			3-O	16
		4 h	2-O	56.6
		Reflux	6-O	9.6
			3-O	33.8
3.	DMF	5 h	2-O	88.2
		Room Temp.	6-O	5.3
		with NaH	3-O	6.5
		307 h	2-O	9.7
			6-O	86.7
			3-O	3.6
4.	pyridine	5 h	2-O	86.9
		Room Temp.	6-O	6.5
		with NaH	3-O	6.5
		162 h	2-O	46.5
			6-O	37.0
			3-O	15.5
5.	DMF	0 h	2-O	96.8
		Room Temp.	6-O	< 1
		with NaOH	3-O	3.2
		1 h	2-O	52.7
			6-O	34.9
			3-O	12.4
		3 h	2-O	42.6
			6-O	46.0
			3-O	11.4
		7 h	2-O	< 1
			6-O	> 98
			3-O	< 1

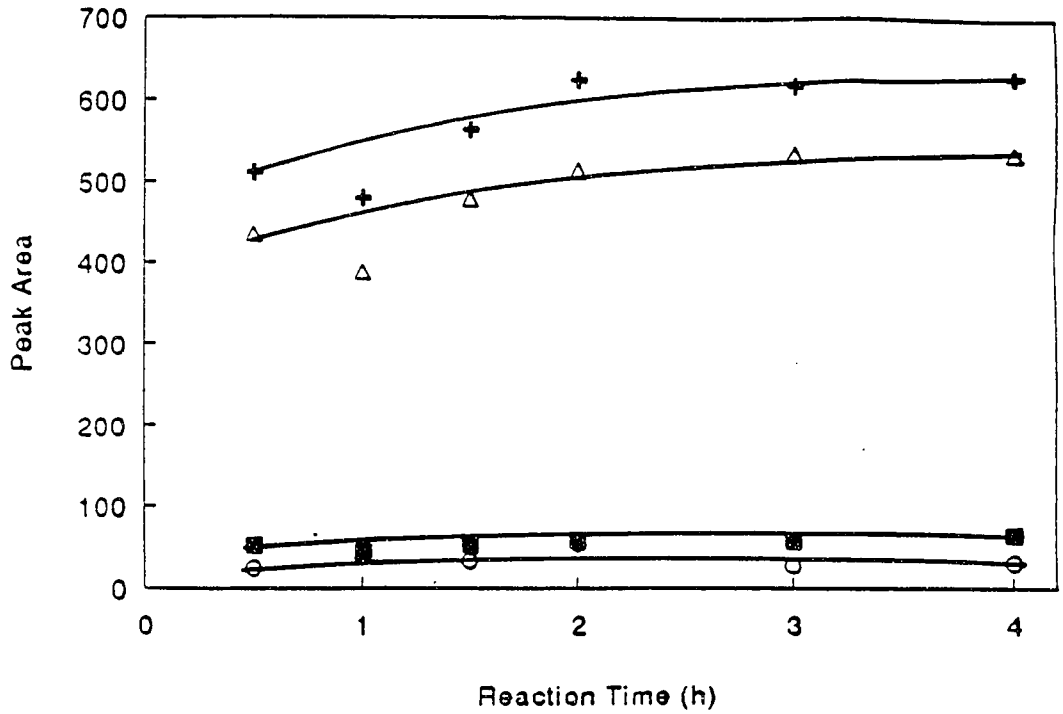

Figure 2.5 Product distribution for the reaction between S-NEIC and β-CD in pyridine (reflux). ▪ SC-2, o SC-3, Δ SC-6, and + all three monosubstitution products.

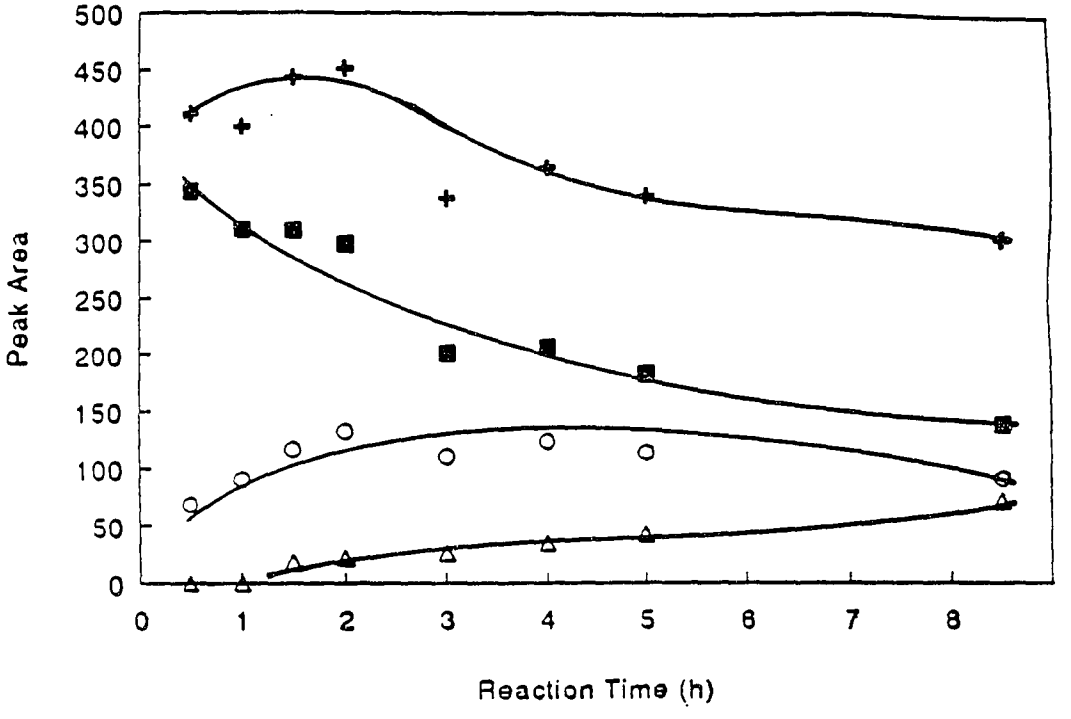

Figure 2.6 Product distribution for the reaction between S-NEIC and β-CD in DMF (reflux). ▪ SC-2, o SC-3, Δ SC-6, and + all three monosubstitution products.

and Exp. 4, respectively. Further stirring of the reaction mixture at room temperature resulted in loss of **SC-2** with concomitant increase in **SC-6**, as shown in Figures 2.7 and 2.8 in the **DMF** and pyridine cases, respectively. After stirring the mixture for 307 h, the relative percentage of **SC-2** and **SC-6** in **DMF** was 10 % and 87 %, respectively. In addition, the combined intensity of all three products was fairly constant over the reaction period.

When pure **SC-2** was treated with NaOH in **DMF**, almost all of **SC-2** converted to **SC-6** (see **Exp. 5** in Table 2.2).

2.4 Discussion

2.4.1 NMR

The large downfield shifts of protons at the substitution site in the carbamoylation reaction made the identification of the point of derivatization possible using proton NMR. In the case of primary substitution, the extent of deshielding of C-6 protons is less than those of H-2 and H-3 protons suggesting less conformational rigidity for the primary sites and the deshielding effect of carbonyl group is minimized. Of the three, H-3 shows the largest deshielding effect (ca. 1.30 ppm), which suggests that

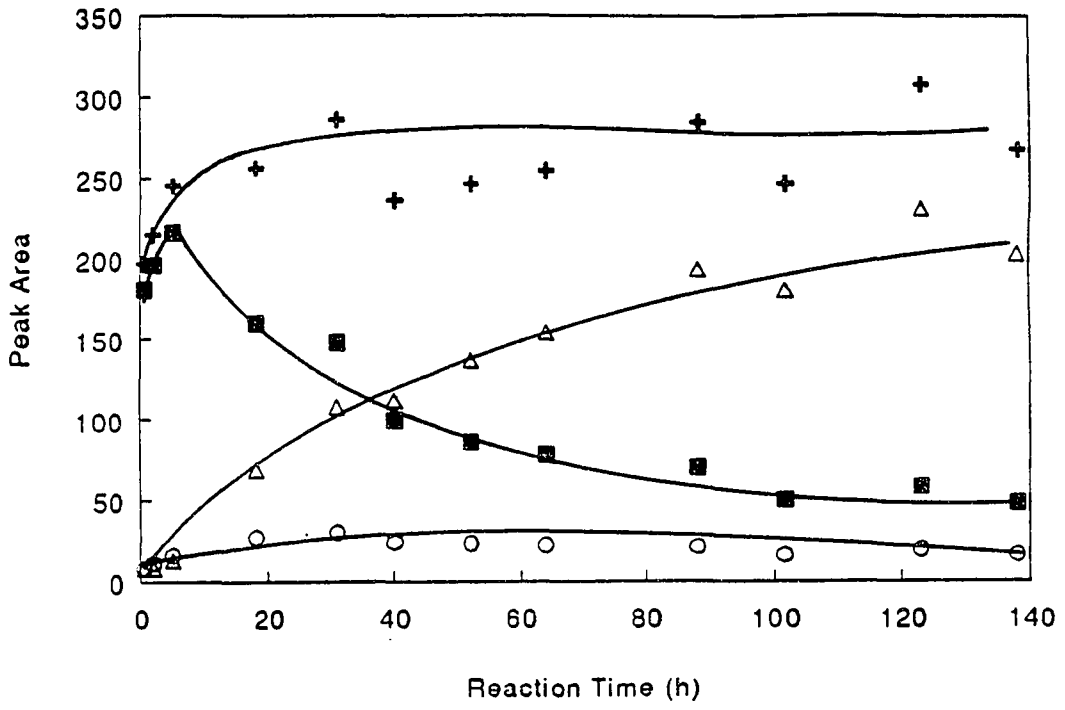

Figure 2.7 Product distribution for the reaction between S-NEIC and β-CD in DMF (with NaH activation at room temperature). ▪ SC-2, ○ SC-3, Δ SC-6, and + all three monosubstitution products.

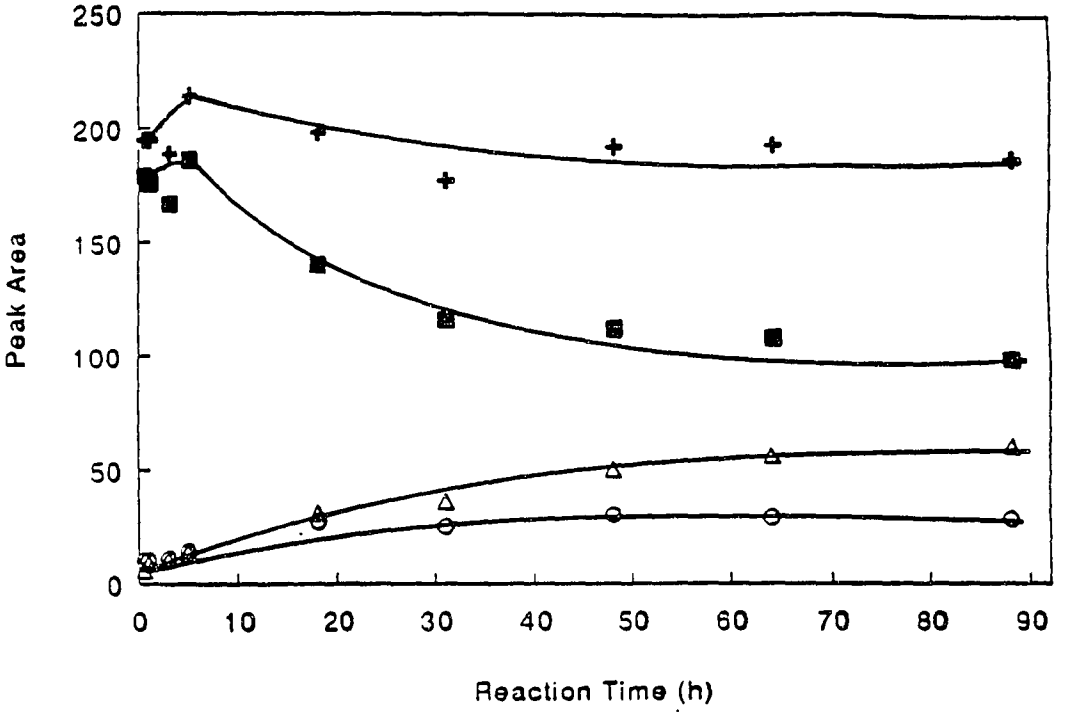

Figure 2.8 Product distribution for the reaction between S-NEIC and β-CD in pyridine (with NaH activation at room temperature). ▪ SC-2, ○ SC-3, Δ SC-6, and + all three monosubstitution products. the

motion of the **NEC** group is more restricted in this molecule. Not much difference in the extent of deshielding of the α protons was observed between the R and S epimers. However, a large difference (0.14 ppm) in the deshielding of the anomeric proton in the case of the C-2 substituted epimers (**SC-2** and **RC-2**) was observed (see Table 2.1). This suggests that the configuration of the substituent affects the geometry around the anomeric proton of the derivatized glucose unit even though the magnitude of the inductive effect of the carbamoyl group upon β protons is same. The large downfield shift of protons in the derivatized residue from the broad envelope from the protons of the non-substituted glucose units of the **CD** should facilitate the study of the degrees and sites of substitution of multiply substituted products which may be more representative of the chiral selector of the **NEC-CD CSPs**.

2.4.2 Synthesis

Several different reaction conditions were employed to synthesize various monosubstituted **NEC-β-CDs**. The reaction schemes used in this work were shown in Figure 2.9. Selective derivatization of the C-2 hydroxyl group of β-**CD** was achieved either employing equimolar NaH to activate C-2 hydroxyl of β-**CD** followed by addition of **NEIC** in pyridine or DMF, or direct reflux of the mixture of β-**CD** and **NEIC** in

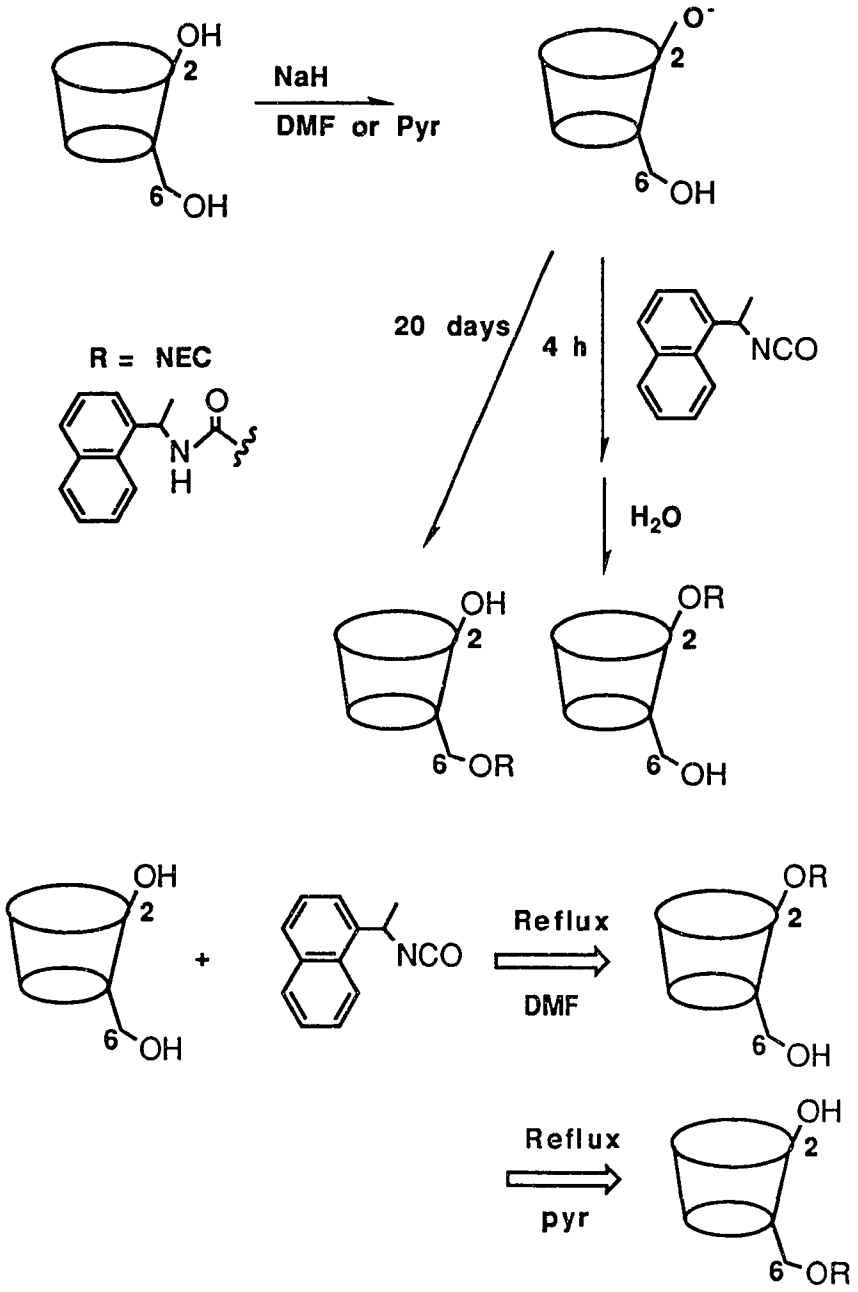

Figure 2.9 Reaction schemes for the synthesis of monosubstituted NEC-β-CDs.

DMF. In pyridine, under reflux condition, the regio-selectivity of the isocyanate-alcohol reaction seems to be controlled by steric factors (e.g., primary more reactive than secondary alcohols) and may explain why the C-6 substitution product predominates. Similar results were reported in the synthesis of monotosylated **CDs**.[97] Reaction of **CDs** with p-toluenesulfonyl chloride in pyridine at room temperature resulted in attachment of a tosyl group at the primary site. Also, in pyridine, there seems to be no significant increase in the concentration of products after 2 h reaction time.

In contrast, the predominant product is the C-2 substituted isomer in **DMF**. The decline in overall product yield compared to pyridine may be attributed to thermal degradation due to the high temperature of **DMF** reflux. The extent of decomposition of the C-2 substituted product, under **DMF** reflux, seems to be higher than that of the primary product.

Product distribution changed with reaction time when a stoichiometric amount of NaH was used to activate hydroxyl groups of **CD** either in **DMF** or pyridine. Despite the fact that the C-2 hydroxyl group is activated and therefore the initial site of substitution, substitution on the primary site yields a product which is more thermodynamically

stable. The proposed mechanism for the conversion of the C-2 substituted isomer to the C-6 substituted is shown in Figure 2.10. On reaction with NaH at room temperature, CD loses a proton of the C-2 hydroxyl group to form an alkoxide which reacts rapidly with an isocyanate resulting in an intermediate I. This intermediate is in equilibrium with intermediate II through proton transfer from a primary hydroxyl group. The resulting primary alkoxide nucleophile may then attact the carbonyl carbon to form an intermediate III. In the presence of excess base, both inter- and intramolecular rearrangements may be possible. Since NaH activation was performed at ambient temperature, the higher rate of conversion in **DMF** over that in pyridine is probably due to the difference in polarity of the solvents with the more polar **DMF** perhaps providing better solvation of intermediates thereby hastening the reaction.

The proposed role of the base in the conversion of secondary to primary is supported by the results obtained upon addition of NaOH to the solution of **SC-2** in **DMF** at ambient temperature.

Modification of the secondary hydroxyl side of **CD**s is thought to be more important for chiral distinction than the primary site because the more open rigid secondary side can more easily accommodate chiral guest molecules. Pyridine

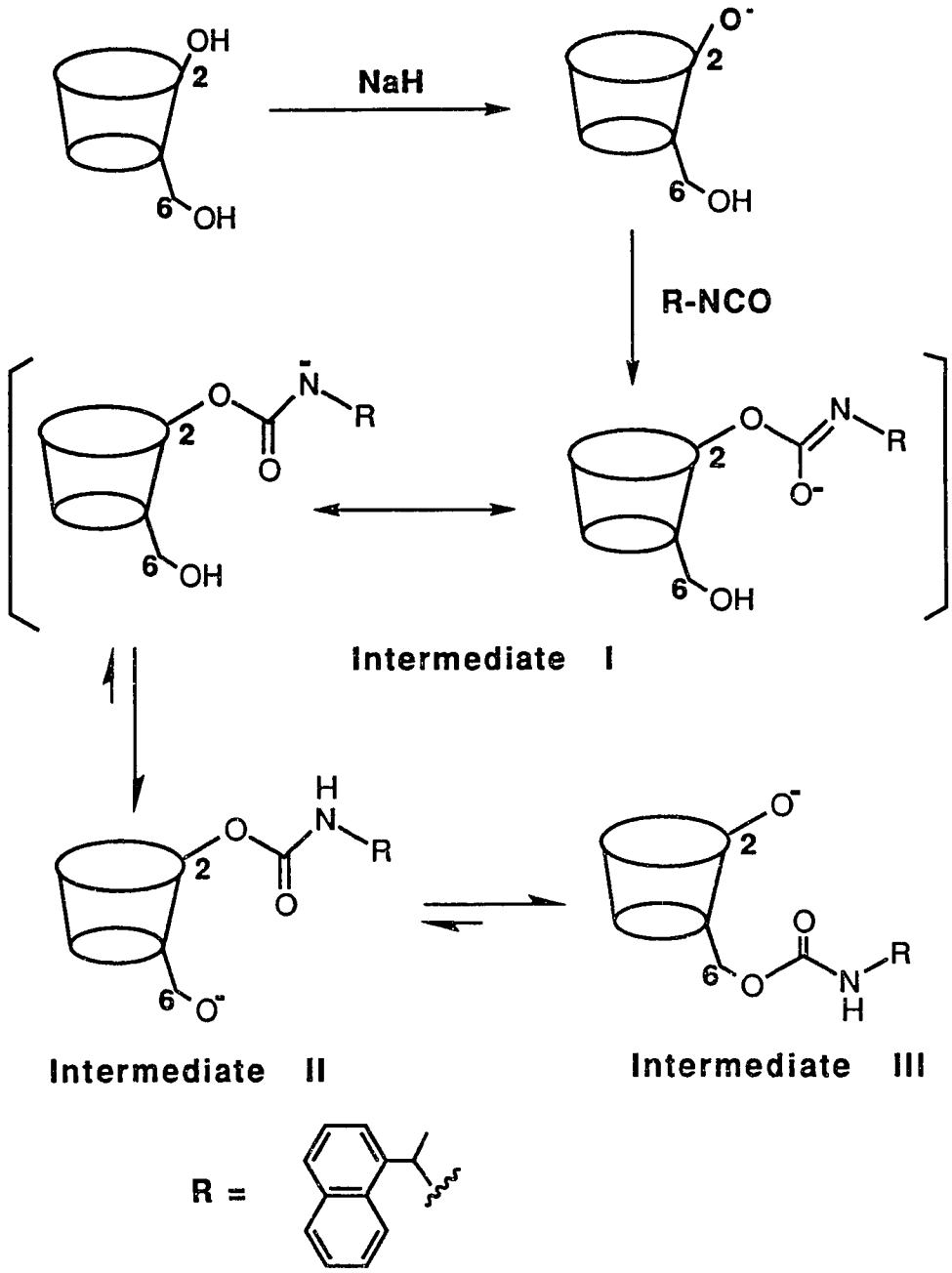

Figure 2.10 Proposed mechanism for the conversion of the C-2 substituted isomer to the C-6 substituted isomer.

was used as a solvent for the preparation of **NEC-CD CSPs**. The usual method for the preparation of **NEC-CD CSPs** involves refluxing **NEIC** and **CD** bonded silica sorbent in pyridine for 4 h. The present results suggest that substitution might occur mostly at the primary sites under these reaction conditions although this effect might be mitigated because of steric hindrance imposed by the linkages through which primary sites of **CDs** are thought to be connected to the silica.[98]

CHAPTER 3

^{1}H AND ^{13}C NMR STUDY OF 2-O-1-(1-NAPTHTYL)ETHYL-CARBAMOYLATED CYCLODEXTRINS

3.1 Introduction

Among several derivatized cyclodextrin based chiral stationary phases (CD-CSPs), the naphthylethylcarbamoylated CD based chiral stationary phase (NEC-CD-CSP) has been used both in the reversed and normal phase modes because of its stability and unique enantioselectivity in both modes.[33-39]

As mentioned previously, several issues about these CSPs remain unanswered: the sites of substitution, the orientation of the substituent and its role in chiral recognition under different mobile phase conditions, and the integrity of the toroidal configuration of CD upon derivatization. Given the ambiguity with regard to sites and degree of substitution, the chiral recognition interaction mechanism of these phases is not clear.

A first step toward understanding of NEC-CD-CSPs may be to make a monosubstitution product to serve as a simple model to represent these phases. Among three possible regioisomeric products, the most relevant model compound may

be the one substituted at the C-2 hydroxyl site, because the inclusion complexation may occur through the wider secondary hydroxyl side than the narrow primary side.[80]

Inclusion of guest molecules in the apolar cavity of CDs has been studied using a variety of techniques including X-ray,[99,100] NMR,[101,102] and computer modeling.[103,104,105] In NMR studies, inclusion of aromatic compounds in the native CD cavity usually induces a net upfield shift of protons H-3, and H-5, located in the cavity.[75,76] Because CD cavity is chiral, complexation of CD with chiral analytes results in diastereomers. Not only the chemical shifts of CD but also those of a guest molecule change upon inclusion complex formation.[106,107] NMR experiments could provide information about the orientation of the guest molecule and its conformation within the cavity.[108]

Monosubstitution of CDs destroys the C_n (n: the number of glucose units) symmetry axis of native CDs.[109] Thus complete assignment of NMR resonances may be possible but challenging and necessitates the use of not only homonuclear correlation experiments (COSY, and TOCSY)[110] but also heteronuclear correlation experiments (HMBC and HMQC).[111,112] The glucose connectivity can be ascertained from the spacial proximity of H-1 and H-4 of neighboring glucose residues through the ROESY correlation

peaks.[113,114] In HMBC, glucose sequential information could be easily obtained by the correlation of C-4 to H-1 of neighboring glucose (one direction) and C-1 to H-4 of neighboring glucose (opposite direction).

In this part of study, the complete assignment of the ^{1}H and ^{13}C NMR spectra of the major conformer of **2-O-(R)-NEC-β-CD (RC-2)** and complete ring connectivity of its epimer, **2-O-(S)-NEC-β-CD (SC-2)** by various 2D NMR techniques is reported. Similarities and differences between the NMR spectra of these two compounds are discussed in conjunction with those of native **β-CD** and computer modeling results. The relative populations of the included and excluded orientation were studied by the ^{1}H NMR. Finally, chiral distinction capability of **RC-2** and **SC-2** was demonstrated by taking ^{1}H NMR spectra with 3,5-dinitrobenzoylated (**3,5-DNB**) phenylglycine (**PG**) in methanol.

3.2 Experimental

3.2.1 Materials

RC-2 and **SC-2** were prepared using the procedures reported in Chapter 2 of the present work. β-CD was obtained from Pfanstiehl Laboratories, Inc. (Waukegan, IL). (R)-(-)- and (S)-(+)-1-(1-naphthyl)ethyl-isocyanate ((R)-**NEIC** and (S)-**NEIC**) and deuterated solvents were obtained from Aldrich Chemical Company (Milwaukee, WI).

3.2.2 NMR spectroscopy

All NMR experiments were performed on a **GE NMR GN-Omega 500 NMR** spectrometer operating at 500.11 and 125.76 MHz for ^{1}H and ^{13}C, respectively. The ^{1}H chemical shifts were determined relative to the residual HDO peak (4.70 ppm at 25 °C). The ^{13}C chemical shifts were referenced to an external dioxane peak (66.5 ppm). The concentrations used were 15 and 10 mM of **RC-2** and **SC-2**, respectively. Data sets for the two-dimensional experiments were acquired routinely using 512 blocks of 2K data points.

The **COSY** spectrum was recorded using the double quantum filtered sequence[115] and detected in the phase sensitive mode[116] in the evolution domain (f_1). The ^{1}H-^{13}C correlation

experiments were recorded using ^{1}H detected techniques. The direct $^{1}H-^{13}C$ correlation experiments (**HMQC**) were obtained using the variation of Muller's reverse polarization sequence[117] reported by Bax and Subramanian[118] and acquired with quadrature detection in f_1. In this sequence, a value of 140 Hz was used for $^{1}J_{H-C}$. The long-range $^{1}H-^{13}C$ correlation experiment was performed using the **HMBC** sequence reported by Bax and Summers.[112] The mixing delay used to transfer information was optimized for $^{n}J_{H-C}$ = 5 Hz.

The phase-sensitive cross correlation experiments with spin locking in the rotating frame (**ROESY**) were acquired by the reported pulse sequence,[119,120,121,122] with varying mixing times of 70, 200, or 350 ms. **TOCSY (2D HOHAHA)** experiments were performed by the reported pulse sequence[123,124] with varying mixing times of 65, and 120 ms.

Data sets were processed using **GE NMR Instruments Omega Software 6.0.2.** All datasets were apodized before transformation in both time domains. A sine-bell weighing function was used in both domains for the **COSY** experiment and a double exponential function was used for both of the **HMQC** and **HMBC** correlation experiments. The **COSY** and **HMQC** experiments were zero-filled to yield a final data set size of 512 by 2K real points and presented in the phase

sensitive mode. The processed data set for the **HMBC** experiment was also 512 by 2K real points and presented in the absolute value mode.

3.2.3 Computer modeling

The calculations were carried out using a **CVFF** force field and the conjugate gradient energy minimization method in Discover of Biosym Technologies. **β-CD** structure was constructed and energy minimized by molecular mechanics calculation. The energy minimized structure was compared with that obtained by X-ray technique and found to be in good agreement.[125] To construct **RC-2** and **SC-2**, one of the C-2 hydroxyl protons of energy minimized **β-CD** was replaced with **(R)-NECM**, or **(S)-NECM**, followed by energy minimization.

3.3 Results and Discussion

3.3.1 Assignment of ^{1}H and ^{13}C resonances of native β-CD

To better understand the NMR spectra of derivatized cyclodextrins, it was necessary to study the NMR spectra of native **β-CD**. **CDs** are cyclic oligomers of 1 -> 4 linked α-D-glucose mononmers. The ^{1}H and ^{13}C NMR spectra of **CDs** are very simple because they have C_n symmetry axis (n: number of

glucose units) and all glucose units are identical in the ^{1}H and ^{13}C NMR time scale. The 500 MHz ^{1}H and 125 MHz ^{13}C NMR spectra of β-CD taken in D_2O are shown in Figure 3.1. Because of the reasons mentioned above, the signals seems to arise from a single glucose unit. Several decoupling experiments were done to assign individual resonances. Irradiation of the doublet at δ 5.09 caused collapse of a doublet of a doublet at δ 3.67. The resonance at δ 5.09, which corresponds to the most downfield resonance of CD signals, arises from the anomeric proton. Therefore, the doublet of doublet at δ 3.67 was assigned as H-2 which shows coupling to the anomeric proton and H-3 with coupling constants of 3.7, and 10.0 Hz, respectively. In the same way, protons H-4, H-5 and H-6s could be assigned. To assign ^{13}C resonances, ^{1}H and ^{13}C **COSY** spectrum was obtained using **HETCOR** pulse sequence as shown in Figure 3.2. Chemical shifts of ^{1}H and ^{13}C resonances of β-CD and coupling constants are listed in Table 3.1.

The anomeric proton resonances, which are well separated from the other protons, and the C-1 resonances which are at δ 103.1 serve as a solid base for the identification of complicated carbohydrates. In addition, the relatively well separated C-4 (at δ 82.4) and C-6 (at δ 61.5) resonances can be used for additional information on assignment.

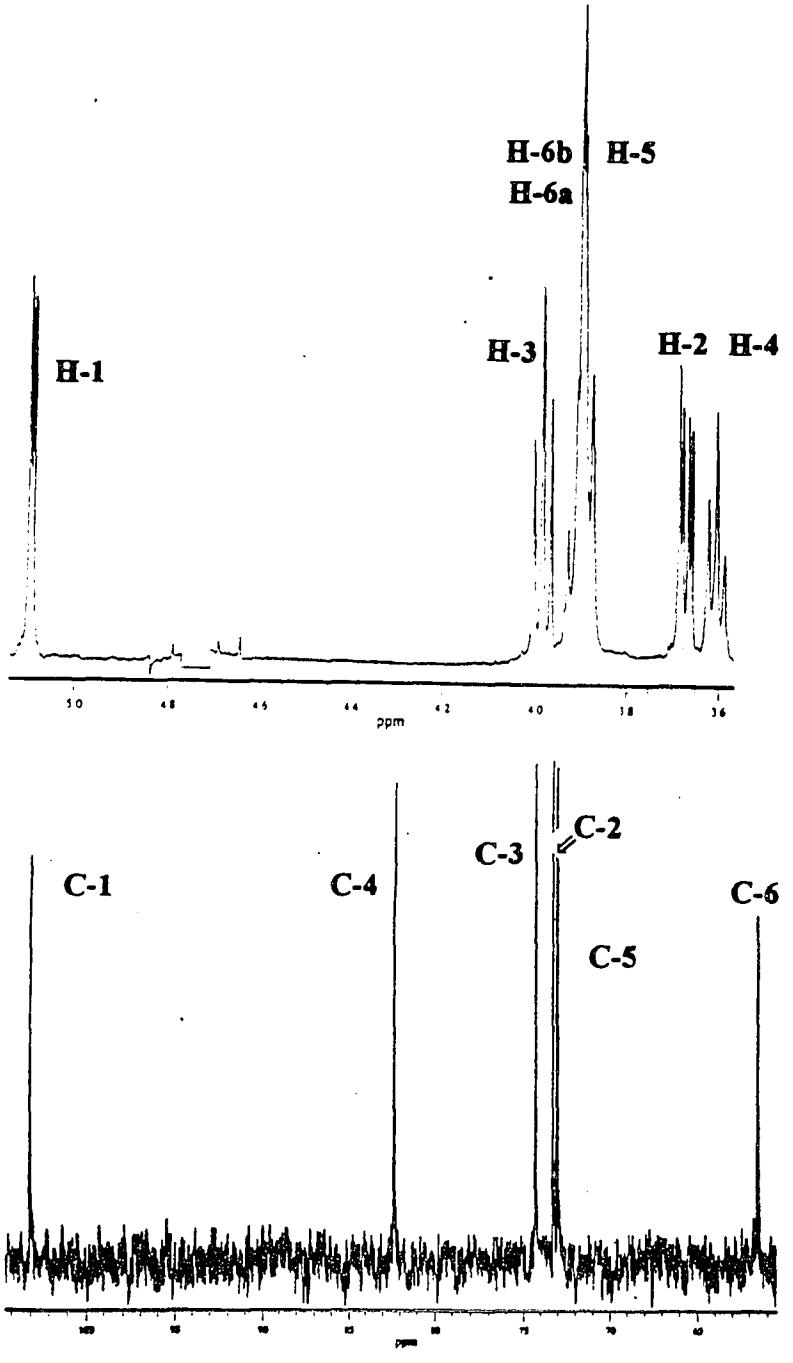

Figure 3.1 The 500 MHz ^{1}H and 125 MHz ^{13}C NMR spectra of β-CD taken in D_2O.

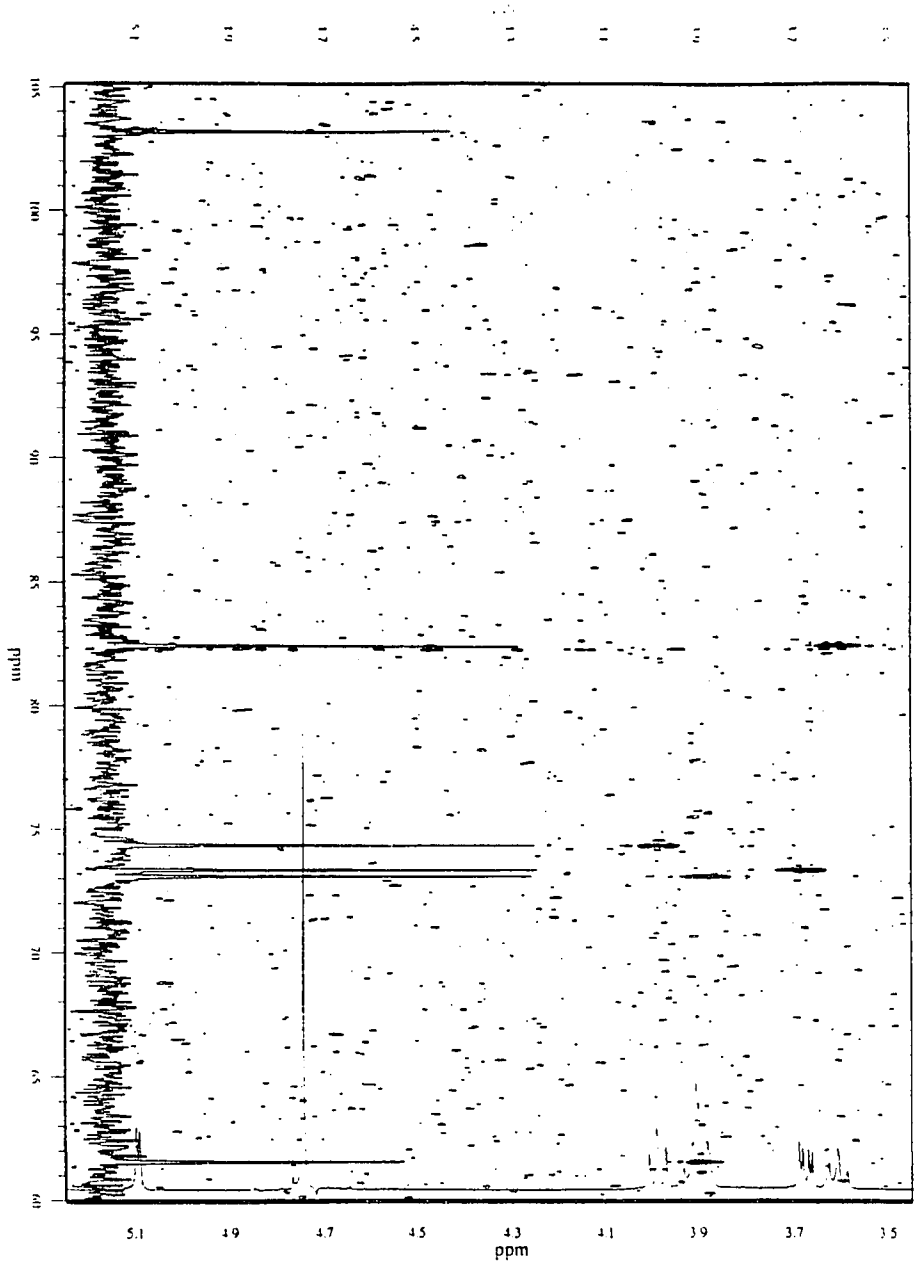

Figure 3.2 ^{1}H and ^{13}C COSY spectrum of β-CD.

Table 3.1 The ^1H and ^{13}C NMR data of β-CD in D_2O.[a]

atom	^{13}C	^1H(multiplicity, J in Hz)
1	103.1	5.09(d, 3.7)
2	73.3	3.67(dd, 3.7, 10.0)
3	74.3	3.99(t, 9.5)
4	82.4	3.60(t, 9.1)
5	73.0	3.89(m)[b]
6	61.5	3.90(m)[b]

a: ^1H chemical shifts were determined relative to the residual solvent peak at $\delta = 4.70$. ^{13}C chemical shifts were determined relative to the external dioxane peak $\delta = 66.5$.

b: Chemical shifts are appoximated by the consideration of ^1H-^{13}C 2D NMR correlation spectra obtained through HETCOR pulse sequence.

3.3.2 Assignment of ^{1}H and ^{13}C resonances of RC-2 and SC-2

Numbering system of the proton and carbon atoms and the seven glucoses of **RC-2** and **SC-2** is shown in Figure 3.3. ^{1}H and ^{13}C NMR spectra of **RC-2** and **SC-2** in D_2O are shown in Figures 3.4 and 3.5. The ^{1}H and ^{13}C NMR spectra of **RC-2** and **SC-2** in D_2O are complicated by severe overlap of the carbohydrate resonances. The doubling of many of the resonances including aromatic resonances indicated the presence of at least two conformers. The presence of conformational exchange adds to the complexity of the spectra for both compounds. The existence of two conformers both in **RC-2** and **SC-2** is clearly demonstrated by the correlation between anomeric protons in the **ROESY** spectrum. For example, the anomeric protons in **SC-2** are well dispersed and easily identified except for the H-1C resonance which is buried under the multiplet centered around 5.07 ppm. The six other anomeric proton resonances have exchanging partners under the huge multiplets as evidenced by the observed cross peaks in the **ROESY** spectrum as shown in Figure 3.6. The integration of two exchanging H-11 resonances of **RC-2** and **SC-2** revealed that there exist predominantly two conformers with the population ratios of 90/10 and 61/39, in **RC-2** and **SC-2** at 25 °C, respectively.

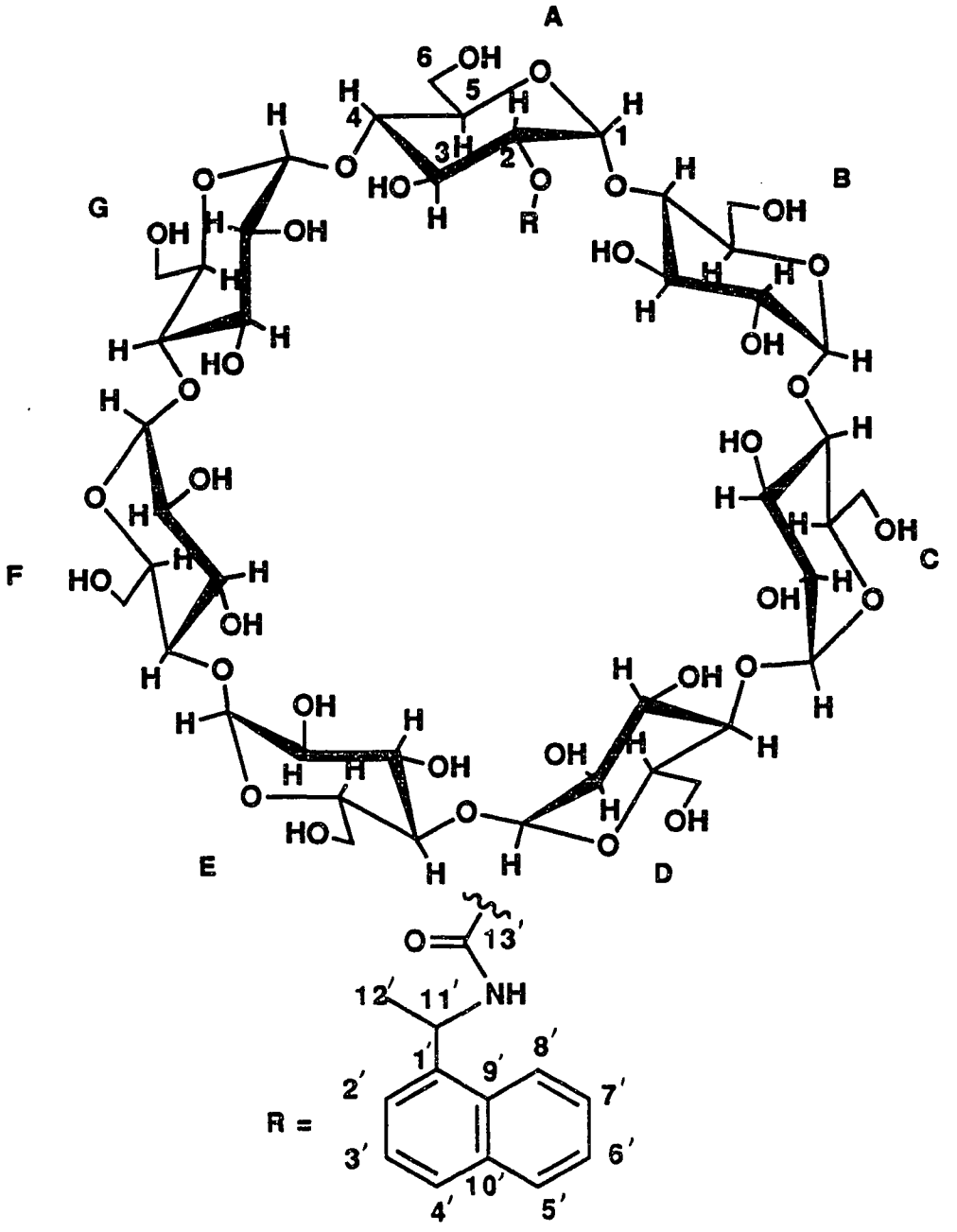

RC-2 : R on the carbon 11

SC-2 : S on the carbon 11

Figure 3.3 Numbering system of the proton and carbon atoms and the seven glucoses of RC-2 and SC-2.

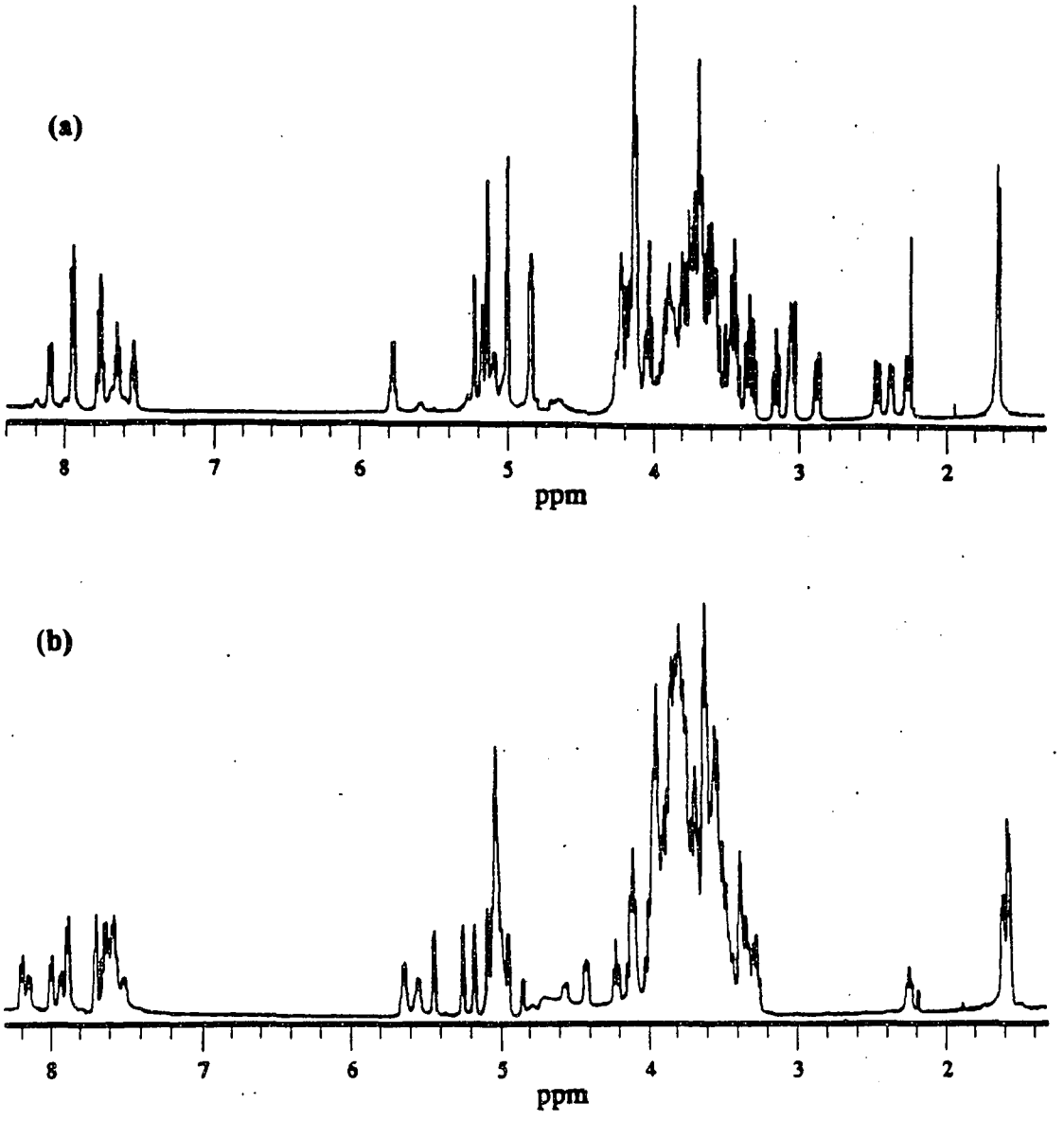

Figure 3.4 The 500 MHz ^1H NMR spectra of (a) RC-2, and (b) SC-2 in D_2O.

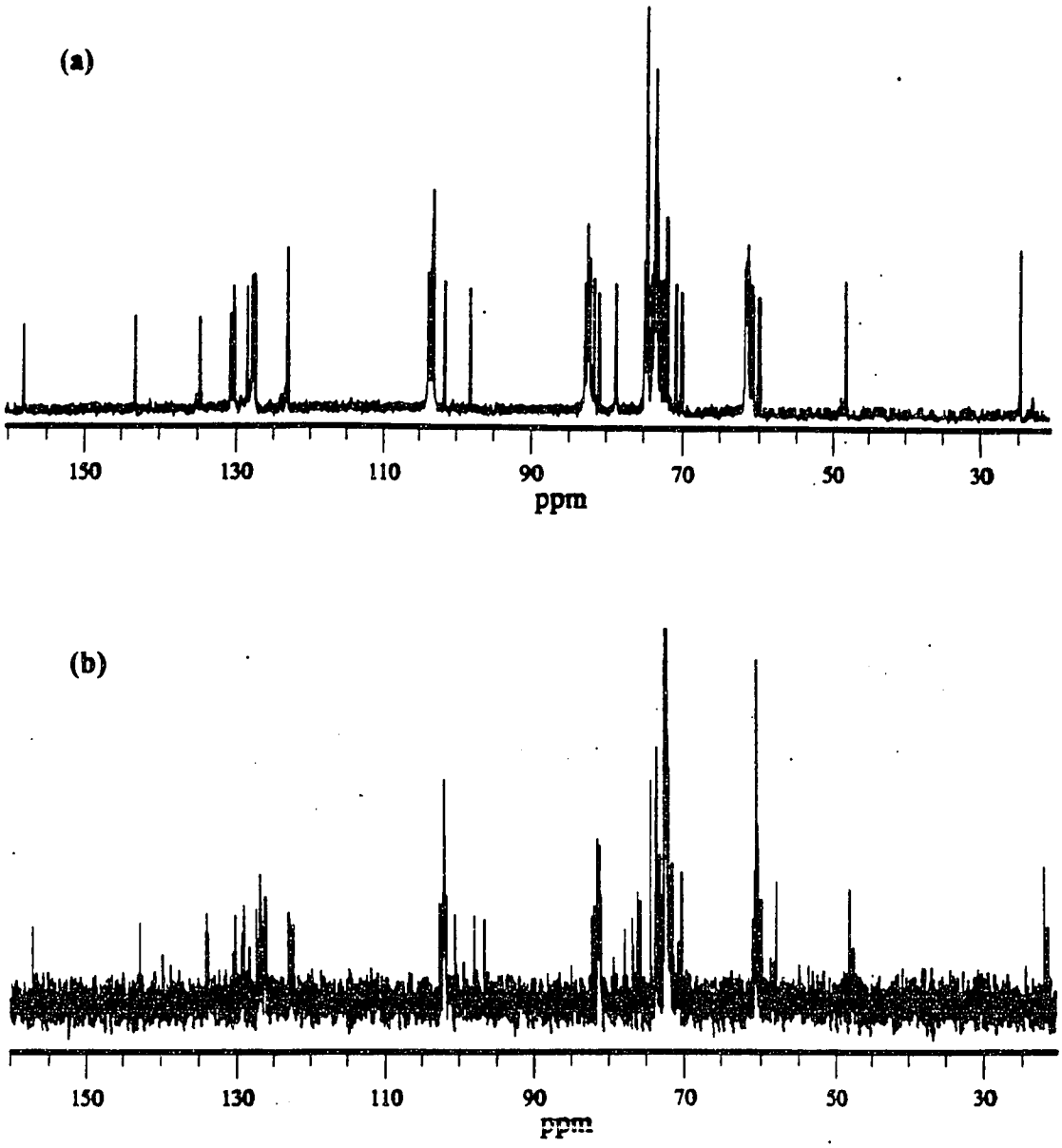

Figure 3.5 The 125 MHz ^{13}C NMR spectra of (a) RC-2, and (b) SC-2 in D_2O.

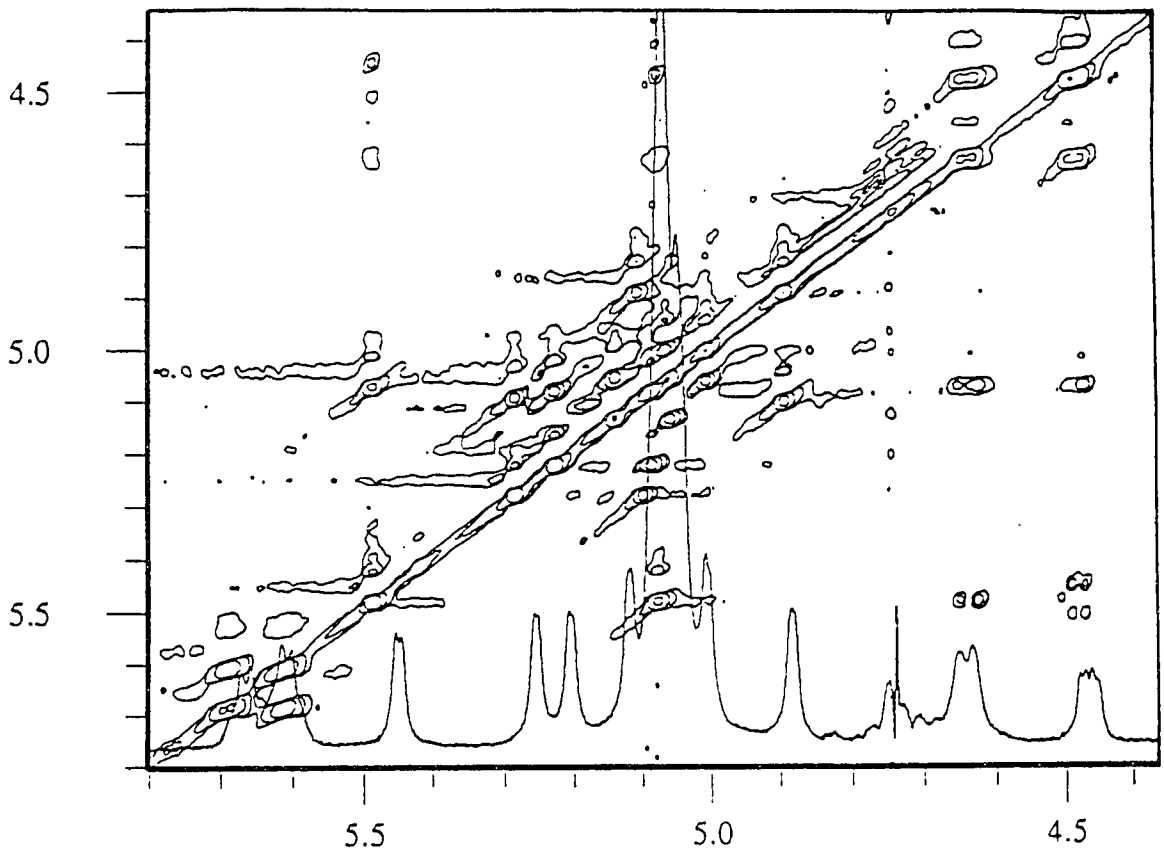

Figure 3.6 The anomeric region of partial ROESY spectrum of SC-2 showing the correlations between the two exchanging conformers.

3.3.2A RC-2: ^{1}H Assignments

The strategy for the assignment of ^{1}H and ^{13}C is shown in Figure 3.7. The first step in the assignment of seven independent glucose spin networks of the major conformer of **RC-2** was to correlate the six anomeric protons with resonances in the main carbohydrate envelope (δ=3 to 4) in the ^{1}H-^{1}H **COSY** spectrum. Six out of seven H-2's (glucose residues B-G) were readily identified in this way as shown in Figure 3.8. The seventh, H-1A, correlates with H-2A at δ = 5.16, shifted downfield by the carbamate linkage. The proton spin systems (H-2 to H-6's) of glucose rings B and E were readily identified using only the **COSY** spectrum. The **NECM** protons could also be unambiguously assigned by **COSY**. The remaining sugar ring resonances required data from additional two-dimensional experiments.

The **TOCSY** spectrum aided in the assignment process by extending the observed correlations throughout the spin systems of the individual glucose units. However, the close positioning of the anomeric proton resonances prevented complete assignments of these signals. Despite a long mixing time (120 ms), only two of the seven correlations (glucose residues B and E) between the anomeric protons and the H-6s were readily identified. Therefore, the remaining resonances were assigned to the individual glucose spin

Strategy for the assignment of ^{1}H and ^{13}C of RC-2 and SC-2

1. **H-1 ⇒ H-2 (COSY)**
2. **H-2 ⇒ H-3, H-3 ⇒ H-4, H-4 ⇒ H-5, H-5 ⇒ H-6s (COSY)**

   and check with H-1 ⇒ H-2, H-3, H-4, H-5 (TOCSY)
3. **H-1 ⇒ C-1 (HMQC)**
4. **H-4 ⇒ C-4 (HMQC)**
5. **H-4 ⇒ C-6 (HMBC)**
6. **Glucose connectivity**

   a. **H-1 ⇔ H-4 of neighboring glucose unit (ROESY)**

   b. **C-4 ⇒ H-1 of neighboring glucose unit (HMBC) (in one direction)**

   c. **C-1 ⇒ H-4 of neighboring glucose unit (HMBC) (in opposite direction)**
7. **H-1 ⇒ C-5 (HMBC), H-1 ⇒ C-3 (HMBC), C-5 ⇒ H-5 (HMQC)**

   C-3 ⇒ H-3 (HMQC), H-2 ⇒ C-2 (HMQC) etc.

8. **Conformational study**

   1. **ROESY correlation between naphthyl protons and sugar protons**

   2. **HyperChem and Insight II (Biosym)**

Figure 3.7 Strategy for the assignment of ^{1}H and ^{13}C resonances of RC-2 and SC-2.

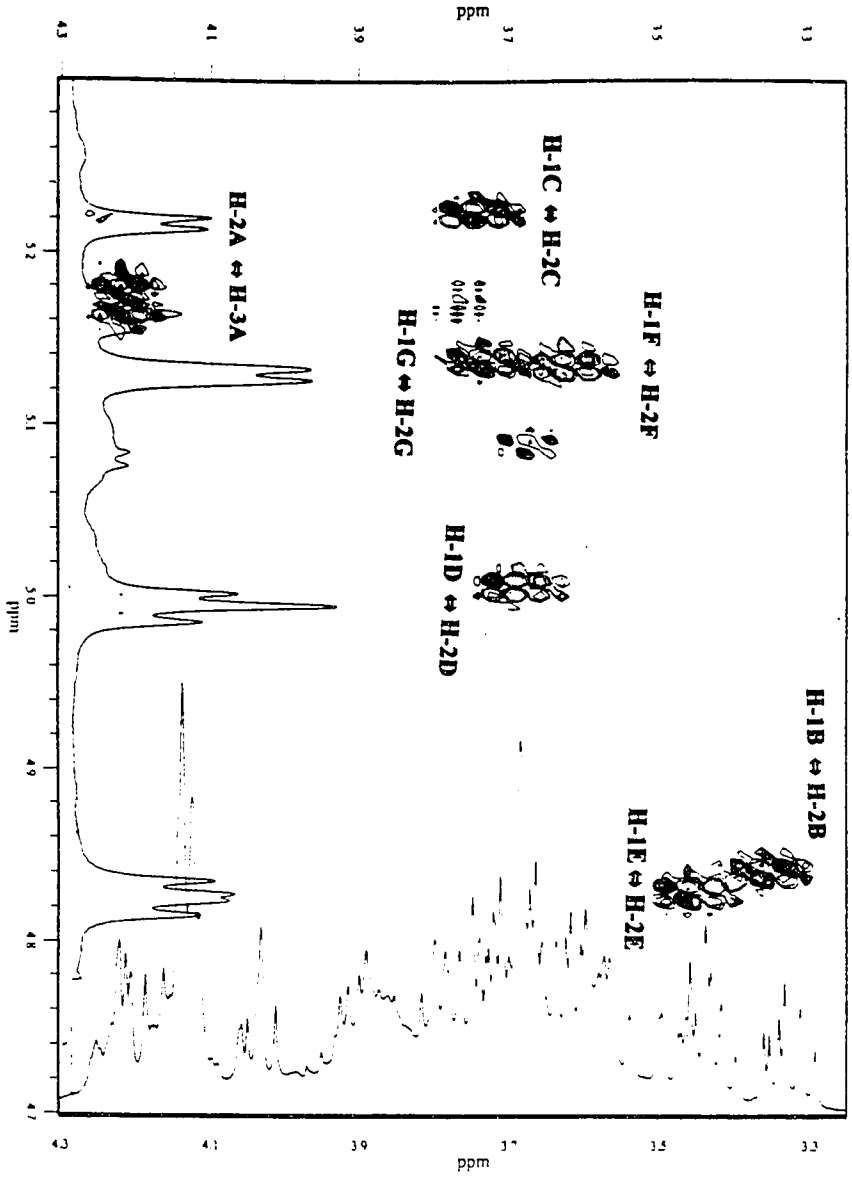

Figure 3.8 Partial ^1H-^1H COSY spectrum of RC-2 in D_2O showing the correlations of anomeric protons and H-2s.

networks through the correlation between the C-4's and H-6's in the **HMBC** experiment (see below).

3.3.2B RC-2: ^{13}C Assignments

Some of the ^{13}C resonances of the carbohydrate units are observed in distinct regions: C-1, δ_{obs} 97 ~ 105, C-4, δ_{obs} 78 ~ 84 and C-6, δ_{obs} 57 ~ 64. This makes it possible to easily identify these resonances from those of C-2, C-3 and C-5, all between 73 and 76 ppm. The first step in the assignment of ^{13}C resonances was the utilization of direct coupling between anomeric protons and C-1s in the **HMQC**. Six correlations between the anomeric protons and C-1s of **RC-2** were observed in the **HMQC** spectrum (The ^{1}H signals of the anomeric protons of glucose residues F and G overlapped and only one cross peak was observed) as shown in Figure 3.9. The assignment of C-2s, C-3s, and C-5s were possible through the correlation of C-5 to H-1 (**HMBC**), C-3 to H-1 (**HMBC**), C-5 to H-5 (**HMQC**), and C-2 to H-2 (**HMQC**) in combination with the **COSY** and **TOCSY** spectra. All seven correlations between H-4s and C-6s were resolved as shown in Figure 3.10. The three bond correlations observed between H-4s and C-6s were much stronger than the two bond correlation between H-5s and C-6s. Therefore, the dispersion of the C-4 resonances yielded experimental data on which to base the assignments of the H-6 resonances. The substitution site of the **NECM** group on C-

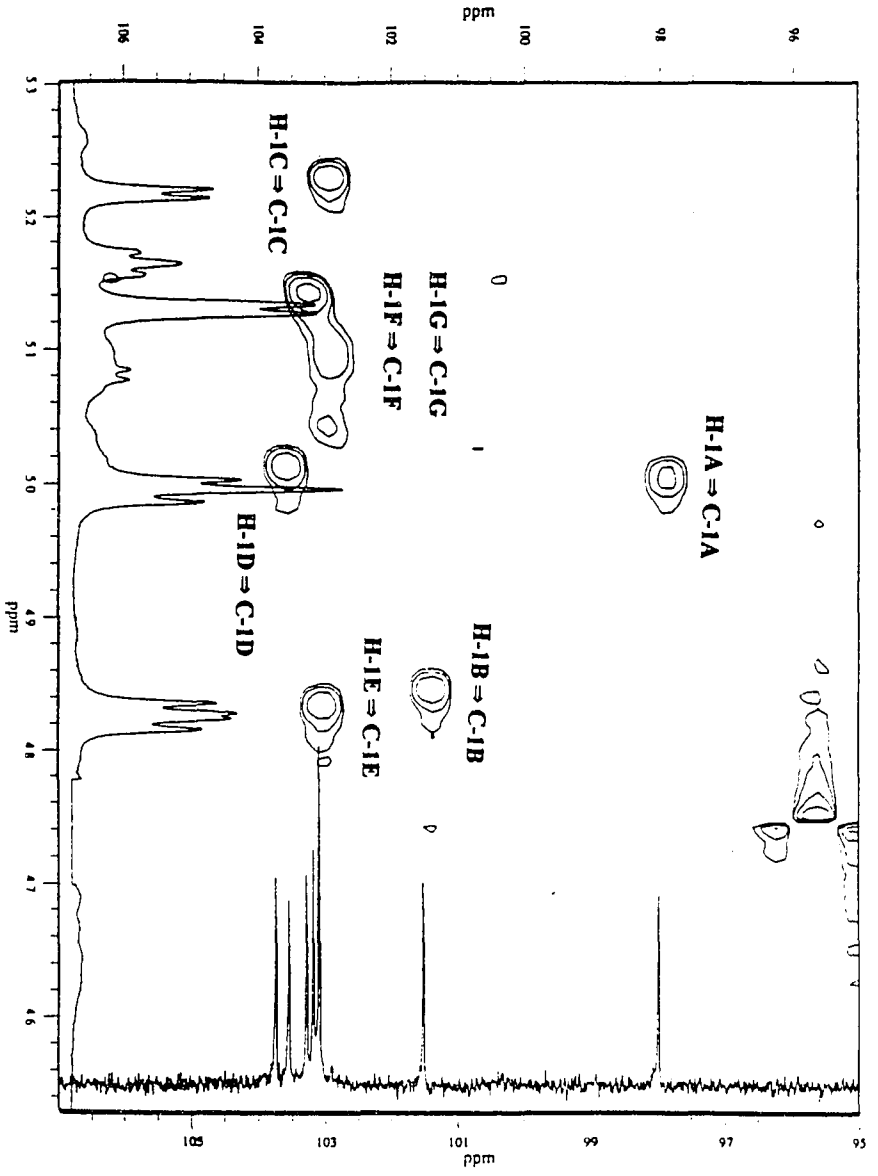

Figure 3.9 Partial HMQC spectrum of RC-2 showing the correlations between H-1s and C-1s.

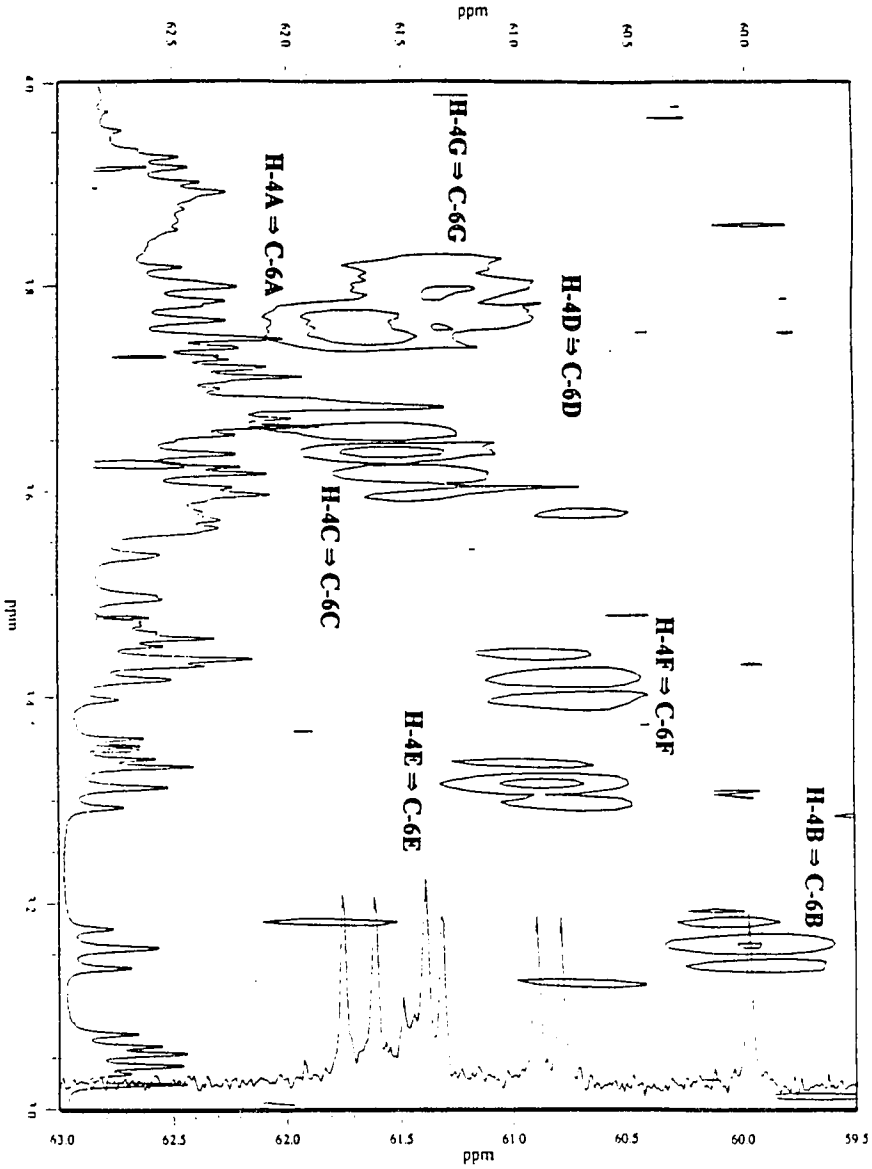

Figure 3.10 Partial HMBC spectrum of RC-2 showing the correlations between H-4s and C-6s.

2A was evidenced by the correlation between H-2A and C-13' in the **HMBC** spectrum as shown in Figure 3.11.

3.3.2C SC-2

The assignment of ^{1}H and ^{13}C resonances of **SC-2** was complicated by the presence of two similarly populated conformers. Further, the significantly lower solubility of **SC-2** in D_2O relative to **RC-2**, resulted in poorer sensitivity for the inverse detected 2-D experiments. However, important cross peaks in the **HMQC** and **HMBC** data were sufficiently developed to derive useful information. Well dispersed anomeric protons of the major conformer served a good basis for the assignment of other protons as well as carbon-13 resonances. Most of the ring proton resonances from the carbohydrates of the major conformer could be readily assigned using **COSY** and **TOCSY** spectra starting from anomeric protons. As in the case of **RC-2**, there was a lack of correlation between the anomeric proton and the H-6s in the **TOCSY** spectrum. However, the severe overlap of the C-6 resonances precluded complete assignment of the H-6's. The resonances of C-2, C-3, and C-5 were also severely overlapped and could not be assigned. The **NECM** protons of both conformers were unambigously assigned using **COSY**. Some of the proton resonances of the minor conformer could be identified by the correlation observed with the resonances

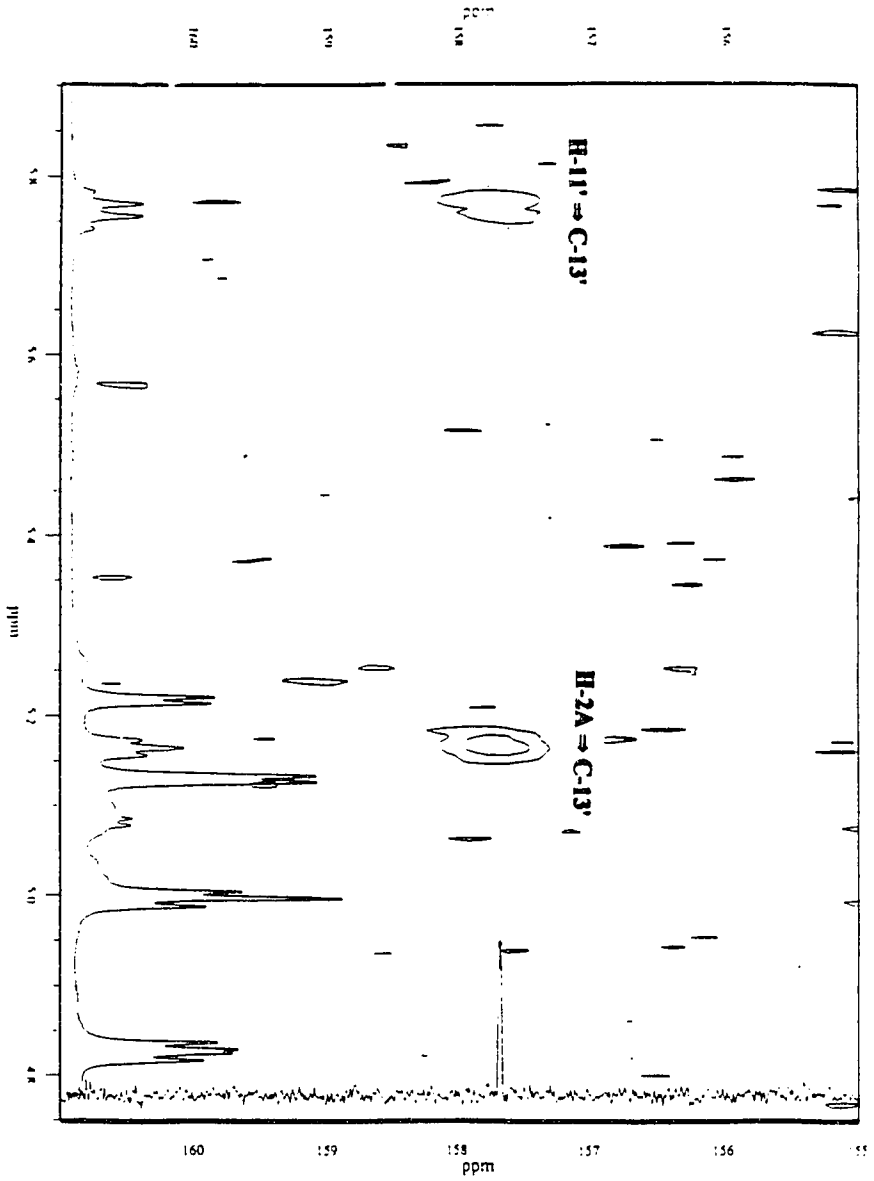

Figure 3.11 The partial HMBC spectrum showing the correlation between H-2A and C-13′ of carbamate indicating the derivatization site.

of the major conformer in **ROESY** spectra. The presence of conformers and the severe overlap of resonances limited the utility of the **HMBC/HMQC** methods employed for complete assignment of **RC-2**. Despite incomplete assignment for **SC-2**, **HMBC/HMQC** techniques did allow for meaningful information regarding connectivity of glucoses as detailed below.

3.3.3 Connectivity of glucoses

The **ROESY** spectra, showing the correlations between H-1A and H-4B, H-1B and H-4C ... H-1G and H-4A, are shown in Figure 3.12 and Figure 3.13 for **RC-2** and **SC-2**, respectively. Cross peaks from the **HMBC** spectra, demonstrating the correlations of C-1G to H-4A, C-1F to H-4G, ... C-1A to H-4B are shown in Figure 3.14 and Figure 3.15, for **RC-2** and **SC-2**, respectively. Cross peaks from the **HMBC** spectra, demonstrating the correlations of C-4B to H-1A, C-4C to H-1B ....C-4A to H-1G are shown in Figure 3.16, for **RC-2**. Almost all of the correlations of C-4s to H-1s were observed in the case of **SC-2** except a correlation between H-1G and C-4A. However, the resonance of C-4A carbon was identified through the correlation of C-4A to H-3A in the **HMBC** spectra. The three self-consistent sets of correlations confirm the assignment of all H-1s, H-4s, C-1s, and C-4s as well as provide glucose sequential information.

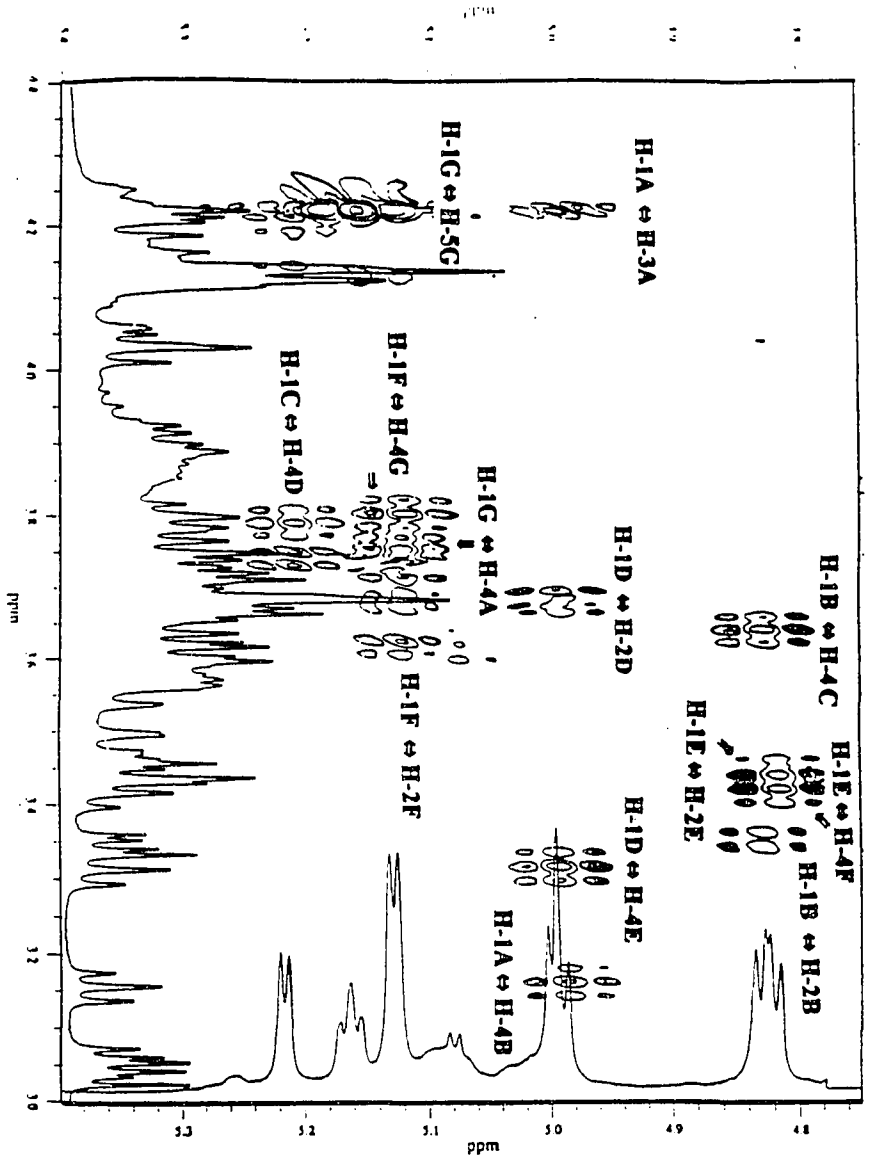

Figure 3.12 Partial ROESY spectrum of RC-2 showing the correlation between H-1 in one glucose and H-4 in neighboring glucose connected through α-(1 -> 4) glycosidic linkage.

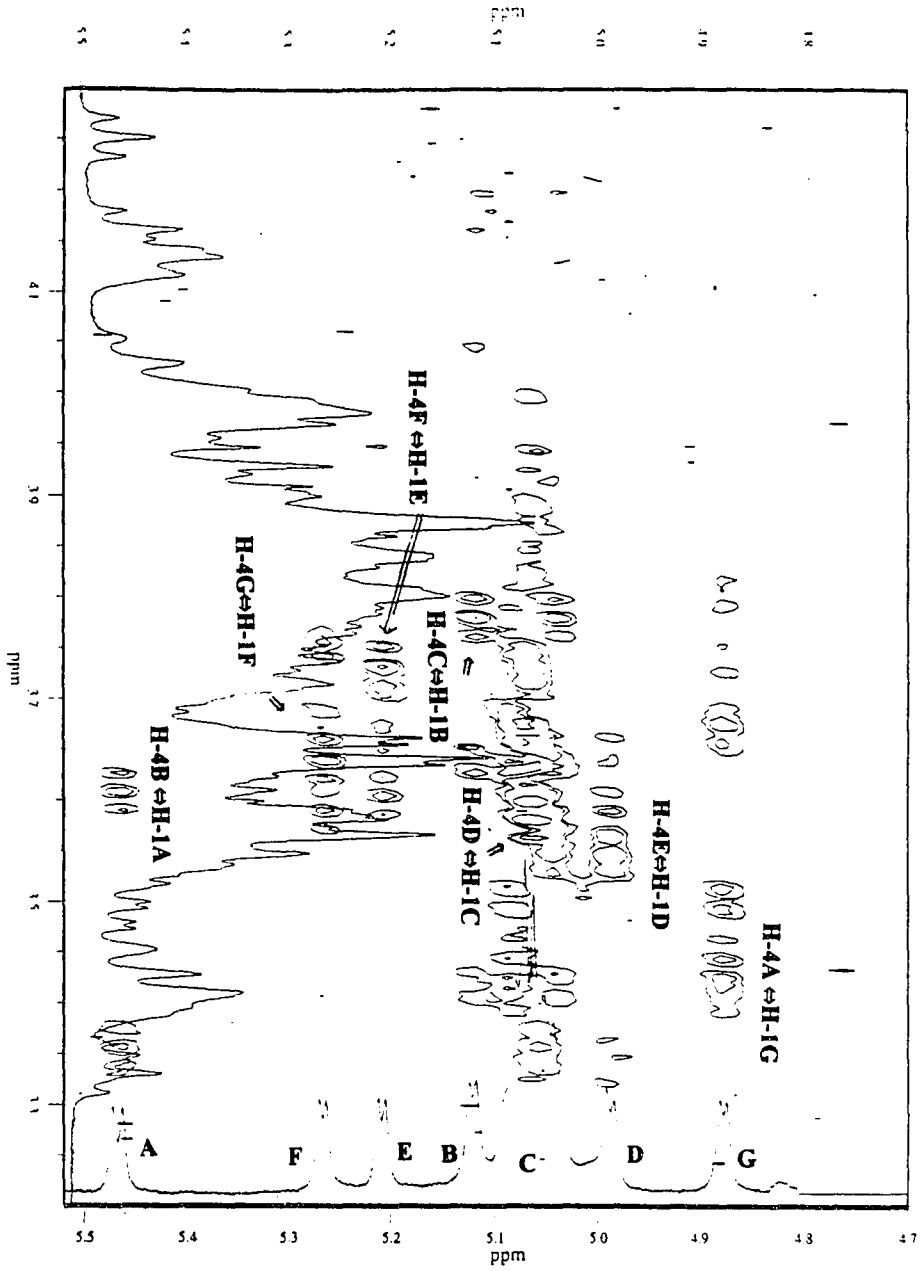

Figure 3.13 Partial ROESY spectrum of SC-2 showing the correlation between H-1 in one glucose and H-4 in neighboring glucose connected through α-(1 -> 4) glycosidic linkage.

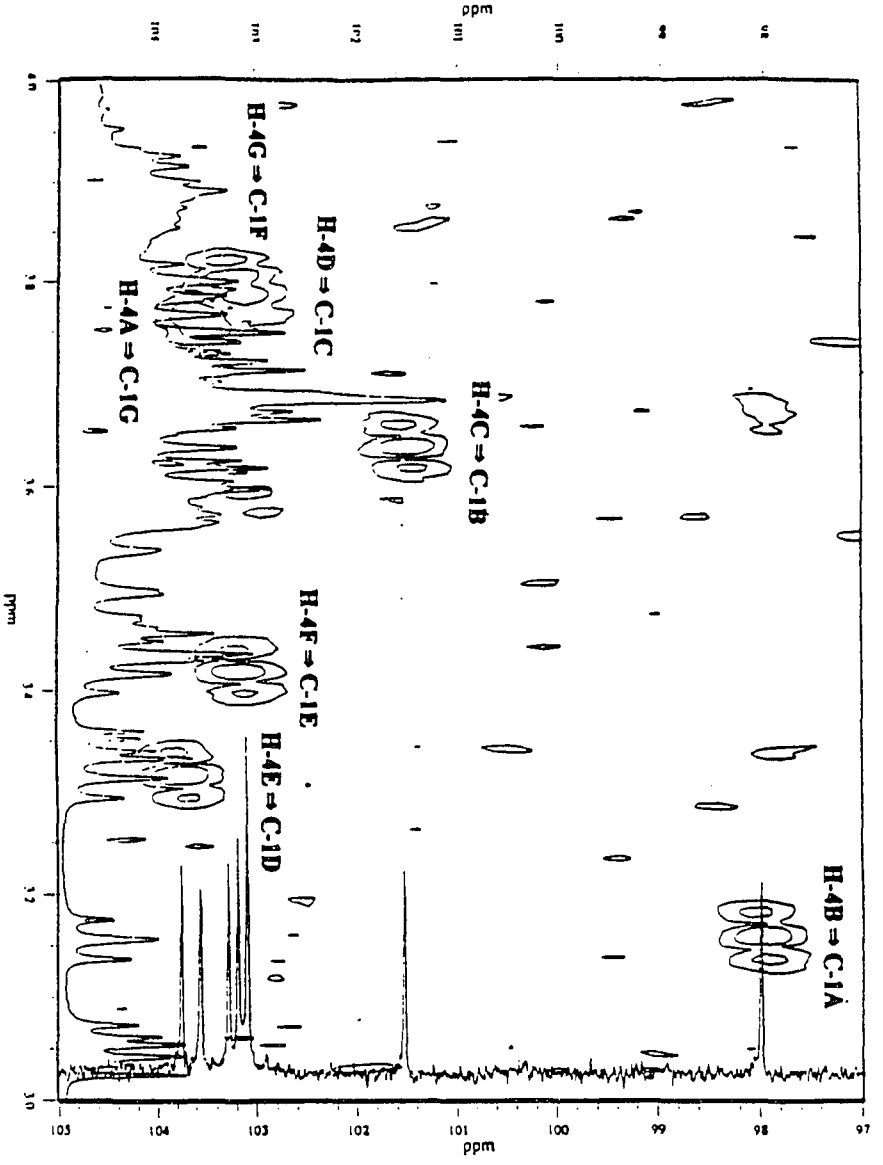

Figure 3.14 Partial HMBC spectrum of RC-2 showing the correlation between H-4 in one glucose and C-1 in neighboring glucose connected through α-(1 -> 4) glycosidic linkage.

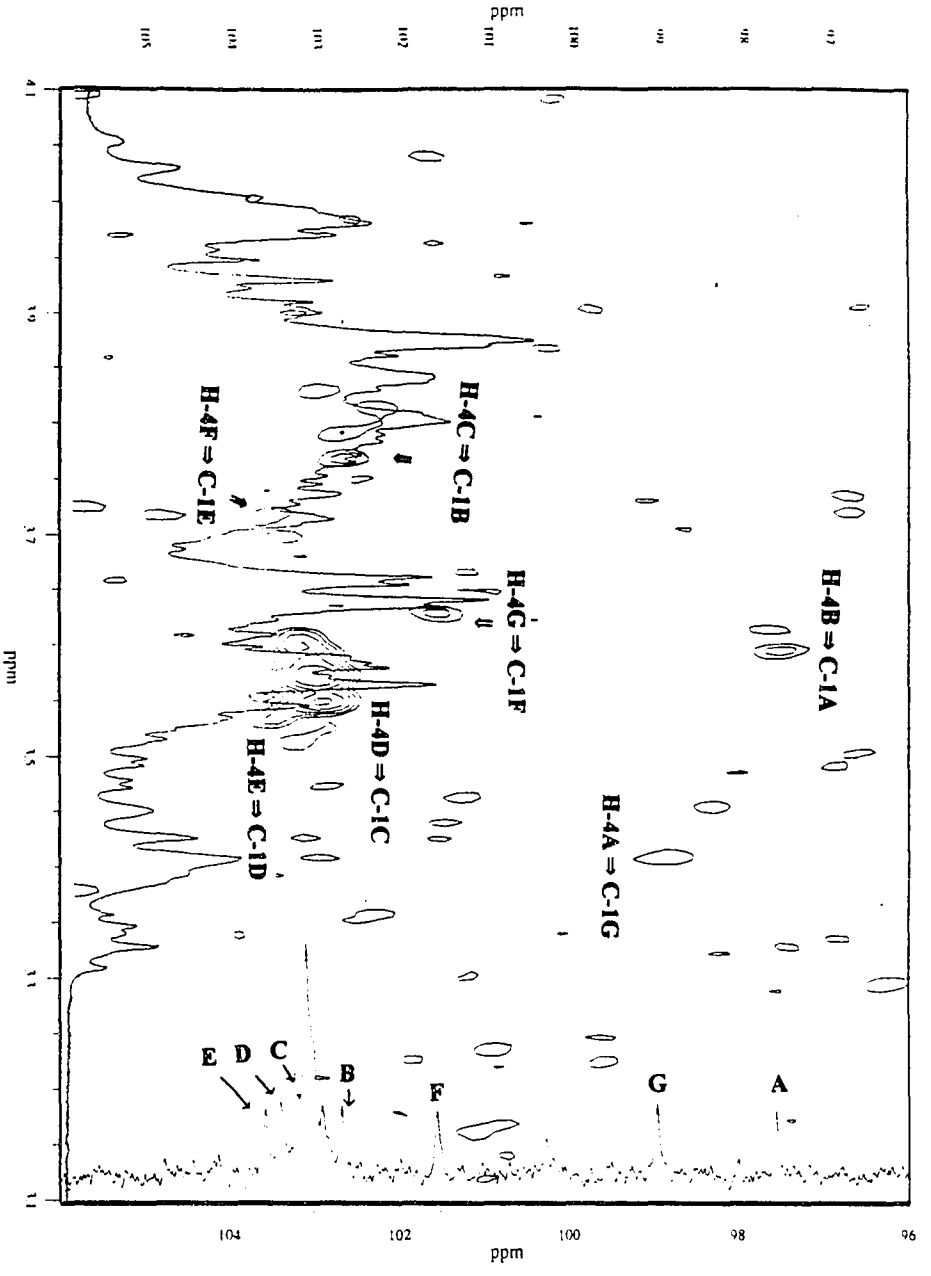

Figure 3.15 Partial HMBC spectrum of SC-2 showing the correlation between H-4 in one glucose and C-1 in neighboring glucose connected through α-(1 -> 4) glycosidic linkage.

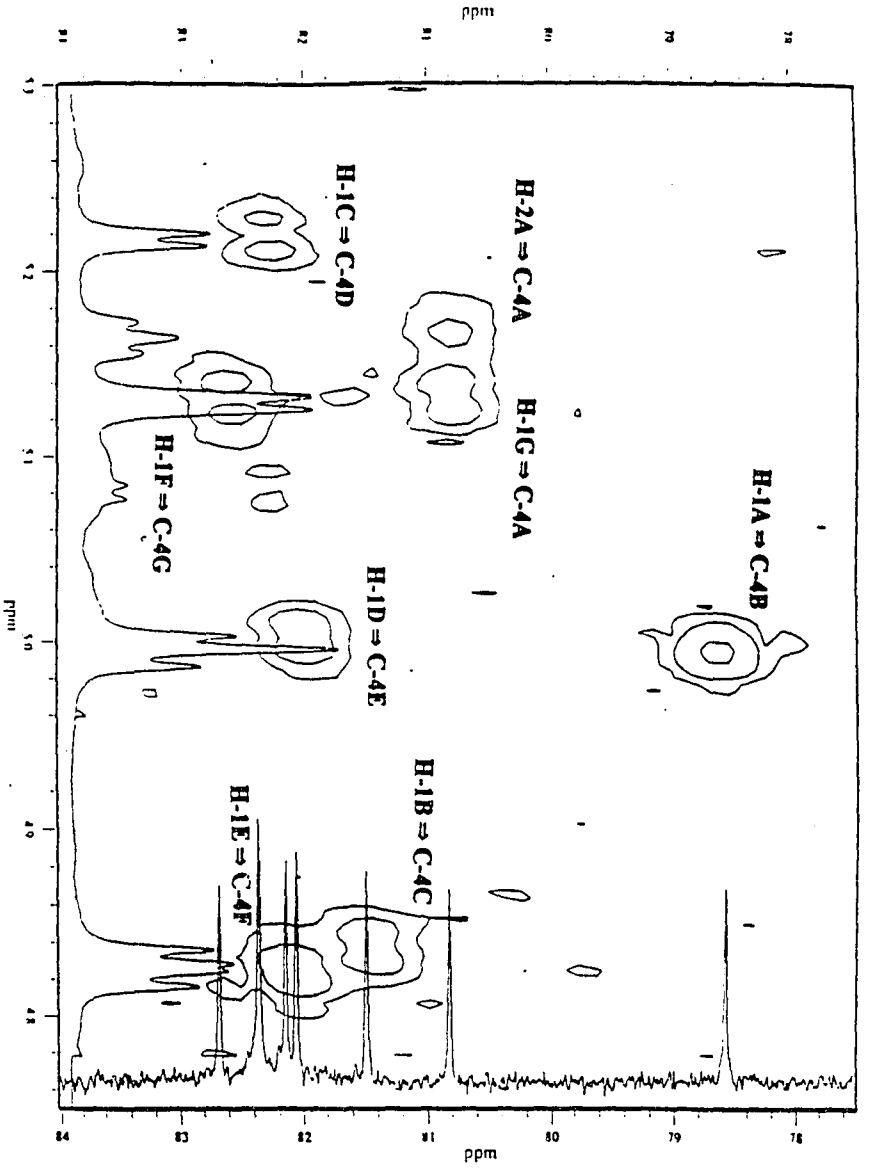

Figure 3.16 Partial HMBC spectrum of RC-2 showing the correlation between H-1 in one glucose and C-4 in neighboring glucose connected through α-(1 -> 4) glycosidic linkage.

3.3.4 Conformational analysis

The substituent chemical shifts (**SCSs**: defined as the difference between the observed chemical shift of **RC-2** or **SC-2**, and **β-CD**; positive value implies deshielding) demonstrate the effect of the **NECM** on the various glucose units through substituent bonding, and anisotropic ring current effect. The ^{1}H and ^{13}C **SCSs** of the carbohydrate part of **RC-2** are listed together with the chemical shifts of **β-CD** in Tables 3.2 and 3.3 for ^{1}H and ^{13}C, respectively. The same data for SC-2 are listed in Tables 3.4 and 3.5. The chemical shifts of the naphthyl groups are listed in Table 3.6.

3.3.4A RC-2

In Table 3.2, ^{1}H resonances of glucoses B, E, and F are upfield shifted whereas those of glucoses C, D, and G are downfield shifted. In general, the extent of shielding on glucoses B and E is more pronounced than that of deshielding on the remaining glucoses. Glucose A does not seem to show clearly either shielding or deshielding effect, which may be due to the proximity of carbamate substituent. H-2A is the most deshielded (1.49 ppm). This can be attributed to the inductive effect of the carbamoylation together with deshielding of the naphthyl group.

Table 3.2 The ^1H chemical shifts of β-CD and SCSs of RC-2 in D_2O. ($SCS = \delta_{obs} - \delta_{CD}$).

^1H	H-1	H-2	H-3	H-4	H-5	H-6a	H-6b
β-CD	5.09	3.67	3.99	3.60	3.89	3.90	3.90
A	-0.10	1.49	0.23[a]	0.16[a]	-0.21[a]	-0.35[a]	-0.11[a]
B	-0.26	-0.32	-0.95	-0.44	-1.63	-1.43	-1.03
C	0.13	0.07[a]	0.22[a]	0.04[a]	0.29[a]	0.01	0.14[a]
D	-0.09	0.01[a]	0.04	0.19[a]	0.26[a]	0.00[a]	0.00[a]
E	-0.27	-0.23	-0.94	-0.29	-1.52	-0.42[a]	-0.32
F	0.04	-0.06[a]	-0.30[a]	-0.18	-0.30[a]	-0.45[a]	-0.20[a]
G	0.04	0.06[a]	0.16[a]	0.20[a]	0.35	0.22[a]	0.22[a]
Ave	5.02 ±0.15	3.59 ±0.16	3.77 ±0.53	3.55 ±0.26	3.50 ±0.85	3.55 ±0.54	3.71 ±0.42
Δ[b]	-0.07	-0.08	-0.22	-0.05	-0.39	-0.35	-0.19

a: Chemical shifts are estimated by ^1H-^1H COSY spectrum.

b: Δ is the chemical shift differences between β-CD and average chemical shift of an individual point. H-2A point was omitted for the calculation of average chemical shift of H-2 position because H-2A is the site of the carbamoylation.

Table 3.3 The ^{13}C chemical shifts of β-CD and SCSs of RC-2 in D_2O. (SCS = δ_{obs} - δ_{CD}).

^{13}C	C-1	C-2	C-3	C-4	C-5	C-6
β-CD	103.1	73.3	74.3	82.4	73.0	61.5
A	-5.1	-3.4	-2.3	-1.5	0.7	0.2
B	-1.5	0.1	1.1	-3.8	-1.2	-1.6
C	0.0	0.0	1.4	-0.9	1.4	0.1
D	0.7	-0.2	1.1	0.0	0.5	-0.1
E	0.1	-0.1	1.0	-0.3	-0.8	-0.6
F	0.2	-0.0	1.1	-0.2	-0.4	-0.8
G	0.5	-1.5	1.0	0.3	0.2	-0.2
Ave	102.3 ± 2.1	72.6 ± 1.3	74.9 ± 1.4	81.4 ± 1.4	73.1 ±0.9	61.1 ± 0.6
Δ^a	- 0.7	-0.7	0.6	-0.9	0.1	-0.4

[a]: Δ is the chemical shift differences between β-CD and average chemical shift of an individual point.

Table 3.4. The ^1H chemical shifts of β-CD and SCSs of SC-2 in D_2O. (SCS = δ_{obs} -δ_{CD}).

^1H	H-1	H-2	H-3	H-4	H-5	H-6a	H-6b
β-CD	5.09	3.67	3.99	3.60	3.89	3.90	3.90
A	0.39	0.80	-1.70	-0.16[a]	-0.45[a]		
A"[b]		0.96	-0.09[a]				
B	0.04	-0.03[a]	0.15	0.04[a]			
B"		-0.26		-0.25[a]			
C	-0.01	0.06[a]	0.18	0.18[a]	0.25[a]		
D	-0.09	-0.13[a]	-0.65	-0.02[a]	-0.28[a]		
E	0.13	0.04[a]	-0.10[a]	-0.06[a]	0.12[a]		
F	0.18	0.07[a]	0.27	0.12[a]	0.12[a]		
G	-0.21	-0.18	-0.21[a]	0.07[a]	-0.48[a]		
Ave	5.15 ±0.20	3.64 ±0.10	3.70 ±0.69	3.62 ±0.12	3.77 ±0.32		
Δ[c]	0.06	-0.03	-0.29	0.02	-0.12		

[a]: Chemical shifts are estimated from ^1H-^1H COSY spectrum.

[b]: Protons of minor conformer are marked with double prime.

c: Δ is the chemical shift differences between β-CD and average chemical shift of an individual point. H-2A point was omitted for the calculation of average chemical shift of H-2 position because H-2A is the site of the carbamoylation.

Table 3.5 The ^{13}C chemical shifts of β-CD and SCSs of SC-2 in D_2O. (SCS = δ_{obs} -δ_{CD}).

^{13}C	C-1	C-2	C-3	C-4	C-5	C-6
β-CD	103.1	73.3	74.3	82.4	73.0	61.5
A	-5.5	0.6	-1.8	-4.6	-1.8	
B	-0.4		2.1	-5.3		
C	0.0		0.8	-0.4		
D	0.3		-0.1	-0.3		
E	0.5			0.5		
F	-1.5			0.7		
G	-4.1			-3.3		
Ave	101.5 ±2.4			80.5 ±2.5		
Δ [a]	-1.5			-1.8		

a: Δ is the chemical shift differences between β-CD and average chemical shift of an individual point.

Table 3.6 ^{1}H and ^{13}C chemical shifts of non-carbohydrate units.

Carbon #	RC-2 ^{13}C	^{1}H	^{13}C	SC-2 ^{1}H	$^{13}C''^{a}$	$^{1}H''^{a}$
1′	143.0		143.6		140.7	
2′	123.0	7.73	123.8	7.73	123.6	7.76
3′	127.5	7.76	127.8	7.67	127.2	7.64[b]
4′	128.2	7.93	128.2	7.93[b]	129.0	7.94[b]
5′	130.0	7.93	130.0	8.03	130.0	7.95[b]
6′	127.2	7.63	127.0	7.61[b]	127.1	7.52[b]
7′	127.4	7.52	127.6	7.66[b]	127.6	7.62[b]
8′	123.0	8.08	123.4	8.24	123.9	8.18
9′	130.4		131.1		131.3	
10′	134.4		134.7		134.8	
11′	48.0	5.76	48.9	5.68	48.5	5.60
12′	24.6	1.62	22.7	1.61	22.5	1.67
13′	157.7		157.4		157.9	

a: Chemical shifts of minor conformer are marked with double prime.
b: Chemical shifts are estimated by ^{1}H-^{1}H COSY spectrum.

Both dihedral angles of (H-1A)-(C-1)-(C-2)-(H-2A) and (H-2A)-(C-2)-(C-3)-(H-3A) are around -43° (4.0 Hz coupling constants of $J_{H1A,H2A}$ and $J_{H2A,H3A}$),[126] as shown in Fig. 3.17, suggesting that the ring of glucose A is distorted, thus allowing the **NECM** group to be centrally located in the cavity. The 4 Hz coupling constant of $J_{H3A,H4A}$ (estimated from **COSY**) also supports the distortion of glucose A.

All of the proton resonances of glucose rings B and E are shielded with H-5B exhibiting the largest upfield shift ($\Delta\delta$ 1.63). The extent of shielding of the protons in rings B and E are similar except H-6's. The upfield chemical shifts of the H-3's, H-5's, and H-6's of glucose rings B and E, suggests that these two glucose residues are located on opposite sides of naphthalene plane, and that the naphthyl group is deep within the cavity, protruding from the narrow rim (i.e., primary alcohol site). Almost 1 ppm difference in the shielding of H-6's suggests that H-6's of glucose B are on the plane of the naphthalene and H-6's of glucose E are a little bit off from the plane. Although the naphthyl ring may occupy the cavity in a variety of orientations (Figure 3.18), the upfield shifts of protons of upper rim (H-3) and bottom rim (H-5) as well as H-6's suggest that the longer C_2 symmetry axis of the naphthalene is somewhat aligned although not parallel with the C_7 symmetry axis of native **CD** as shown in Fig. 3.18(c). This orientation seems

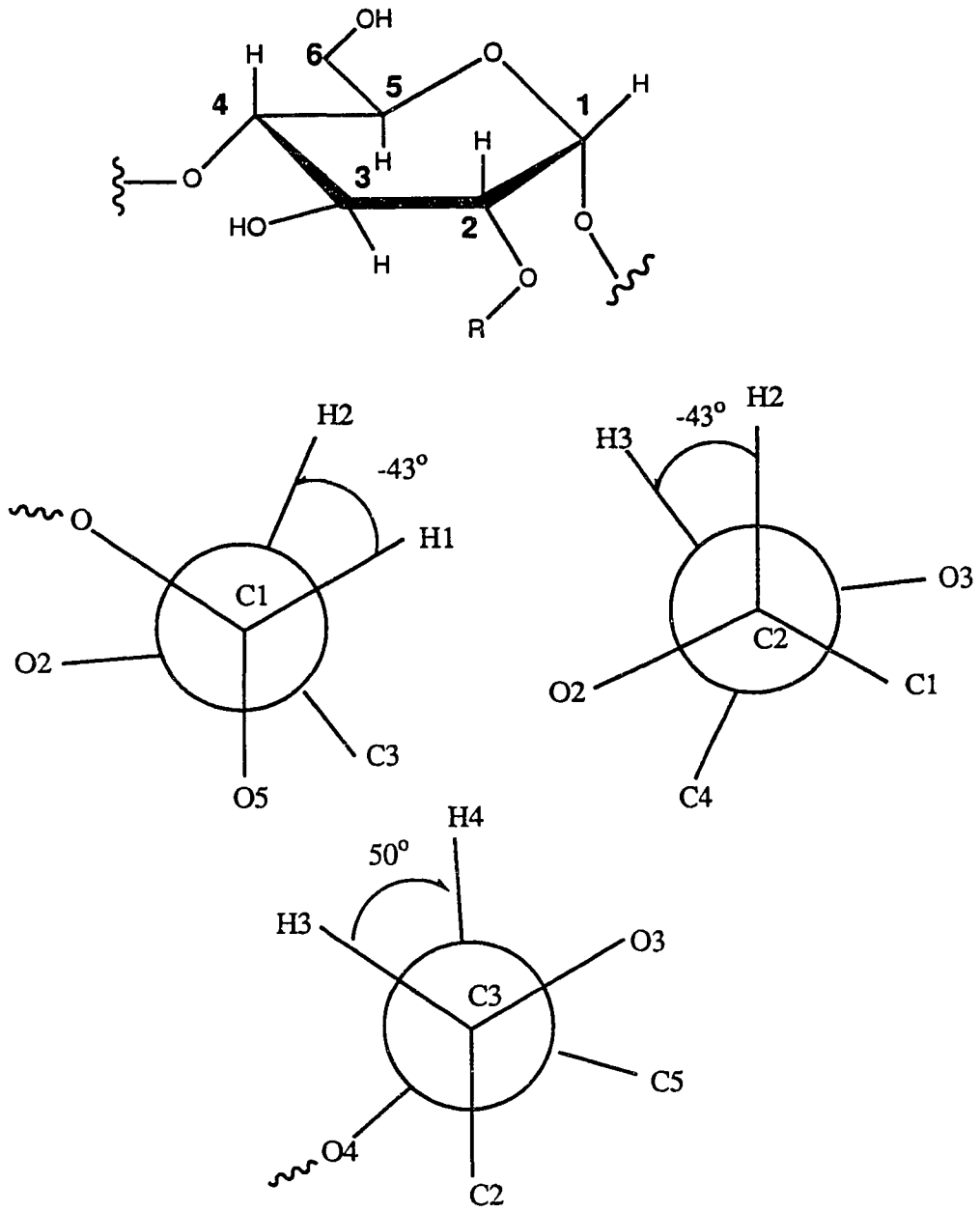

Figure 3.17 The structure of glucose A of RC-2.

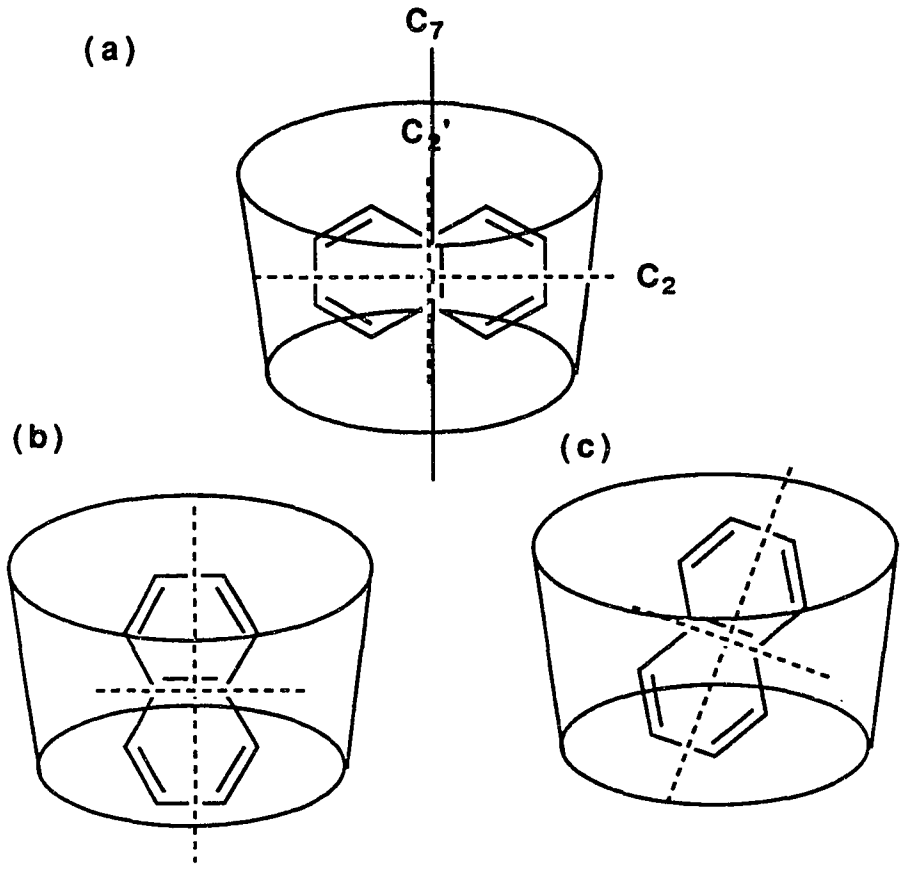

Figure 3.18 The schematic diagram showing several possible inclusion modes. (a) shorter C_2' axis of the naphthalene is parallel to C_7 axis of native CD. (b) longer C_2 axis of the naphthalene is parallel to C_7 axis of CD. (c) longer C_2 axis of the naphthalene is a little tilted.

reasonable because it results in less steric crowding of the naphthalene ring in the cavity compared to the conformation where the shorter C_2 symmetry axis of the naphthalene is aligned with the CD axis. The ^1H resonances of ring F, except H-1, are also shielded, indicating that part of ring F are in the shielding region of the naphthalene plane.

The downfield shift of the proton resonances (except H-1D) of residues C, D and G also suggest that naphthalene is in the cavity and oriented in such a way that these glucose residues face the edge of the naphthalene plane where ring current deshielding effect is maximized. The comparable magnitudes of proton shielding or deshielding of glucoses B, E, and glucoses C, G, respectively, especially for the protons orientated toward the center of the cavity, suggests that the plane of the naphthyl group is relatively parallel to the C_7 molecular axis of β-CD and that the distances from the naphthalene to those protons are similar.

The average chemical shift of the proton and carbon-13 resonances of the same position in each glucose units were also calculated and listed in Tables 3.2 and 3.3. As mentioned earlier, all seven sets of protons showed an average upfield shift with the extent of shielding on the protons orientated toward to the cavity much more prominent.

Interestingly, the average calculated chemical shift of the ^{13}C resonances of C-3's and C-5's are deshielded, relative to native **CD**. This is exactly opposite to that observed for protons attached to these carbons. The shielding of C-6 resonances is also notable which suggests that generalization of shielding or deshielding effect, as in the case of ^{1}H, is not valid for the ^{13}C resonances.

The inclusion of the naphthyl group in the cavity deduced from the **SCS** table was confirmed through homonuclear nOe's detected in the **ROESY** experiments. In Figure 3.19, strong correlations from H-8' to H-5G and from H-4' to H-5D and H-5C indicate that these protons are proximate. The medium intensity correlation from H-7' to H-6G and the stronger correlation of H-8' to H-5G than H-3G indicate that the naphthyl group is deep in the cavity as was postulated based on the **SCS** values of H-6's of glucose rings B and E discussed above. Further information regarding orientation can be derived from the correlations of the aromatic H-3' resonance to the H-3D, H-3C and H-5C resonances. The absence of any correlation between H-6' and the **CD** suggests that H-6' is away from any **CD** protons oriented to the center of the lower rim (primary hydroxyl side) of the **CD**. These observations together with other weak cross-peaks indicate that the naphthalene is in the cavity with the H-3',4' side of the ring in close proximity to residues C and D, and the

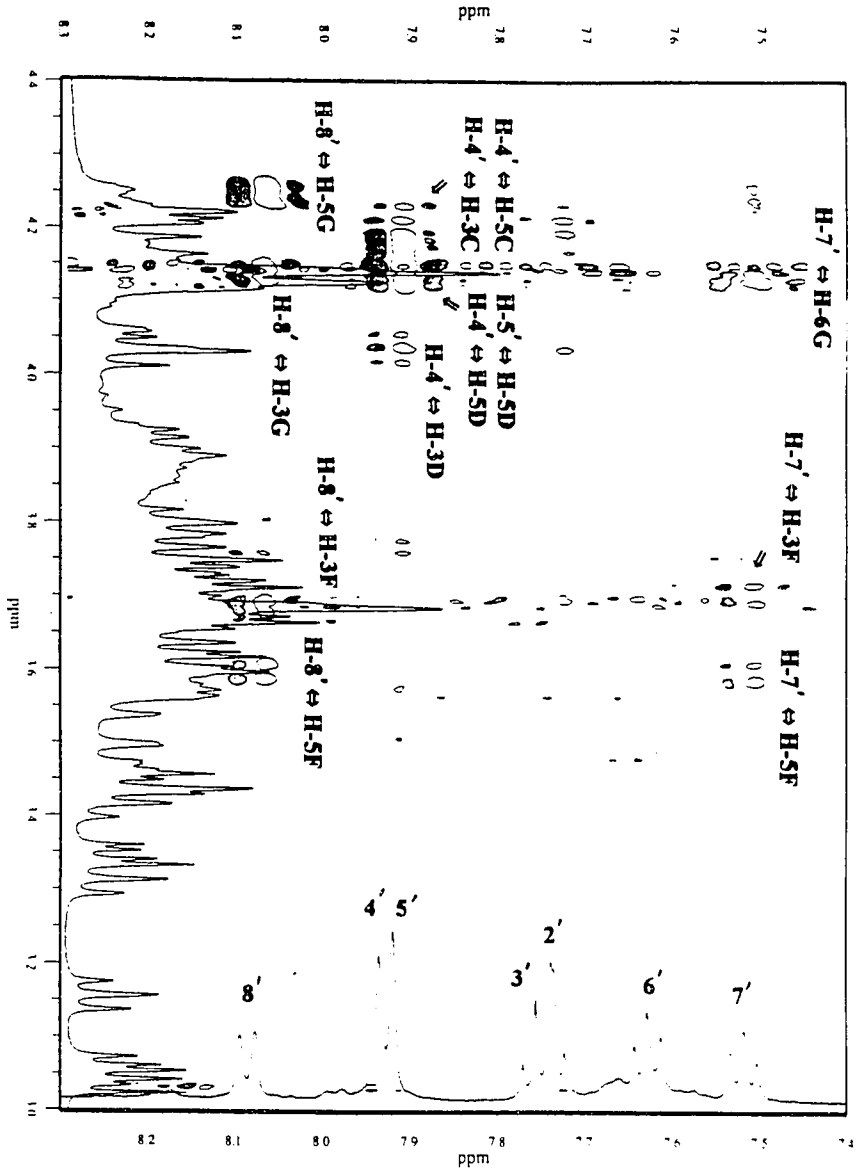

Figure 3.19 Partial ROESY spectrum of RC-2 showing the correlations between naphthyl protons and carbohydrate protons.

H-7′,8′ side of the ring close to residues G and F. In addition, the C_2 axis of naphthalene is not parellel to C_7 axis of β-CD but is skewed a little toward glucose B and C as shown in Fig. 3.20. The strong correlations of H-11′ to H-3G and H-3F indicate that the skewed nature of the C_2 axis of naphthalene is correct and that the methyl group (C-12′) is oriented outside the cavity to minimize steric crowding with any carbohydrate protons.

RC-2 may be a good model for the study of inclusion phenomena, because the naphthyl group is predominantly within the CD cavity.

3.3.4B SC-2

The well dispersed anomeric proton signals of one conformer of SC-2 and the overlap of the corresponding protons in the other conformer indicate that the naphthyl group is inside and outside the CD cavity, respectively. Inclusion of the naphthyl group in the cavity induces different magnetic environment around the CD torus and is well reflected in either the anomeric protons or carbons. In contrast, the exclusion of the naphthyl group from the cavity, removes the anisotropic influences imposed on CD protons and thus the H-1s have similar magnetic environment

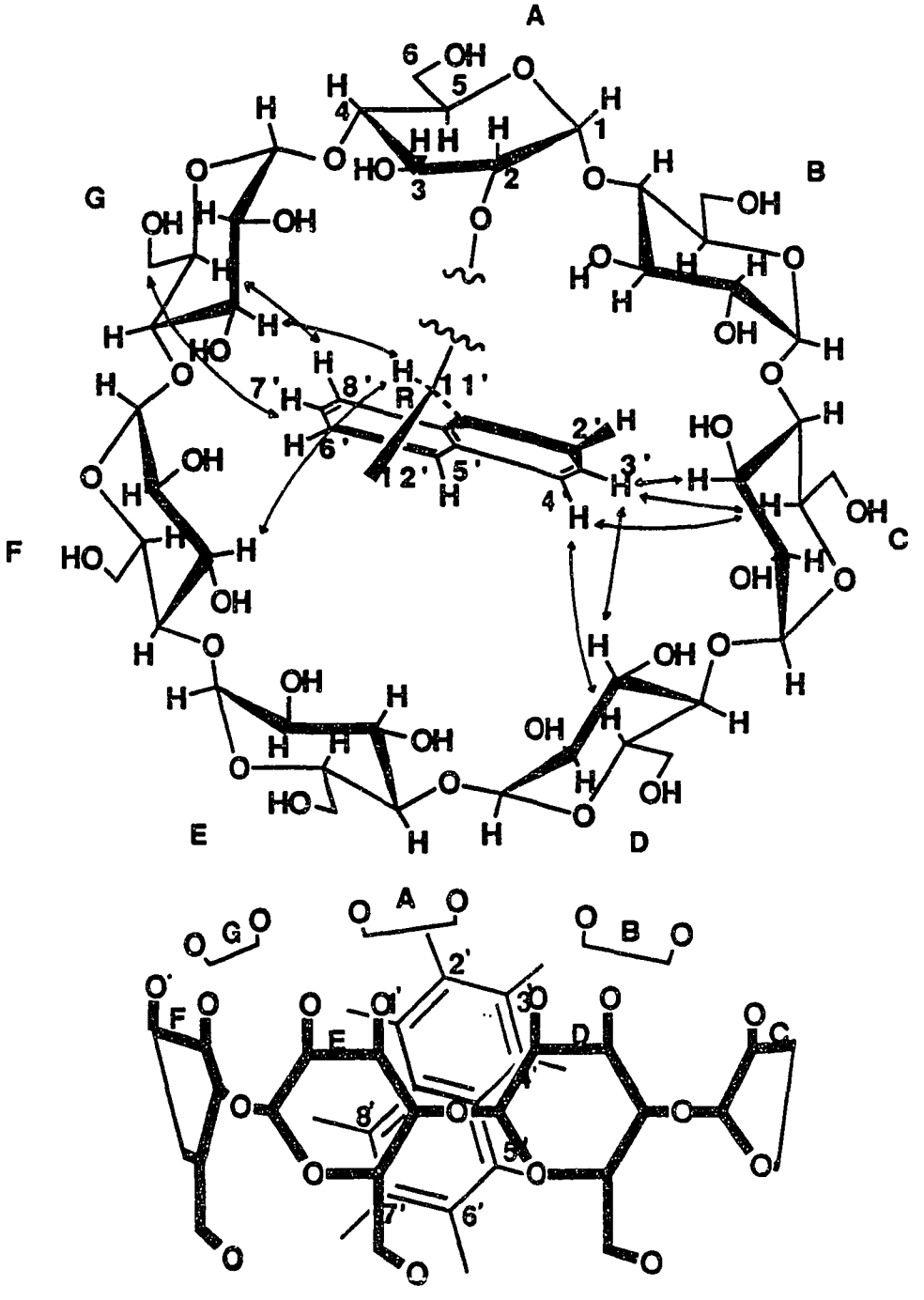

Figure 3.20 The schematic diagram illustrating a possible geometry of RC-2 deduced from the NMR experiments. (↔: nOe correlations)

resulting in clustering of these resonances in narrow range of chemical shifts. Supporting experimental evidence for the assignment of NMR resonances of the included and excluded states was obtained by examining the proton NMR spectra of **SC-2** in the various volume fractions of methanol and water. The simplified proton NMR spectrum taken in 100% methanol corresponds to the excluded conformer. The increasing population of the excluded conformer with decreasing solvent polarity is demonstrated in the series of proton NMR spectra in Fig. 3.21.

It is notable that, in general, the extent of shielding on the **CD** protons seems much smaller than those observed in **RC-2** (see Tables 3.2 and 3.4). This trend is well reflected in the average calculated chemical shifts of **RC-2** and **SC-2**. Only H-3's of **SC-2** show an appreciable shielding effect. The smaller extent of shielding of H-5's (-0.12 vs -0.39 ppm for **SC-2** and **RC-2**, respectively) and lack of prominent shielding of H-6's suggest that the naphthyl group does not penetrate the cavity as deeply as in **RC-2**.

The upfield shift of the H-3's and H-5's of glucose residues A and D of **SC-2** suggests that the naphthyl group is oriented such that residues A and D are on the plane of the naphthalene. The downfield shift of the H-3s of glucoses B, C, and F suggests that these glucoses are on the edge of the

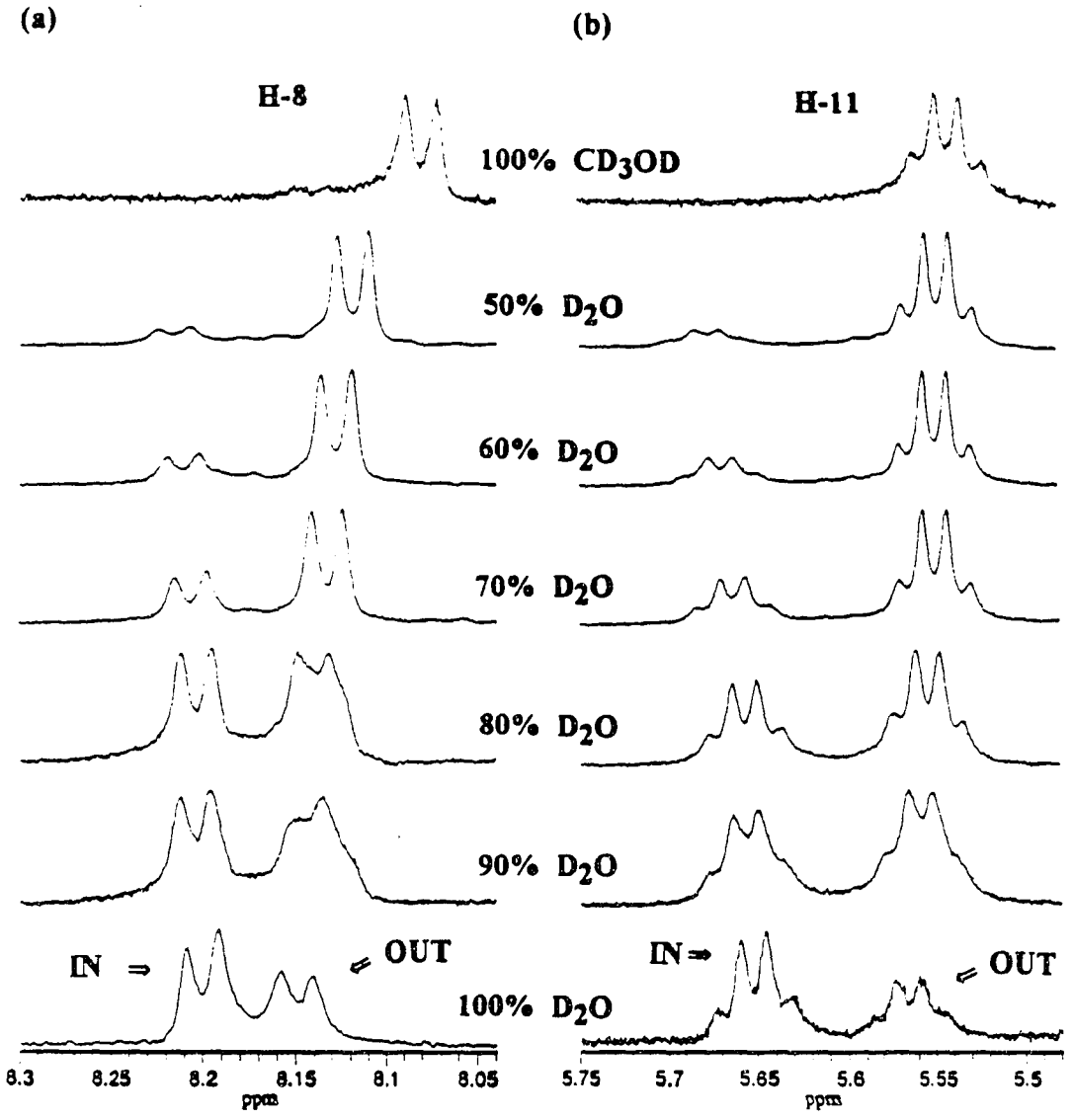

Figure 3.21 Series of ^{1}H NMR spectra of SC-2 showing the effect of solvent polarity on the populations of in- or excluded conformers.

naphthalene ring. The coupling constants of $J_{H1A,H2A}$ (4.5 Hz), $J_{H2A,H3A}$ (9.4 Hz), and $J_{H3A,H4A}$ (9.5 Hz) suggest that, unlike **RC-2**, the derivatized glucose is not appreciably distorted. The most striking feature is the 1.70 ppm shielding of H-3A. This seems to be a combination of the naphthyl and carbamate anisotropic shielding and suggests that H-3A is orientated toward the center of the naphthalene plane. Further, it suggests that the naphthalene plane is not parallel with the C_7 symmetry axis of **β-CD** but is skewed a little toward glucose A such that the distance from the naphthyl plane to H-3A is shorter than that to H-3D as shown in Fig. 3.22. This skewed orientation of the naphthalene plane and shallow penetration into the cavity may explain why the extent of shielding on glucose D is not as strong as on glucose A and why there is less prominent overall shielding or deshielding in **SC-2** than in **RC-2**. One face of the naphthalene seems to be oriented toward the outside of the cavity.

The inclusion state was further investigated by **ROESY** experiment. The correlations between the aromatic protons and carbohydrate protons (e.g. H-4′ and H-5′ with H-3F and H-3E; H-7′ and H-8′ with H-3B and H-3C) in Figure 3.23 indicate that naphthalene is in the cavity with the H-4′,5′ side of naphthalene between E and F, and the H-7′,8′ side between B and C. The stronger correlation of H-8′ with H-3B

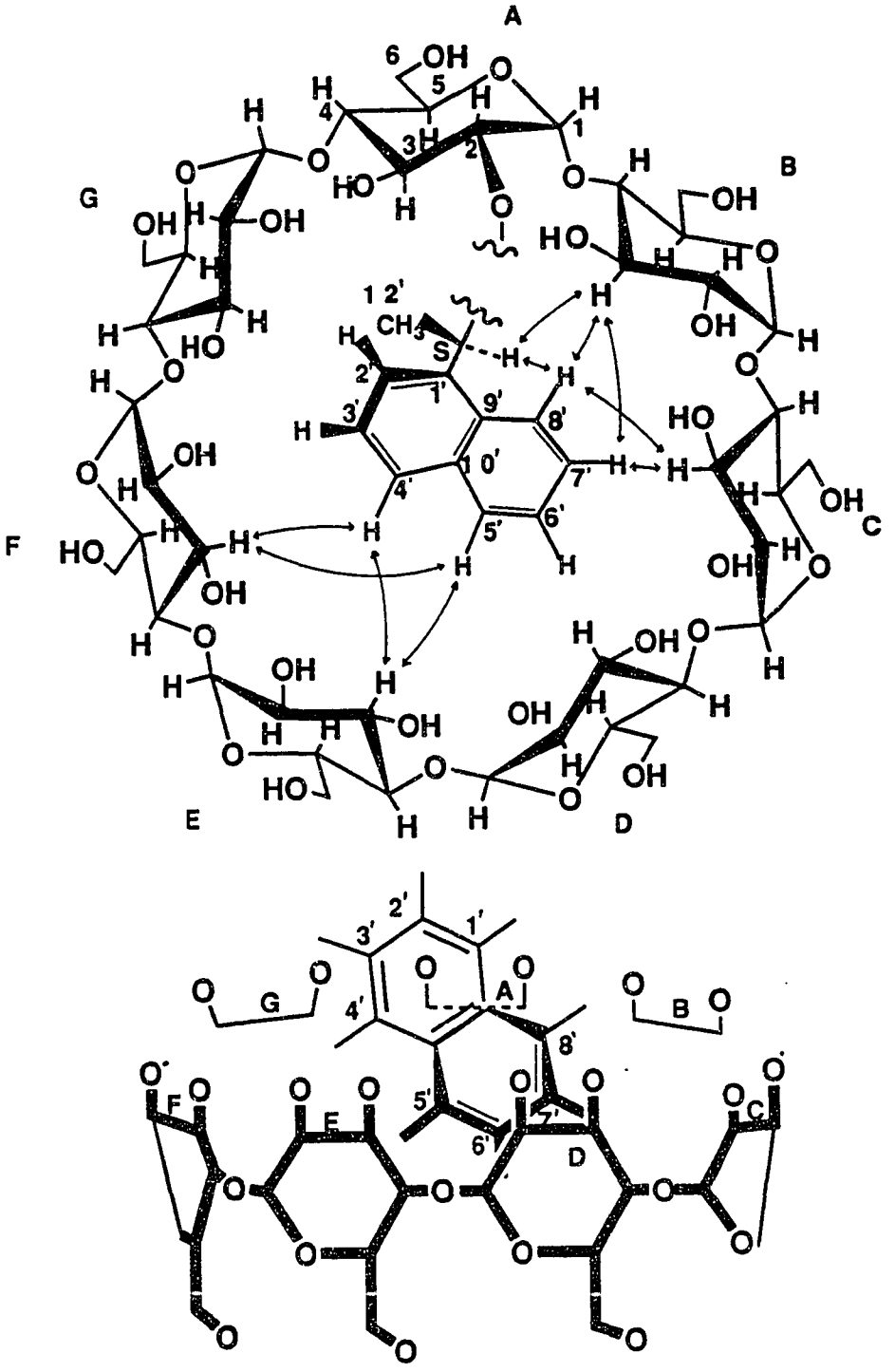

Figure 3.22 The schematic diagrams of SC-2 deduced from the NMR experiments. (↔: nOe correlations)

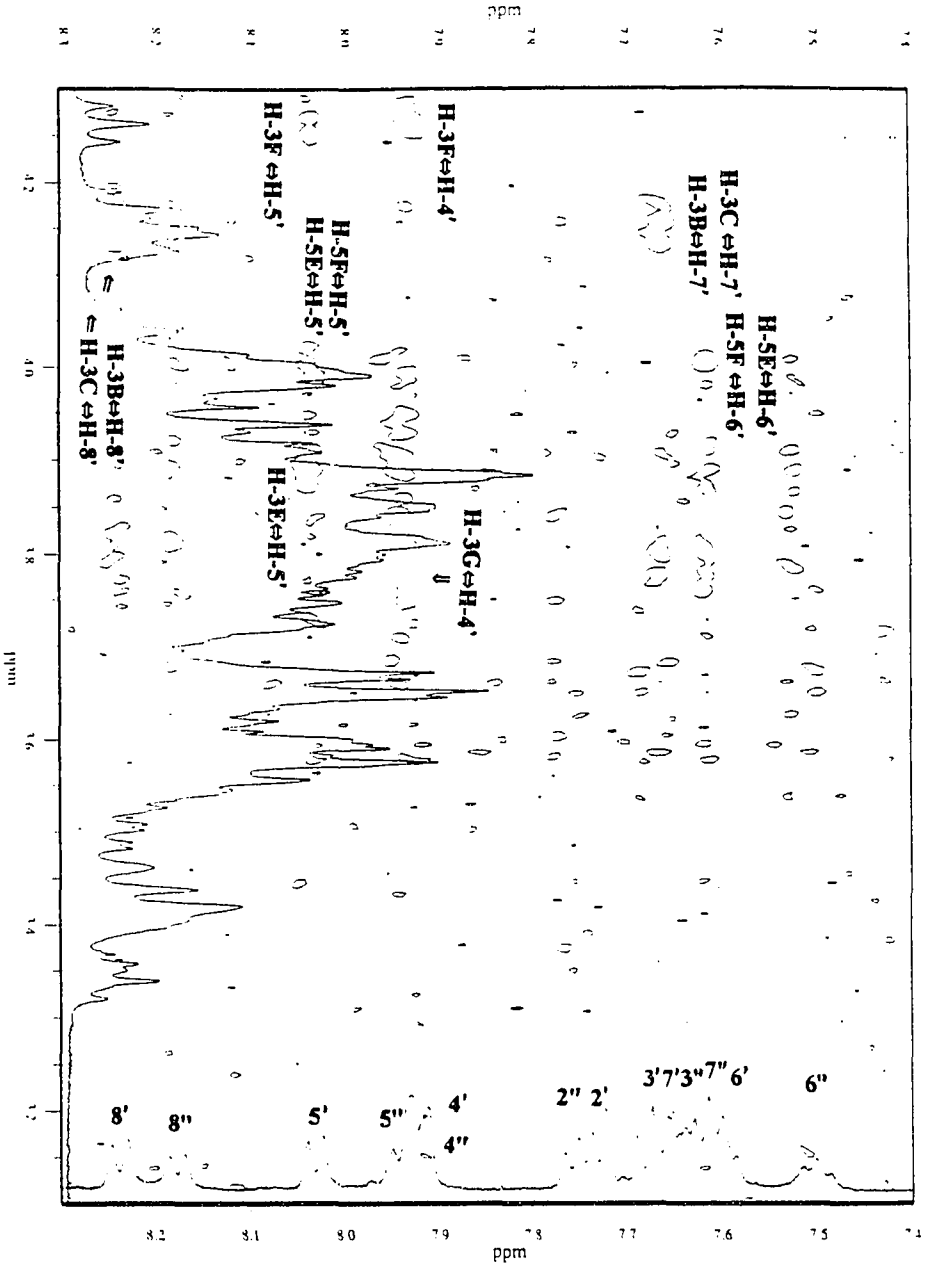

Figure 3.23 Partial ROESY spectrum of SC-2 showing the correlations between naphthyl protons and carbohydrate protons.

and H-3C than H-8′ with H-5B and H-5C also indicates that the naphthyl group does not penetrate the cavity as deeply as in **RC-2**. The strong correlation of H-11′ with H-3B indicates close proximity of these two protons. No observable correlation between the methyl group (C-12′) and carbohydrate protons indicates that the methyl group is orientated outside the cavity. The strong correlation of H-11′ with H-8′ precludes the possible rotational conformer along the single bond between C-11′ and C-1′ of the naphthyl group. The lack of strong correlations between protons of the minor conformer (aromatic H-2", 3", 5", and 6") and any carbohydrate protons suggests that the naphthyl group is outside the cavity.

3.3.4C The differences in the conformations of RC-2 and SC-2

Considering that **RC-2** and **SC-2** differ in only one chiral center, the differences in the inclusion states are remarkable. To better understand this phenomena, it is required to know the role of the carbamate linkages in the overall geometry of these molecules.

The geometry of **RC-2** including all of the naphthalene protons except the carbamate linkage itself is well understood utilizing the **SCSs** and **ROESY** correlations as

described earlier. Pirkle reported previously that diastereomeric carbamates, derived from NEIC, existed preferentially as the Z-rotamer.[127] With this rotameric stability in mind, the carbamate linkage was constructed as shown in Figure 3.24. Possible hydrogen bonding between the carbonyl oxygen and the C-3B-OH is shown using the broken line. Stabilization through this hydrogen bonding and deep inclusion of the naphthyl group into the cavity overcomes the strain energy induced by distorting glucose A. By inverting the configuration of C-11', a hypothetical structure of SC-2 was constructed and this structure reveals possible crowding of the methyl group (oriented into the cavity in this hypothetical structure) near glucoses F and G. This possible steric crowding may explain, in part, why SC-2 undergoes totally different inclusion as described below.

Using similar arguments as in the case of RC-2, the carbamate linkage was connected to construct SC-2 as shown in Figure 3.25. In this case, two possible hydrogen bondings are noted between C-3A-OH to the carbonyl oxygen and C-3B-OH to C-2A-O. The stabilization provided by the two hydrogen bondings may hinder the naphthyl ring from being centered in the cavity. Inverting the configuration of C-11' reveals possible crowding of the methyl group (oriented into the cavity in this hypothetical structure)

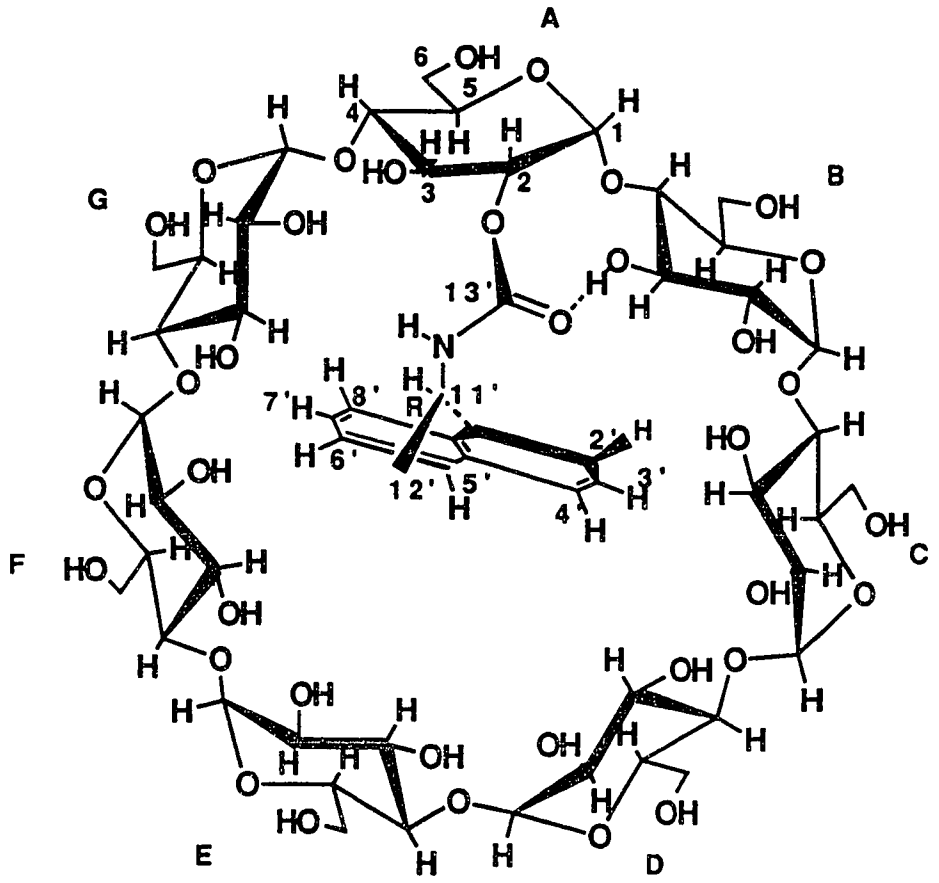

Figure 3.24 Proposed structure of RC-2 including carbamate linkage and possible hydrogen bonding between carbamate linkage and carbohydrate.

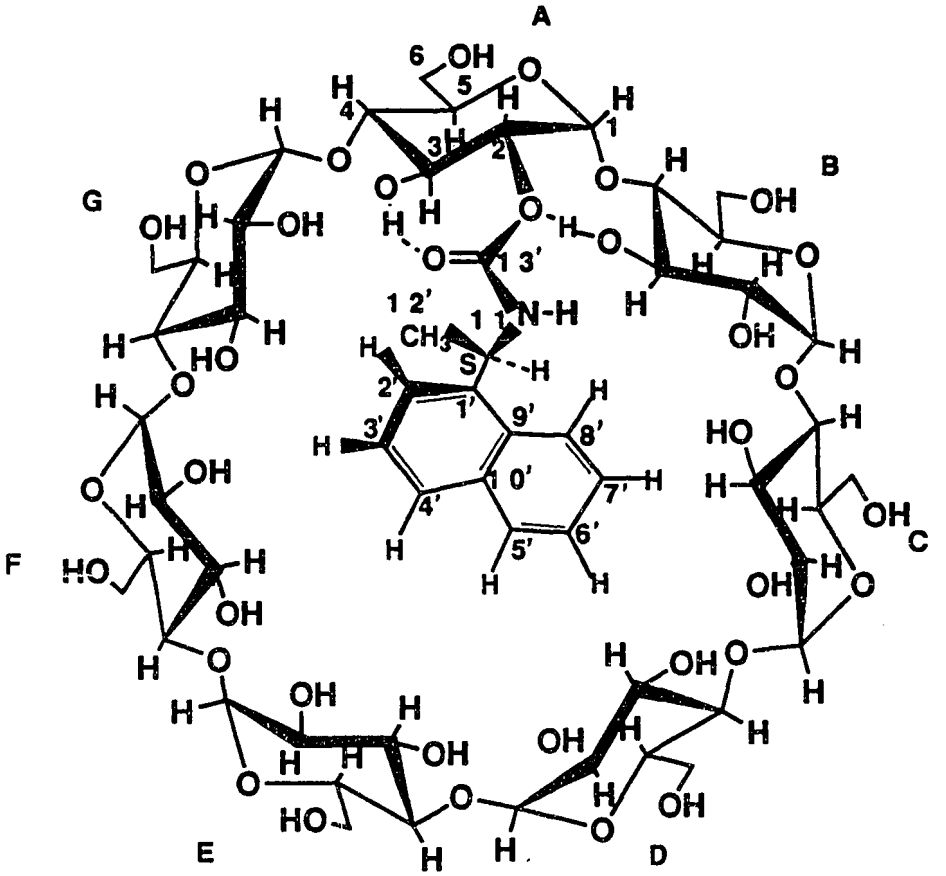

Figure 3.25 Proposed structure of SC-2 including carbamate linkage and possible hydrogen bondings between carbamate linkage and carbohydrate.

near glucoses A and B, thus producing a different orientation of the naphthyl ring with respect to the cavity than observed with **RC-2**.

3.3.5 Molecular modeling

Stick models of the energy minimized structure of **RC-2** by molecular mechanics calculation are shown in Figure 3.26. The **CD** torus appears to be more oval in shape than in the native **CD** in order to accommodate the naphthyl moiety. The dihedral angles of O=C-N-H and H-(C-11′)-N-H are 147° and 17°, respectively. The tilted orientation of the longer C_2 symmetry axis of the naphthalene is obvious with the H-7′,8′ side of the naphthalene ring between glucoses F and G and with the H-2′,3′ side of the naphthalene ring between glucoses C and D. The glucose residues C, D, F, and G were pushed away from the center of the cavity to lessen the steric hindrance imposed by the inclusion of the naphthyl moiety. Most of the structural features of inclusion mode of the naphthyl group in the cavity by the computer generated model are supported by the experimental observations discussed above. The orientation of the carbamate is the same as that proposed in the NMR section thus enabling hydrogen bonding between the C-3B-OH to the carbonyl oxygen. One notable discrepancy between the NMR and calculated model is that the dihedral angles of (H-1A)-

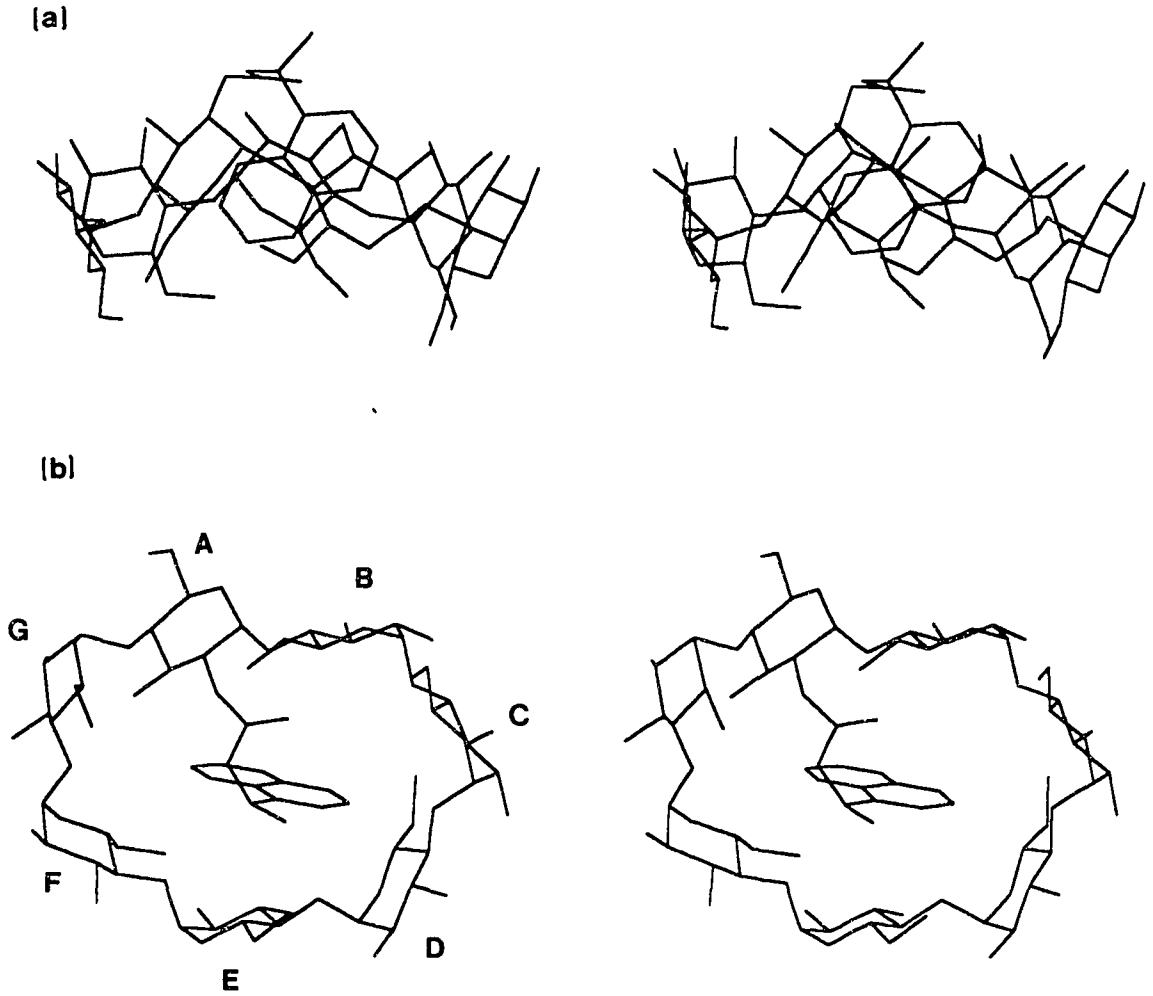

Figure 3.26 Computer generated stereographic views of RC-2. (a) side view with secondary hydroxyl side up. Glucoses A and B are back. Glucose E is in front. (b) View from the secondary hydroxyl side. Hydrogen atoms are omitted for clarity.

(C-1)-(C-2)-(H-2A) and (H-2A)-(C-2)-(C-3)-(H-3A) are 57° and -179°, respectively, in the calculated model, implying that the distortion of glucose A is much less than that deduced from NMR experiment. Of course, the computer generated model does not consider solvent effects.

Stick models of the energy minimized structure by molecular mechanics calculation of **SC-2** are shown in Figure 3.27. Computer modeling of **SC-2** reveals two equally stable isomers in which the **NECM** group is positioned outside the cavity. The two conformers are rotameric isomers along the single bond between C-11′ and C-1′ of the naphthyl group. The two conformers, cis and trans with respect to H-11′ and H-8′, sit atop the **CD** cavity, as shown in Figure 3.27 (a) and (c). The **CD** torus is not twisted in these two structures. The orientation of the naphthyl group of the trans conformer is much like that deduced from NMR experiment. The distances between H-5′ of the the naphthyl group and H-3F and H-3D of the calculated structure are 803 pm, and 306 pm, respectively. Of course, this geometry does not explain the correlation observed between H-5′ and H-3F and no correlation between H-5′ and H-3D in **ROESY** spectra. No structure similar to that deduced from the NMR experiment was observed. The most probable explanation of the failure of the computer modeling experiment to produce the included conformer may be attributed to the lack of the consideration

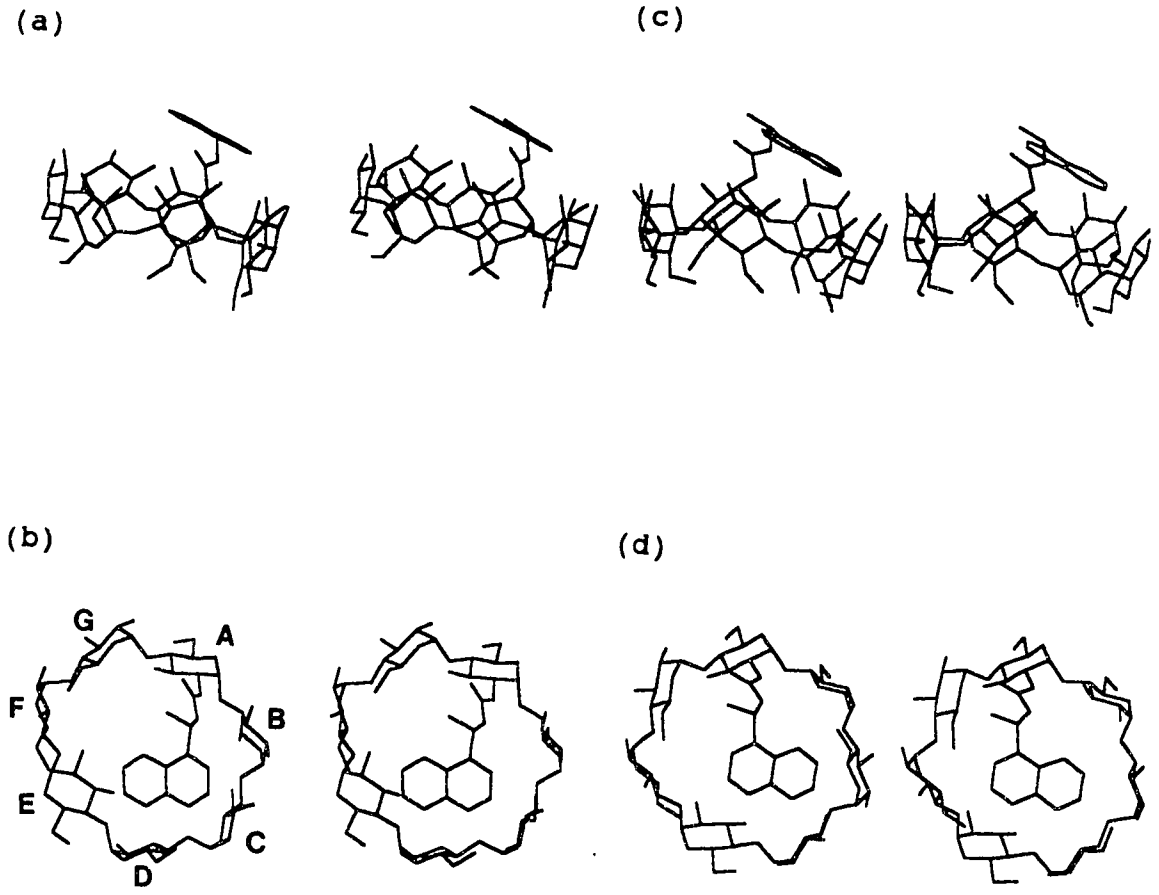

Figure 3.27 Computer generated stereographic views of SC-2. Side views of (a) cis conformer and (c) trans. Top views of (b) cis and (d) trans.

of the solvent effect in the molecular mechanics calculation. Hydrophobic interactions no doubt drive the naphthyl moiety into the cavity, thus leading to the structure which is similar to that deduced from NMR experiments. The calculated dihedral angles of O=C-N-H and H-(C-11')-N-H of the cis conformer are -180° and 77°, respectively. The dihedral angles of (H-1A)-(C-1)-(C-2)-(H-2A) and (H-2A)-(C-2)-(C-3)-(H-3A) are 48° and -170°, respectively, implying no significant distortion of glucose A. These two conformers could represent the 40 % populated excluded conformer. The single set of ^{1}H resonances for these conformers suggests rapid interchange between the cis and trans conformers.

3.4 The effect of solvent polarity on the populations of in- or excluded conformers

The increasing populations of the excluded conformer for both **RC-2** and **SC-2** with decreasing solvent polarity is demonstrated in the series of ^{1}H NMR spectra taken in the various volume fractions of methanol and water as shown in Figure 3.28 (only the region of H-11' is shown in the figure) for RC-2. The simplified spectrum in the higher volume fraction of methanol corresponds to the excluded conformer. The relative population ratio (excluded over included conformers K) was obtained through the integration

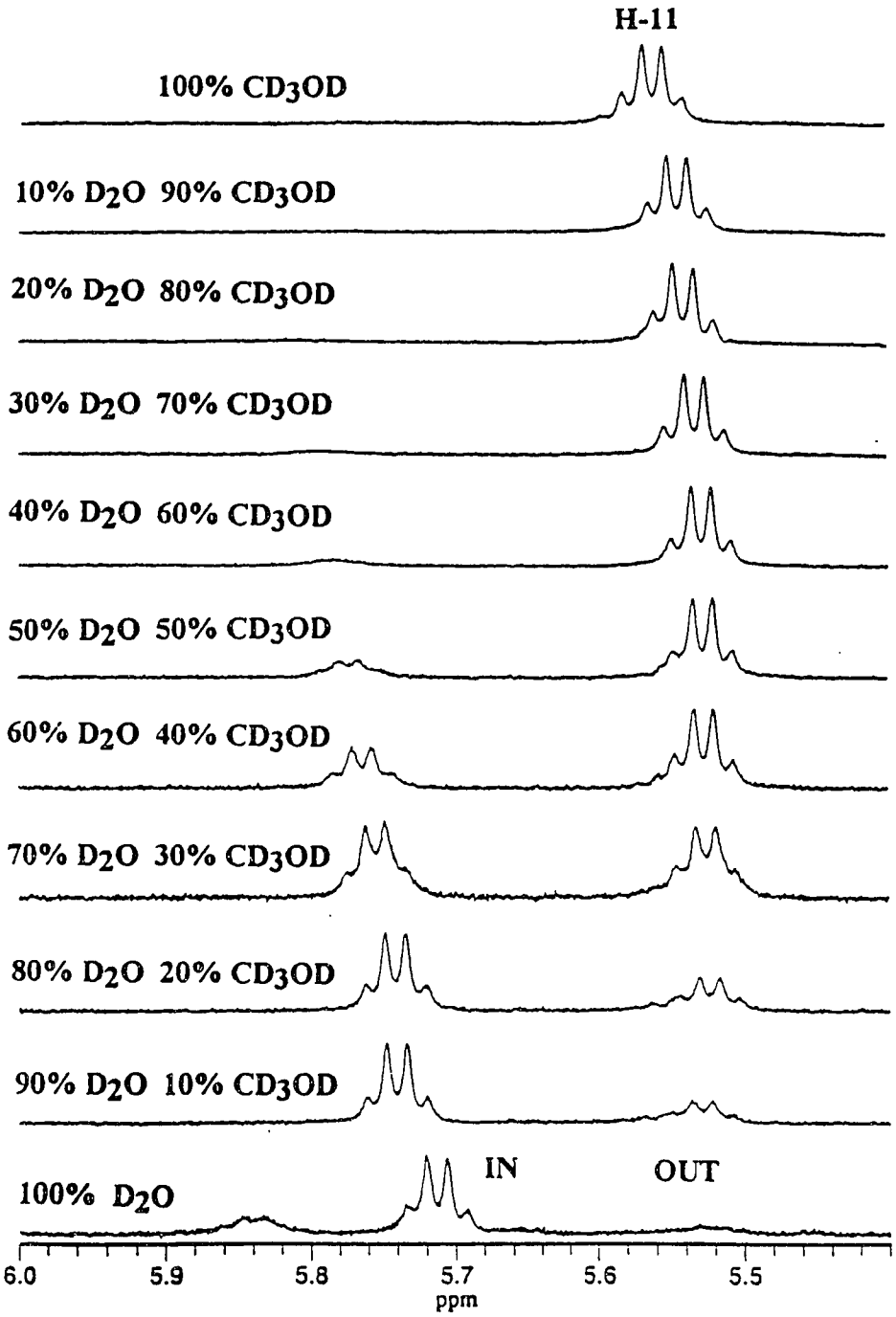

Figure 3.28 Series of ^{1}H NMR spectra of RC-2 in the various volume fractions of methanol and water.

Table 3.7 The equilibrium dependence of included and excluded conformers of RC-2 in various volume fractions of methanol in methanol/water system. (K = [OUT]/[IN])

volume % of MeOH	K (IN ⇔ OUT)	ln K
0%	0.12	-2.12
10%	0.40	-0.92
20%	0.56	-0.58
30%	1.06	0.06
40%	1.86	0.62
50%	3.74	1.32
60%	8.87	2.18
70%	20.48	3.02
100%	∞	

Correlation parameters: ln K = 0.069 volume % of methanol - 1.96
correlation coefficient r = 0.99

Table 3.8 The equilibrium dependence of included and excluded conformers of SC-2 in various volume fractions of methanol in methanol/water system. (K = [OUT]/[IN])

volume % of MeOH	K (IN ⇔ OUT)	ln K
0	0.77	-0.26
10	1.28	0.25
20	1.43	0.36
30	2.43	0.89
40	3.68	1.30
50	5.59	1.72
100	∞	

Correlation parameters: ln K = 0.039 volume % of methanol - 0.26
correlation coefficient r = 0.99

of H-11' resonances and listed in Tables 3.7 and 3.8 for **RC-2** and **SC-2**, respectively. Good linear correlations were found between ln K vs volume % of methanol as shown in Figure 3.29 and the curve fitting data are listed in the Tables 3.7 and 3.8. The trend of the increasing population of the excluded conformer with decreasing solvent polarity is quite understandable however, detailed thermodynamic treatment of the correlation data is subject to future work.

3.5 Chiral recognition of RC-2 and SC-2 toward several 3,5-dinitrobenzoylated amino acids

Chiral recognition of **RC-2** and **SC-2** was studied for 3,5-dinitrobenzoylated (**3,5-DNB**) phenylglycine (**PG**), phenylalanine (**PA**), and homophenylalanine (**HPA**) by using ^{1}H NMR. The structures of the **3,5-DNB** amino acids used in the study are shown in Figure 3.30. In deuterated methanol, both **RC-2** and **SC-2** show splitting of the ^{1}H resonances of the **3,5-DNB** group of **3,5-DNB-PG**, suggesting diastereomeric complexation as shown in Figure 3.31. The splitting of the ^{1}H resonances of the **3,5-DNB** groups of **PA** and **HPA** were also observed when they are complexed in the methanolic solution with **RC-2** and **SC-2**. Although the potential chiral distinction is apparent in methanol, more work is needed to study the chiral interaction mode in detail. This is subject to future work.

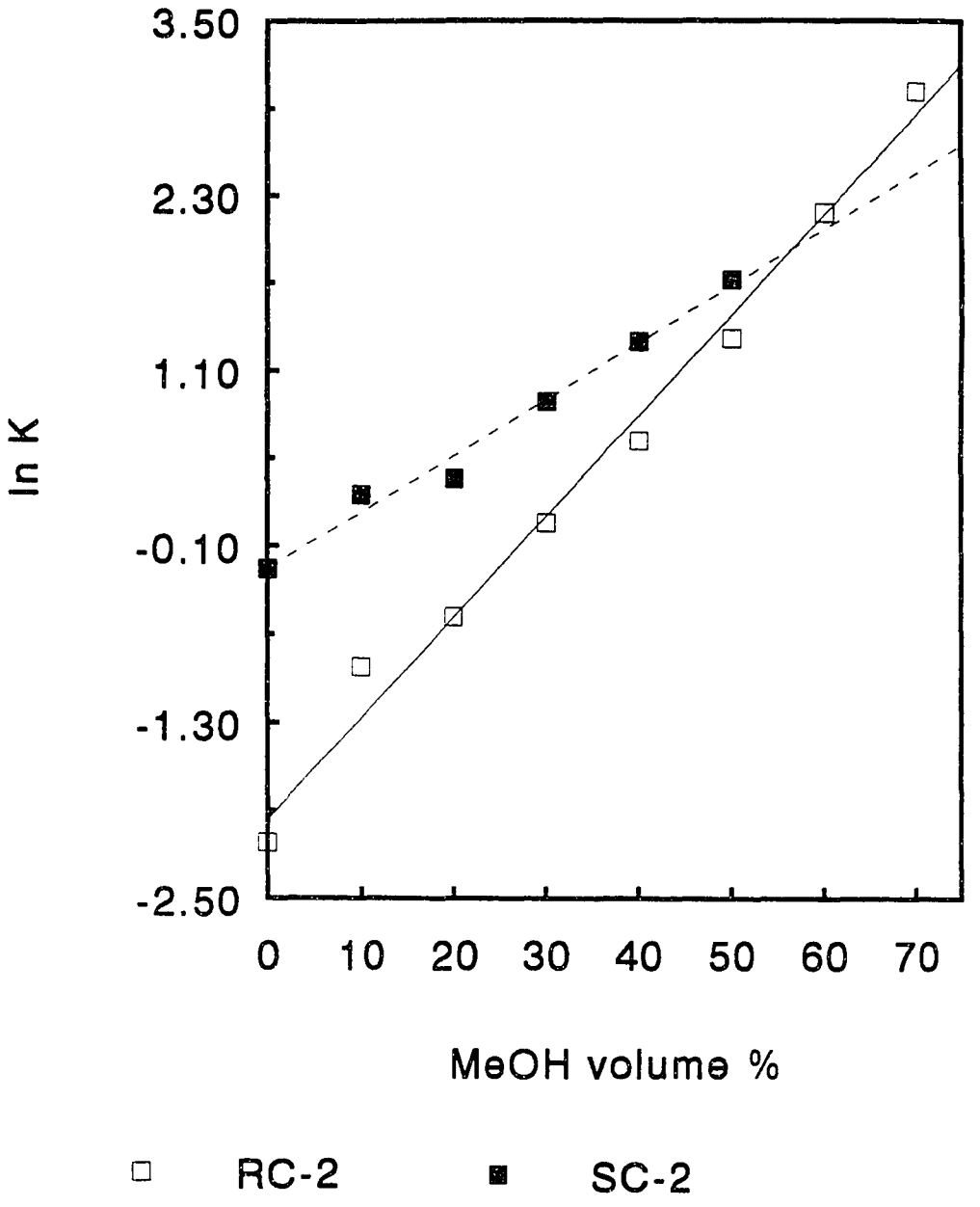

Figure 3.29 Linear correlations between ln K vs volume % of methanol for RC-2 and SC-2.

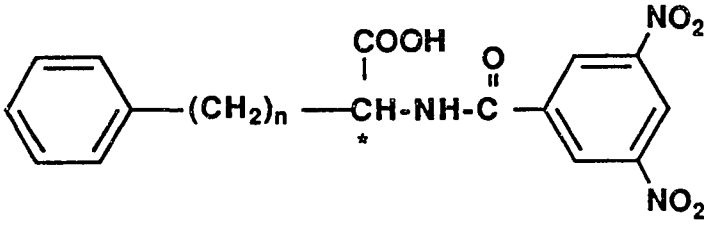

3,5-DNB-HPA n = 2
3,5-DNB-PA n = 1
3,5-DNB-PG n = 0

Figure 3.30 The structures of the 3,5-DNB derivatives of homophenylalanine, phenylalanine, and phenylglycine.

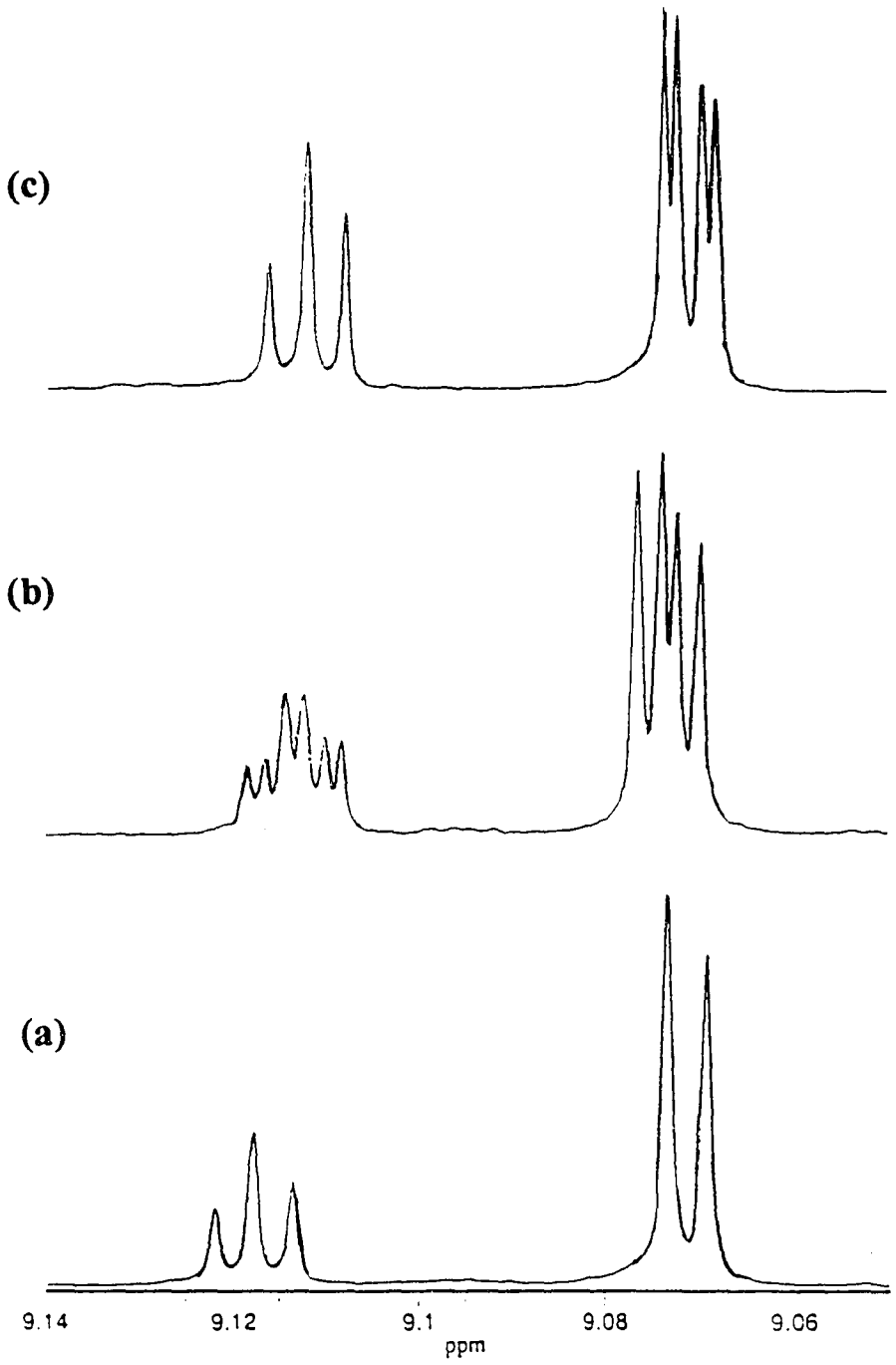

Figure 3.31 The partial NMR spectra of protons of 3,5-DNB group of racemic 3,5-DNB-phenylglycine (a), and complexed with SC-2 (b) and with RC-2 (c).

CHAPTER 4

STUDY OF NAPHTHYLETHYLCARBAMOYLATED β-CYCLODEXTRINS BY CAPILLARY ZONE ELECTROPHORESIS (CZE)

4.1 Introduction

As mentioned previously, there are several ways to achieve chiral separations including crystallization, and various forms of chromatography. Capillary zone electrophoresis (CZE), a rapidly expanding separation technique, has been demonstrated as a powerful chiral separation method.[39,40] In CZE, either addition of a chiral mobile phase additive (CMA) to buffer or fixation of chiral selector into the capillary wall is a common method for the resolution of chiral compounds.[128]

Among several chiral selectors, native CD and their derivatives have been widely used as chiral additives. Among many possible derivatized CDs, permethylated CD have been the most widely used.[58-60]

In this study, monosubstituted naphthyethyl-carbamoylated β-CDs (NEC-β-CDs) as well as native β-CDs were employed as CMA in CZE. Through the use of regio-isomerically pure chiral selectors, it was possible to study the chiral recognition of these new materials. The 3,5-

dinitrobenzoyl (3,5-DNB) derivatives of homophenylalanine (HPA), phenylalanine (PA) and phenylglycine (PG) were chosen for the study because these three amino acids are homologues and their retention data on various NEC-CD-CSPs were readily available.[35-37]

First, interaction between the analytes and native β-CD was studied and compared with those studied from β-CD-CSP. Second, evaluation of interaction between the analytes and NEC-β-CDs was possible by comparing those with various NEC-CD-CSPs.

4.2 Experimental

4.2.1 Chemicals

β-CD was obtained from Pfanstiehl Laboratories, Inc., (Waukegan, IL, U.S.A.). β-CD was dried overnight under vacuum in a drying gun using toluene and phosphorous pentoxide. (R)-, (S)-1-(1-naphthyl)ethylisocyante (NEIC), NaH, N-(3,5-dinitrobenzoyl)-phenylglycine (3,5-DNB-PG) and underivatized phenylalanine (PA), homophenylalanine (HPA), 3,5-dinitrobenzoyl chloride and all deuterated solvents were obtained from Aldrich Chemical Co. (Milwaukee, WI).

4.2.2 Synthesis of 3,5-DNB-HPA, and PA

3,5-DNB-HPA and PA were synthesized by treating 10 mg of appropriate amino acids with 15 mg of dinitrobenzoyl chloride in acetone at 60 °C. 3,5-DNB-PA reaction product was further purified using HPLC under reversed phase conditions.

4.2.3 Electrophoretic conditions

A Waters CZE Quanta 4000 capillary electrophoretic system was used. The length of capillary from anode to detector was 51.4 cm and 7.6 cm from detector to cathode. The I.D. of the capillary was 75 μm. The UV detector was operated at 214 nm. The samples were hydrostatically (2 sec) introduced into the anodic end of the capillary. The analysis was done at ambient temperature (22 ± 1°C). A positive voltage of 15 KV was used for all the electrophoretic analysis. A phosphate buffer (50 mM, pH 6.5) was used unless otherwise specified.

The concentration of amino acids was 0.1 mg/ml, when using native β-CDs as a chiral additive and 1 mg/ml when using NEC-CDs as the CMA. The higher analyte concentration in the presence of the derivatized CD was necessary because of the presence of strong background UV absorption from the

naphthalene chromophore. The concentration of **β-CD** was varied from 0-17 mM for determination of the complexation constants. Over this range, no additive (e.g., urea) was needed to solublize the **CD**. The concentration of **NEC-CDs** used as chiral additives, was 9.7 mM. When **3,5-DNB-AAs** were used as **CMA** (**3,5-DNB-PA**: 8.4 mM; **3,5-DNB-HPA**: 6.7 mM; **3,5-DNB-PG**: 8.7 mM), the concentrations of the **NEC-CDs** and **β-CD** were 0.3 mg/ml and 5 mg/ml, respectively.

4.3 Results and discussion

4.3.1 Theory: calculation of complexation constant

As described by Guttman et al.,[65] the electrophoretic mobility (μ) of a solute can be represented by a weighted sum of mobility in free state and that in complexed state as shown in (1.13)

$$\mu = \frac{\mu_f + K[CD]\,\mu_c}{1 + K[CD]} \qquad (1.13)$$

Rearrangement of (1.13) yields a clear relationship between [CD], the complexation constant and the mobility as shown in (4.1)

$$[CD] = \frac{(\mu_f - \mu)}{K(\mu - \mu_c)} \qquad (4.1)$$

The vector diagram for the migration behaviour of a negatively charged analyte in a buffer with β-CD as CMA was shown in Figure 4.1. Application of (4.1) to the calculation of the complexation constant from the experimental data requires that the electroosmostic flow (EOF) be considered. Because the electrophoretic mobility is a vector quantity, the apparent mobility of an analyte, μ_{app}, is the vector sum of the electroosmotic mobility (μ_{eof}) and the electrophoretic mobility (μ_{ep}) as shown below

$$\mu_{app} = \mu_{eof} + \mu_{ep} \qquad (4.2)$$

Expressing the mobility in terms of the migration time (t_{app}), the length of the capillary from injector to detector (L_d), the length from injector to the cathodic end of the capillary (L_t), and the applied potential (V), with rearrangement of (4.2) yields (4.3)

$$\mu_{ep} = \frac{t_{ep}\, L_d\, L_t}{t_{app}\, t_{eof}\, V} \qquad (4.3)$$

Substitution of (4.3) into (4.1) yields the relationship between [CD], the complexation constant and the migration times as shown in (4.4)

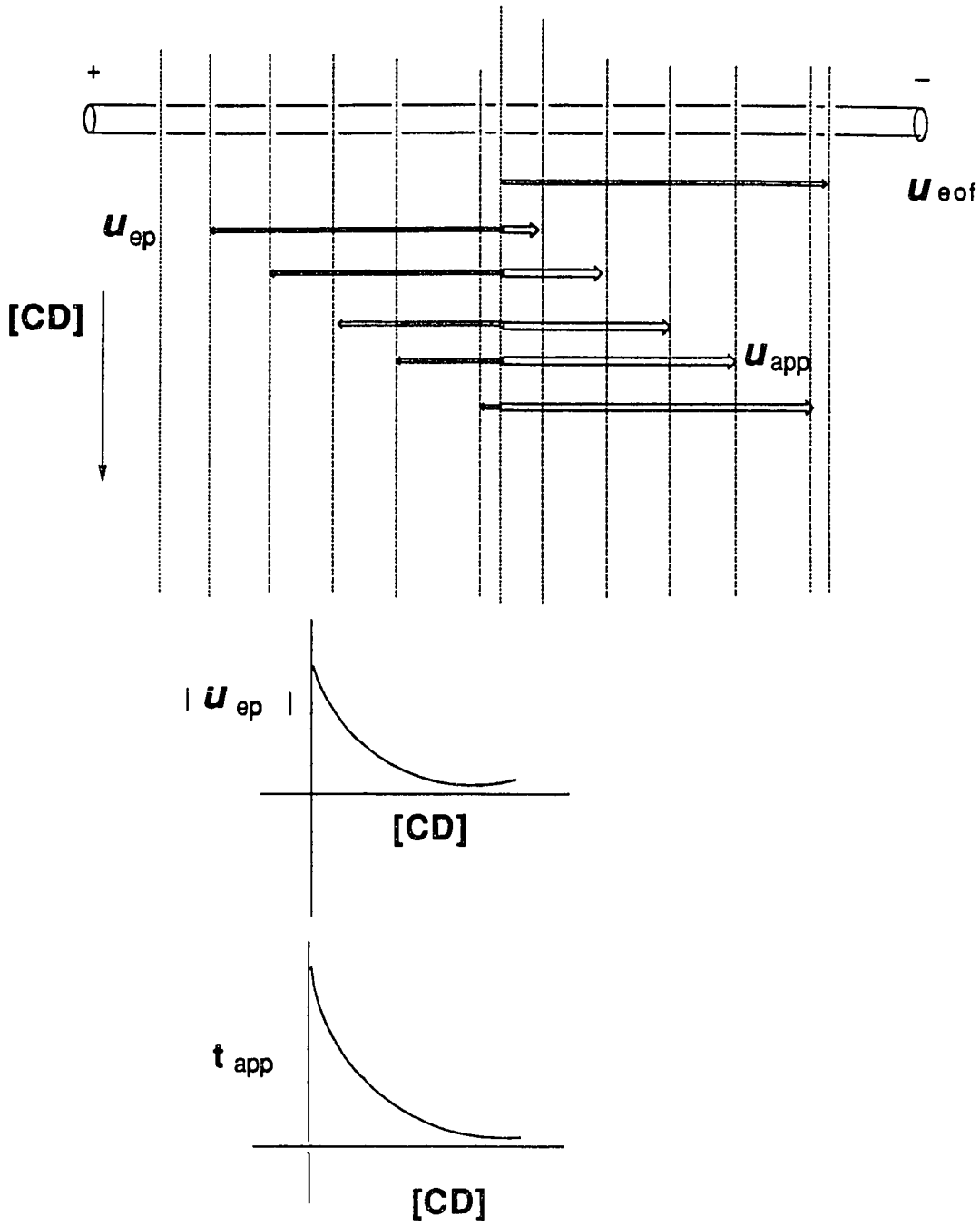

Figure 4.1 Vector diagram for the migration behaviour of a negatively charged analyte in a buffer with β-CD as CMA.

$$[CD] = \frac{t_{app,c}\ (t_{ep,f} - t_{ep})}{K\ t_{app,f}\ (t_{ep} - t_{ep,c})} \qquad (4.4)$$

where $t_{app,c}$: total electrophoretic migration time of the complex; $t_{app,f}$: measured migration time of the analyte in the absence of CD; $t_{ep,f}$: net electrophoretic migration time of an uncomplexed analyte; $t_{ep,c}$: net electrophoretic migration time of complexed species and t_{ep} is the net electrophoretic migration time of the analyte at any concentration of **CMA**, defined as $t_{app} - t_{eof}$. To obtain the association constant from the slope of $(t_{ep,f} - t_{ep})/(t_{ep} - t_{ep,c})$ vs. [**CD**], the complexed state migration time must be estimated from extrapolation to the infinite concentration of the graph of t_{ep} vs [**CD**]. A linear least square fitting program based on (4.4), written in BASIC for an **IBM PC**, allowed determination of the best correlation coefficient and $t_{ep,c}$. According to Altria et al.[129] in the concentration range of **β-CD** used in this study, the viscosity of the electrolytes increased by only 3%. Therefore, the effect of [**CD**] on electroosmotic flow was neglected.

4.3.2 β-CD as a chiral mobile phase additive (CMA)

Typical electropherograms of the **3,5-DNB-** derivatives of **HPA**, **PA**, and **PG** with and without **β-CD** as a chiral

selector are shown in Figure 4.2. The electrophoretic data are listed in Table 4.1. **PA** was generally the best separated and **PG** was not separated when **β-CD** was employed as **CMA**. The dependence of the retention behaviour of the three **3,5-DNB-AAs** on [**CD**] (up to 17.3 mM) is shown in Figure 4.3.

At pH 6.5, the analytes are all negatively charged and resist the electroosmotic flow. The decrease in the migration time of analytes with increasing concentration of **CD** is evident from Table 4.1 and Figure 4.3. This trend can be understood because **CD**, as a neutral molecule, migrates with the electroosmotic flow. The higher the complexed fraction of analyte, the more the migration rate of the neutral **CD** is reflected in the mobility of the analyte.

Linear plots using eq. (4.4) for the calculation of binding constant are shown in Figure 4.4. Association constants are listed in Table 4.2. Enantioresolution of **HPA** and **PA** over the concentration range of **CD** is shown in Figure 4.5. The existence of an optimum concentration of a chiral additive for the best chiral resolution of analytes was previously noted by Wren et al.[66,67] According to Wren et al.,[66] the optimum concentration of **CD** for **HPA** and **PA** are predicted to be 2.1 and 4.9 mM (eq. 1.16). In the present study, the optimum concentration of **CD** for the best chiral resolution of **HPA** and **PA** was found to be approximately 5 mM,

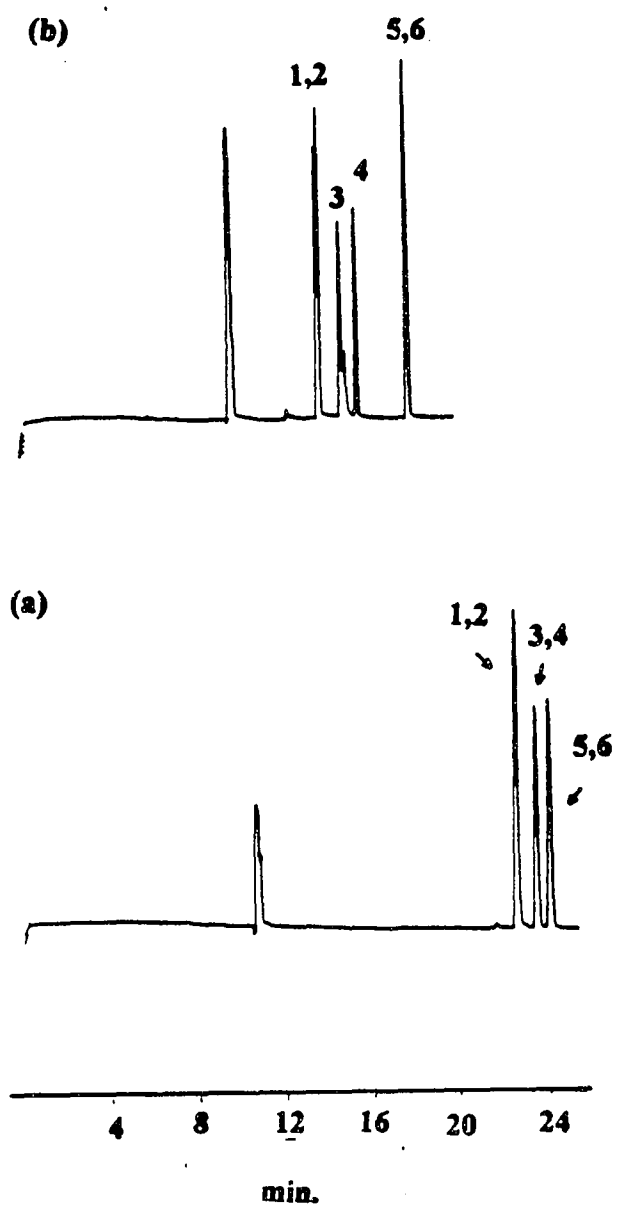

Figure 4.2 Electropherograms of 3,5-DNB-derivatives of L-HPA(1), D-HPA(2), L-PA(3), D-PA(4), L-PG(5), and D-PG(6) with and without chiral additives in 50mM phosphate buffer; (a) no CD (pH 6.5), (b) 7.84 mM β-CD (pH 6.5).

Table 4.1 CZE data of separation of 3,5-DNB-HPA, PA, and PG using β-CD

[CD]x1000 (M)	e.o.f..[a] (min.)	t_{ep}[b] (min.)	$t_{ep,f}$[c] (min.)	$t_{ep,c}$[d] (min.)
L-HPA				
0	10.78		11.35	2.79[e]
0.38	10.00	8.94		
1.65	9.77	7.20		
2.77	10.04	5.78		
4.84	9.68	4.72		
7.84	9.68	4.08		
11.9	9.77	3.63		
17.3	9.94	3.40		
D-HPA				
0	10.78		11.35	2.79[e]
0.38	10.00	8.94		
1.65	9.77	7.35		
2.77	10.04	5.92		
4.84	9.68	4.85		
7.84	9.68	4.14		
11.9	9.77	3.72		
17.3	9.94	3.40		
L-PA				
0	10.78		12.16	2.98[e]
0.38	10.00	9.90		
1.65	9.77	8.73		
2.77	10.04	7.21		
4.84	9.68	5.98		
7.84	9.68	5.09		
11.9	9.77	4.49		
17.3	9.94	4.05		

continued

Table 4.1 (Continued) CZE data of separation of 3,5-DNB-HPA, PA, and PG using β-CD

[CD]x1000 (M)	e.o.f..[a] (min.)	t_{ep}[b] (min.)	$t_{ep,f}$[c] (min.)	$t_{ep,c}$[d] (min.)
D-PA				
0	10.78		12.16	2.98[e]
0.38	10.00	10.08		
1.65	9.77	9.30		
2.77	10.04	7.87		
4.84	9.68	6.72		
7.84	9.68	5.78		
11.9	9.77	5.11		
17.3	9.94	4.58		
DL-PG				
0	10.78		12.72	3.17[f]
0.38	10.00	10.81		
1.65	9.77	10.76		
2.77	10.04	9.59		
4.84	9.68	8.78		
7.84	9.68	8.15		
1.19	9.77	7.66		
1.73	9.94	7.19		

[a]: Electroosmotic flow.
[b]: Electrophoretic (net) migration time (defined as apparent migration time - e.o.f.).
[c]: Electrophoretic (net) migration time in free state.
[d]: Electrophoretic (net) migration time of complexed species.
[e]: Estimated by computer fitting program to get the best correlation coefficient.
[f]: Estimated by the consideration of mobility as a function of $MW^{(-1/3)}$.

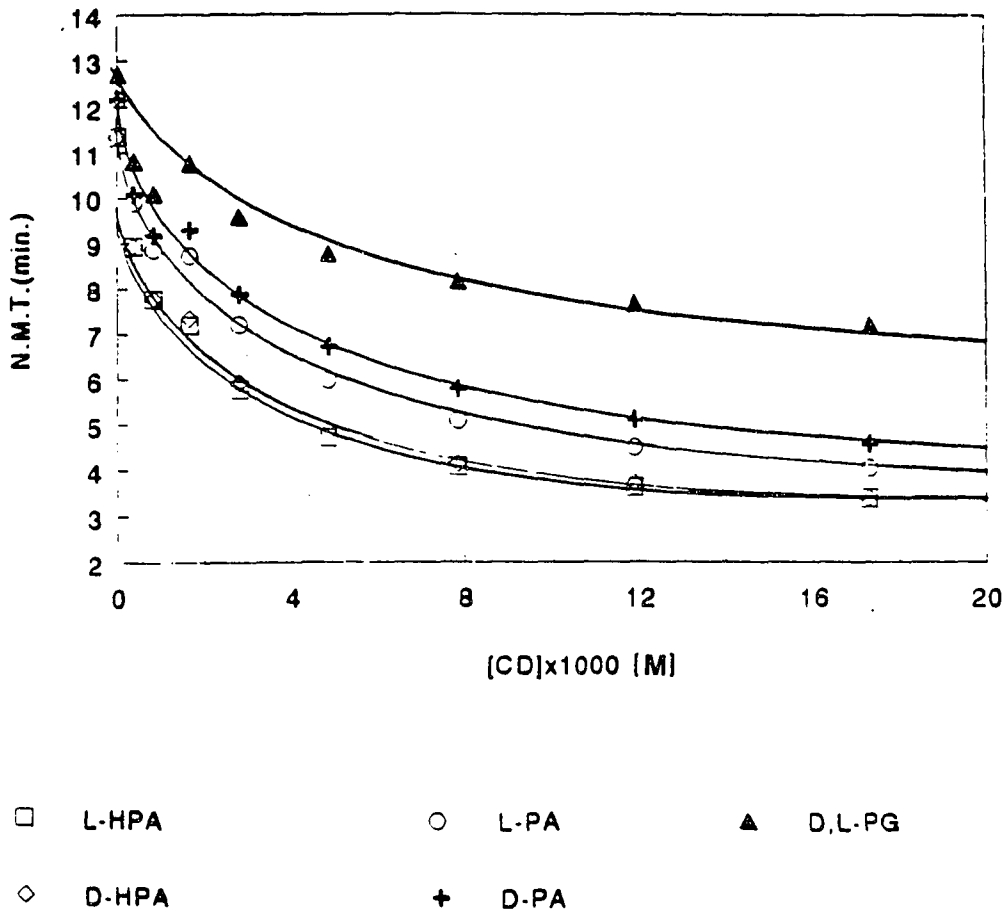

Figure 4.3 Graph demonstrating the dependence of migration times of analytes upon [CD].

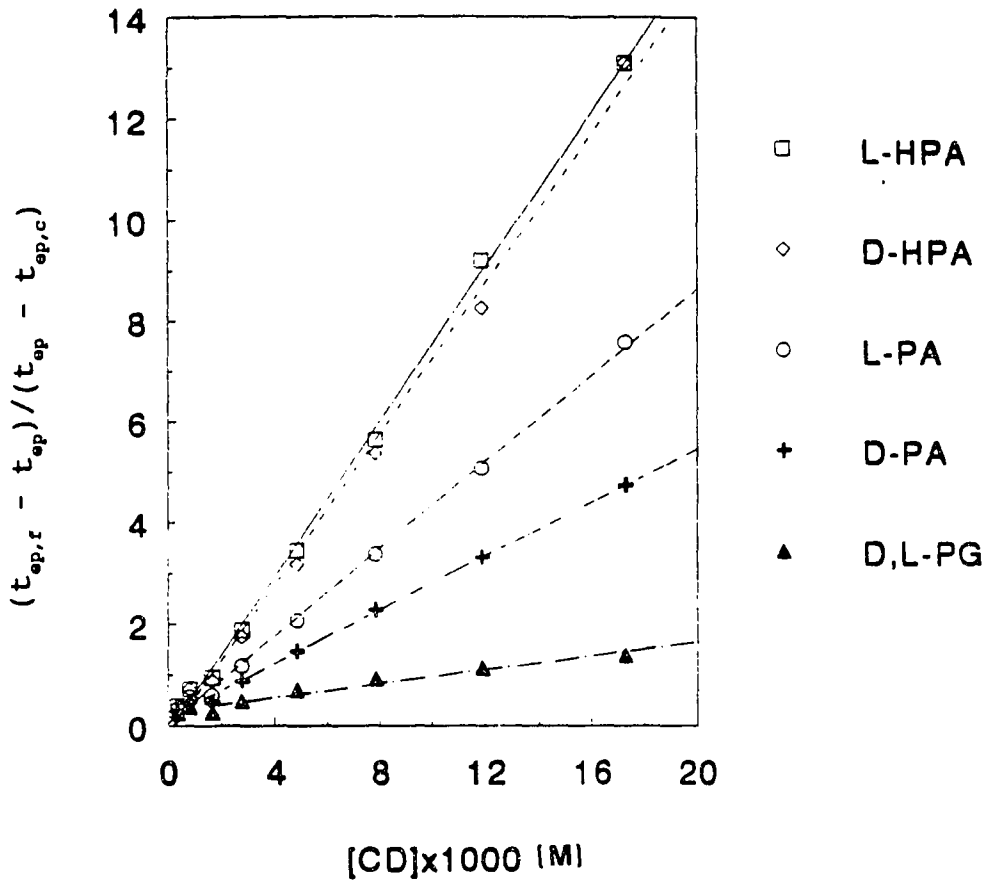

Figure 4.4 Plot of $(t_{ep,f} - t_{ep})/(t_{ep} - t_{ep,c})$ vs [CD].

Table 4.2 Association constants between 3,5-DNB-HPA, PA, and PG with β-CD and line fitting data.

Compound	slope	correlation coefficient (r)	association constant (K in M^{-1})
L-HPA	0.7710	0.9992	473 ± 9
D-HPA	0.7559	0.9978	460 ± 10
L-PA	0.4342	0.9993	260 ± 4
D-PA	0.2678	0.9993	161 ± 3
D,L-PG	0.0723	0.9784	43 ± 4

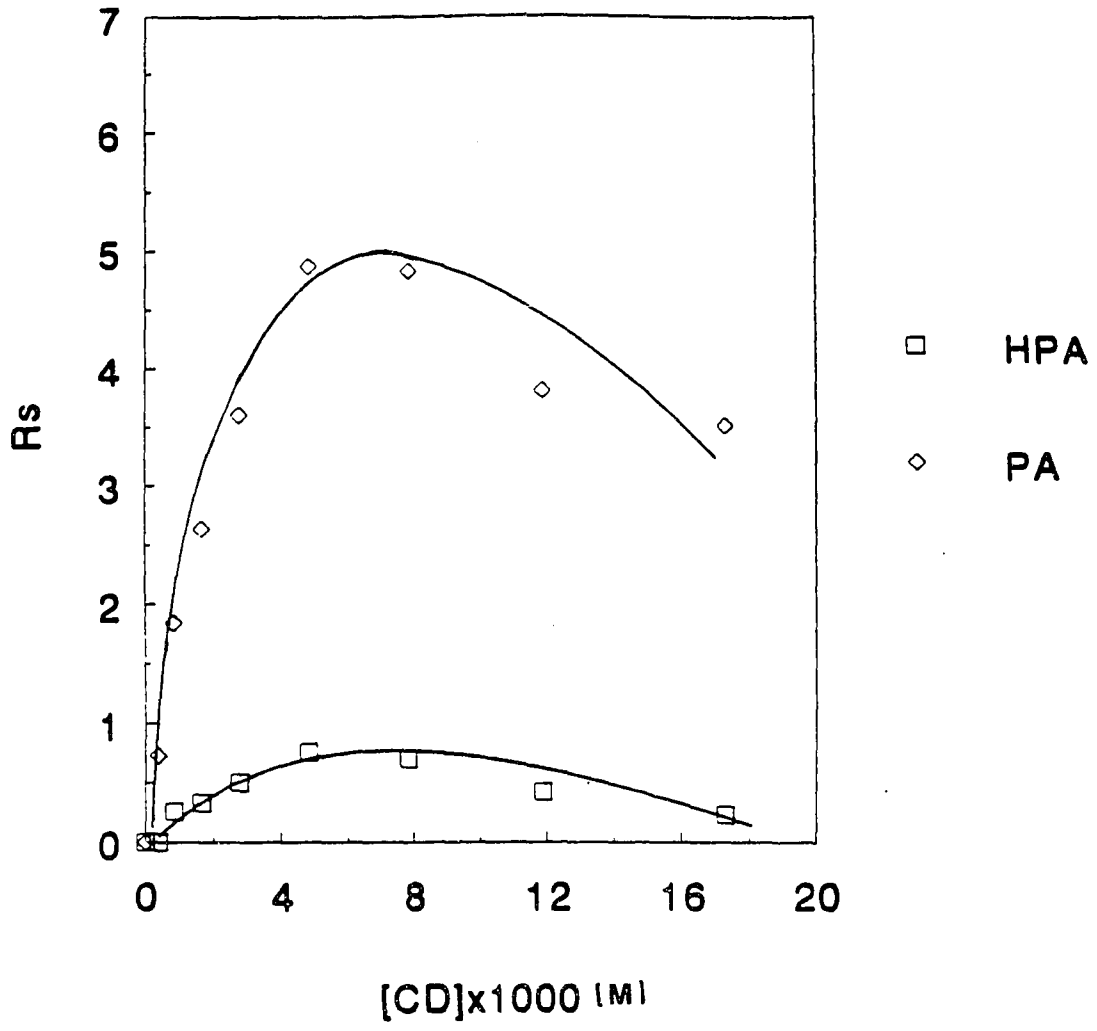

Figure 4.5 Dependence of enantioresolutions of HPA and PA on [CD].

which is in reasonably good agreement with the calculated values.

As in the case of CD-based CSP, the interaction mechanism between **β-CD** and the **3,5-DNB-AAs** seems to involve an inclusion process for chiral recognition. Proper **CD** cavity size for tighter interaction has been reported to be important for the observed enantioseparations. Further, it has been reported that meta substituted benzenes are sterically inhibited from complexation with the **β-CD** cavity.[130] Therefore, the **DNB** moiety of these analytes is not expected to participate directly in inclusion complexation. **HPA** is the most strongly bound with **β-CD** followed by **PA** and **PG**. The order of the binding constants suggests that the benzylic group of the amino acids may penetrate into the cavity and that the longer the hydrocarbon chain from the chiral center to the benzylic group, the deeper inclusion occurs, thereby resulting in a stronger association. It should be noted, however, from the poor enantioresolution of **HPA** and the better enantioresolution of the more weakly bound **PA** that stronger binding apparently does not always produce better chiral resolution.

The results from the **CZE** experiments were compared to those obtained by HPLC using **β-CD-CSP** with the same buffer as used in **CZE**. As can be seen from Figure 4.6, the chromatographic separation of these three amino acids mirror the results obtained from the **CZE** experiments. For instance, **PG** elutes last in **CZE** in the presence of **β-CD** as **CMA** yet elutes first from the analogous **β-CD** HPLC column. In addition, in the case of **PA**, the L enantiomer elutes before the D enantiomer in **CZE** but elutes later from the analogous HPLC column. Similarly, the lack of resolution for **3,5-DNB-PG** with fair resolution of **3,5-DNB-PA** and poor resolution of **3,5-DNB-HPA** in both **CZE** and HPLC further highlights the fact that the chiral separation mechanism involved in the **CZE** and HPLC of **β-CD-CSP** are similar.

4.3.3 NEC-β-CDs

All six possible monosubstituted **NEC-β-CDs** were separated using HPLC under reversed phase conditions. **SC-3** and **RC-3** were not used for the study. As reported by Gahm et al.[131] derivatization of **CD** with **NEIC** under a variety of reaction conditions yielded only minimal amounts of C-3 substitution (<10% of the total regioisomers). Hence, it is assumed that this regioisomer exists only in minor

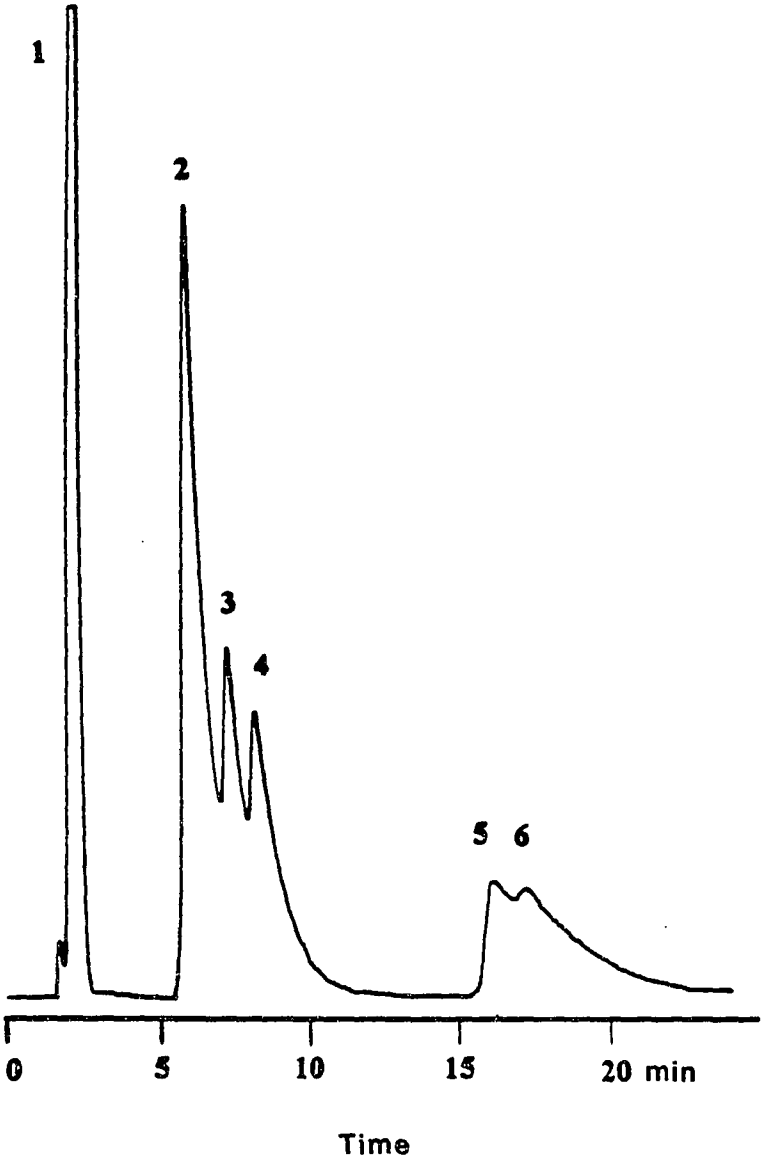

Figure 4.6 HPLC separation of 3,5-dinitrobenzoic acid (1), 3,5-DNB-rac-PG (2), D-PA (3), L-PA (4), D-HPA (5), and L-HPA (6) on β-CD column using 50 mM phosphate buffer at pH 6.5.

concentrations and contributes very little to the enantioseletivity of **NEC-β-CD-CSPs**. Therefore, the C-3 derivatization products were not included in this study.

4.3.3A NEC-β-CDs as CMA

The enantioselectivity of monosubstituted **NEC-CDs** were studied in **CZE** with **3,5-DNB-HPA, PA,** and **PG** as the analytes. The electropherograms using the various chiral selectors are shown in Figure 4.7. The electrophoretic data are listed in Table 4.3. In all cases, the elution order was **HPA, PA,** and **PG**. Interestingly, in all cases where **HPA** and **PA** were enantioresolved, the L enantiomer eluted first followed by D-enantiomer suggesting that the L-enantiomers bind more strongly with the derivatized **CDs** than the D enantiomers. This elution order is identical with that obtained using the native **β-CD** as **CMA**. In the case of **PG**, the L enantiomer eluted later than D counterpart. Interestingly, as in the case of the **NEC-β-CD CSP**, the elution order of the three racemates was unaffected by the configuration of the substituent. Hence, the dominant chiral interactions are with the **CD**.

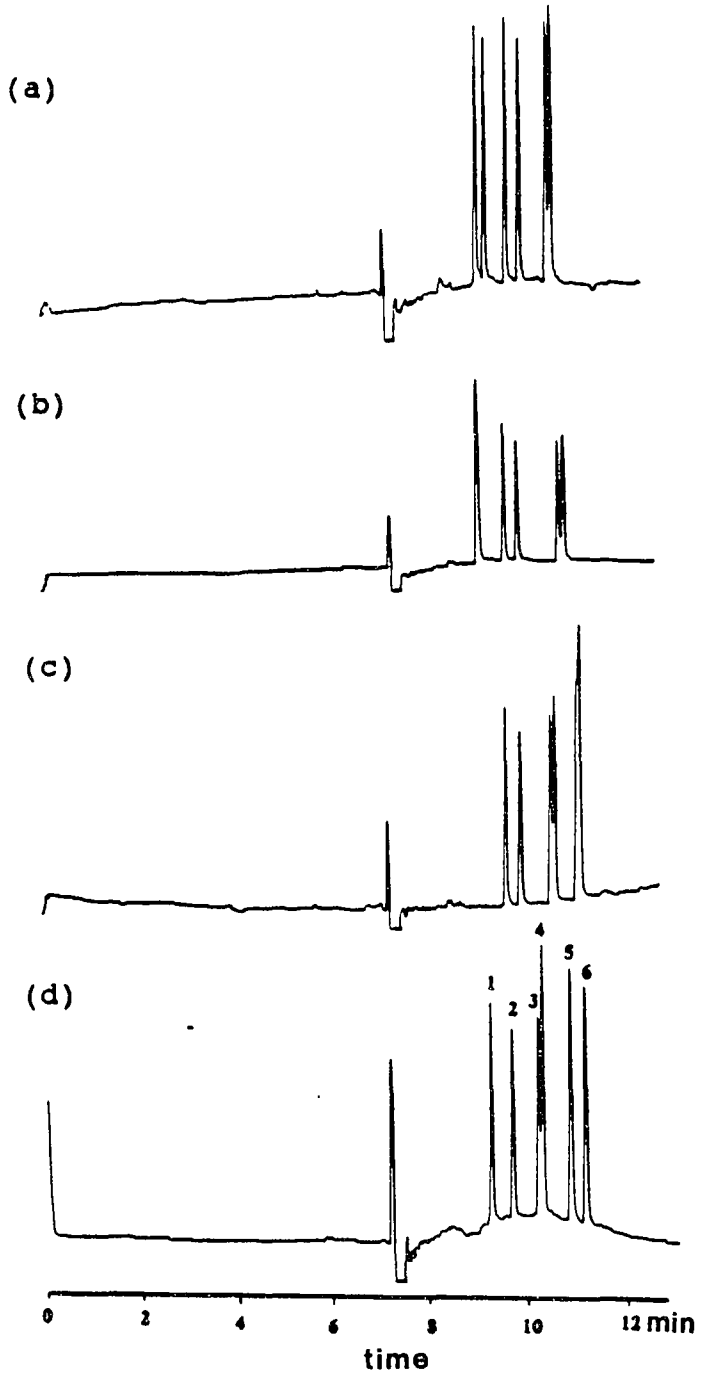

Figure 4.7 Electropherograms of 3,5-DNB-AAs using various NEC-β-CDs as chiral selectors. (a) SC-2, (b) SC-6, (c) RC-2, and (d) RC-6. 1:L-HPA, 2:D-HPA, 3:L-PA, 4:D-PA, 5:D-PG, and 6:L-PG.

Table 4.3 CZE data of separation of 3,5-DNB-HPA, PA, and PG using various monosubstituted naphthylethylcarbamoyl β-CDs

Compound	current (μA)	e.o.f. (min.)	L-HPA	D-HPA	Rs	L-PA	D-PA	Rs	D-PG	L-PG	Rs
SC-2	62.5	7.55	9.13	9.30	1.85	9.74	10.00	2.55	10.58	10.67	0.90
SC-6	60.5	7.72	9.04	9.04	0	9.54	9.80	2.68	10.63	10.73	0.87
RC-2	68.8	7.37	9.68	9.94	3.16	10.60	10.68	0.78	11.19	11.19	slight
RC-6	62.1	7.57	9.25	9.87	4.25	10.39	10.49	0.63	11.05	11.35	2.21

4.3.3B SC-2 as a CMA

Enantioselective interactions with the native CD are thought to occur primarily with the secondary side hydroxyls. Thus, substitution on the secondary hydroxyl side with a naphthylethylcarbamate group should alter the chiral selectivity either through sterically inhibiting analytes from entering the CD cavity or reducing the availability of the secondary hydroxyls for chiral interaction. Hence, it is somewhat surprising that in the current CZE conditions, SC-2 seems to be the best CMA for the overall separation of the three AAs employed in the study. All three AAs were well separated when SC-2 was used as a chiral selector as shown in Figure 4.7(a). The enantioseparation of PG together with the much improved resolution of HPA relative to that obtained with the native β-CD (see Figure 4.2) suggests that derivatization of CD with S-NEIC enhanced the chiral recognition of the β-CD. The overall slightly longer migration times of the analytes in the presence of SC-2 as CMA relative to the β-CD suggests that the binding ability of SC-2 toward PA and HPA was reduced relative to β-CD and will be discussed in more detail later. However, inclusion complex formation still seems to contribute to the observed chiral resolution because the elution order of the three AAs and that of an individual racemate was identical with that obtained using

native β-CD. As mentioned previously, in an aqueous environment, the naphthyl group of SC-2 may spend an approximately equal amount of time either included within the CD cavity or excluded from the cavity.

4.3.3C SC-6 as a CMA

Because, as mentioned previously, enantioselective interactions are thought to arise from interactions with the secondary hydroxyl side, substitution on the primary side should not dramatically alter the analyte/CD interactions. As expected, the similar resolution of PA and lack of resolution of HPA as well as the same elution order as those obtained with native CD suggests that the enantioselectivity of this compound is similar to native CD. The results obtained with the primary substitution product, SC-6, in Figure 4.7(b) strengthens the argument that the inclusion complexation between CDs and AAs is the main contribution to enantioselectivity.

4.3.3D RC-2

As discussed in the previous chapter, in an aqueous environment, the naphthyl group of RC-2 residues almost exclusively in the CD cavity. Thus, the analyte is inhibited from entering the CD cavity thereby resulting in

weaker analyte/chiral selector interactions than in the case of the native β-CD. The overall longer migration times of the analytes in the presence of this CMA, relative to the times obtained when using the other CDs, would tend to support this (see Figure 4.7(c)). Although the analyte/chiral selector interactions may be weakened by the presence of the naphthyl substituent, there may be other chiral interactions from the substituent or the substituent may remove some nonstereoselective interactions existing in native β-CD, thus resulting in enhanced chiral resolution.

4.3.3E RC-6

The best enantioseparations for HPA and PG were obtained when RC-6 was used as an additive as shown in Figure 4.7 (d). The results obtained using RC-6 are remarkable considering that substitution on the primary side, as stated previously, should not significantly perturb the chiral recognition of the CD. Even though the strength of binding with the three amino acids was slightly reduced through the derivatization on primary site, there might be more chance for the analytes to interact enantioselectively with CD.

4.3.4 Relative strength of binding of NEC-β-CDs toward AAs

The presence of the naphthyl substituent complicated determination of binding constants because the derivatives are not UV transparent as in the case of the native CD. In addition, dimer formation between derivatized CD may further obscure the analyte/CD interactions. However, the relative strengths of the association between the analytes and the CD may be ascertained from the relative migration rates of the various CD, as solutes, in the presence of the AAs, as additives. NEC-CDs and native CD are all neutral and migrate with the electroosmotic flow at pH 6.5. Complexation between the CD and AA results in slower migration of CD than the electroosmotic flow. Therefore, stronger interactions between the CDs and the AAs results in longer electrophoretic migration times.

Racemic 3,5-DNB-PA was used as the mobile phase additive and a mixture of the NEC-CDs and the native β-CD was introduced into the CZE as analytes. The resultant electropherogram is shown in Figure 4.8. Fortuitously, complexation between the native CD and the additive enabled direct determination of the migration time of the native CD. The electrophoretic data is listed in Table 4.4. From Figure 4.8, the relative binding of CDs with racemic 3,5-

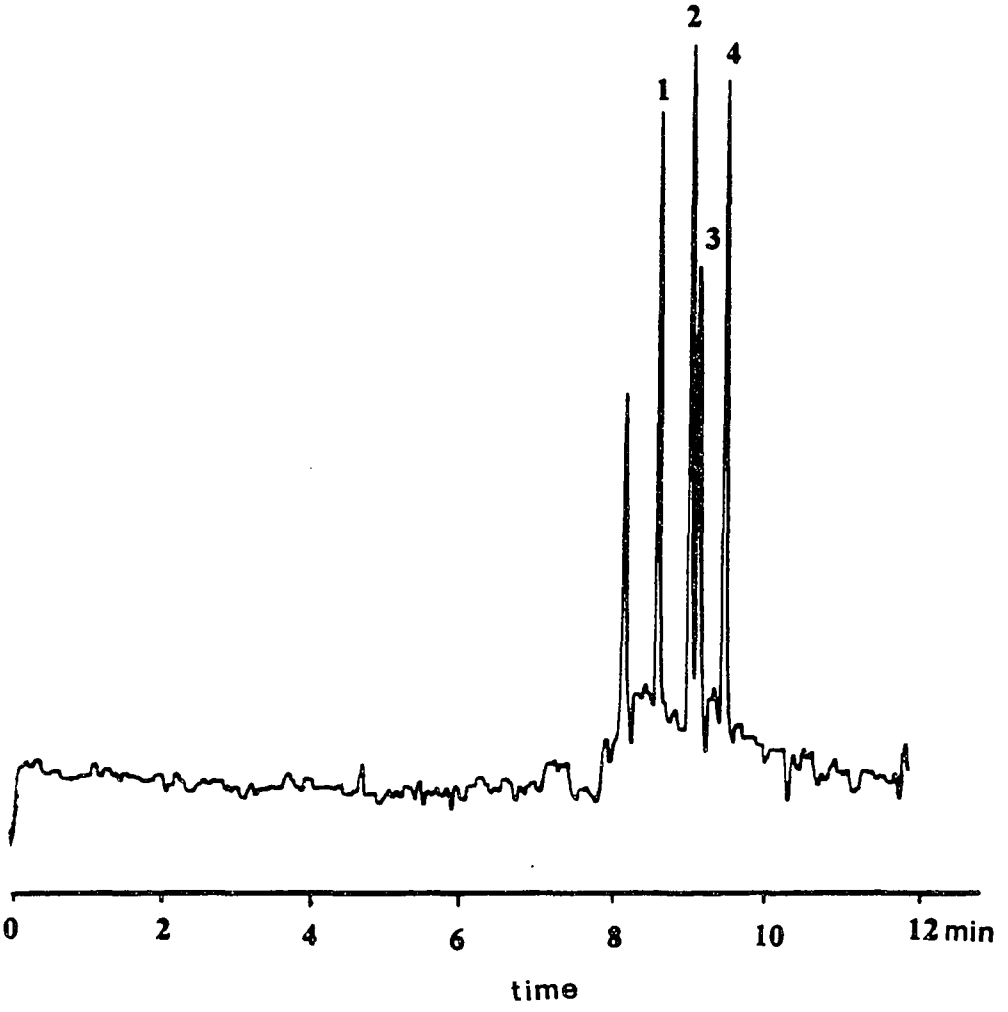

Figure 4.8 Electropherograms of the separations of NEC-CDs including β-CD using 3,5-DNB-PA as an additive. 1:RC-2, 2:RC-6, 3: β-CD, 4:SC-6.

DNB-PA was found to be SC-6 > β-CD > SC-2 = RC-6 > RC-2. (RC-6 coeluted with SC-2).

The general separation and elution orders of the various monosubstituted NEC-β-CDs as well as β-CD were unchanged when 3,5-DNB-L-PA was used as the buffer additive. RAC-3,5-DNB-HPA as an additive produced identical results. In the case of 3,5-DNB-D- or D,L-PG, the elution order of the derivatized CD was the same as that obtained with the other AAs. Unfortunately, the minimal complexation between the native CD and the PG additive precluded direct determination of the migration times of the native CD as was possible in the other cases.

It is interesting to note that, independent of the configuration of the pendant group, stronger binding between the AAs and the CD is seen with the primary rather than the secondary substituted isomer (RC-6 vs RC-2; SC-6 vs SC-2). This seems reasonable given that substitution on the secondary side should sterically inhibit inclusion complexation. It is also not too surprising that, with the exception of SC-6, derivatization of the CD decreases the binding between the AA and the CD. The fact that SC-6 has the strongest affinity for the AAs, greater even than the native CD, again highlights the fact that stronger binding does not necessarily improve chiral recognition.

Table 4.4 CZE data of naphthylethylcarbamoylated β-CDs and β-CD using amino acids as additives to an eletrolyte

Additive	current (μA)	e.o.f. (min)	RC-2	RC6=SC-2	β-CD	SC-6
D,L-PA(8.35mM)	73.7	8.13	8.57	8.98	9.09	9.43
L-PA(8.35mM)	72.9	8.53	9.13	9.52	9.75	9.99
D,L-HPA(6.70mM)	74.5	6.96	7.60	7.91	8.03	8.21
D,L-PG(8.69mM)	71.6	7.30	7.48	7.60	not detected	7.71

4.3.5 The origin of enhanced enantioselectivity

One of the notable characteristics of the various **NEC-β-CDs** applied as **CMAs** is the unique enantioselectivity exhibited by each of the isomers toward the three **AAs**. Even though it is difficult to clearly identify the contribution of the **NEC** group for the overall observed enantioselectivities, several possibilities are worth consideration. First of all, derivatization may induce a change in the toroidal configuration of the **CD**, resulting in an optimum enantiospecific interaction which may be augmented by the **NEC** group, possibly through π-π interaction. It should also be noted that chiral analytes may form a variety of associations with the chiral selector. Not all of these interactions may lead to chiral recognition.[133] The presence of the **NEC** group may diminish contributions from some nonstereospecific interactions as well as providing another chirogenic interaction site.

4.4 Conclusion

Successful application of regiospecifically monosubstituted **NEC-β-CDs** as chiral additives in **CZE** was reported. **HPA** interacted the most strongly with all of the **CDs** studied followed by **PA** and **PG**. Despite the presence of the **CD** substituent, an inclusion process seems to be the

most important prerequisite for the observed chiral separation.

In almost all cases, the presence of the naphthyl substituent diminished the analyte/CD binding constant. However, the inhibition of binding interactions was found, in many cases, to improve the enantioselectivity. The enhanced enantioselectivity was attributed to the fact that the presence of the **NEC** group diminishes contributions from some nonstereospecific interactions as well as provides another chirogenic interaction site.

CHAPTER 5

CONCLUSIONS AND SUGGESTIONS FOR FURTHER EXPERIMENTS

5.1 Conclusions

Several different investigations have been carried out to study **NEC-β-CD CSPs**. First to understand the substitution sites of this chiral stationary phases, monosubstituted **NEC-β-CDs** were regiospecifically synthesized and characterized by NMR and MS spectrometry. Regioselective reactions of **NEIC** with **β-CD** were studied under several different reaction conditions, including NaH activation, direct reflux condition either in pyridine or DMF. The C-2 substitution product predominated when the reaction was carried out either by using NaH activation method with relatively short reaction times (approximately 4 hrs) or by direct reflux of the reaction mixture in DMF without NaH activation. Primary hydroxyl substitution product was regioselectively synthesized with NaH activation with much longer reaction time (approximately over 10 days at room temperature). The usual reaction conditions for the preparation of **NEC-CD-CSPs**, (eg., direct refluxing **NEIC** and **CD** bonded silica sorbent in pyridine) was also employed to study the substitution site and it was found that the substitution occurred at the primary site.

Among several regioisomers, C-2 substituted products were extensively studied using NMR spectroscopy. In an aqueous environment, the naphthyl group was found to be in dynamic equilibrium between included and excluded states. In RC-2, the naphthyl group is almost exclusively residing inside cavity, whereas in SC-2, it is included in the cavity approximately 50 % of time. The difference between these epimers, comes from the difference in their configuration around the chiral center of NEC group. From the present study, it is found that the subtle difference in geometry results in totally different stabilization process, resulting in large difference in final equilibrium conformation. It was also found that computer modeling of these molecules was generally successful to predict solution conformation. In particular, the computer generated model is very close to the structures for RC-2 deduced from the NMR experiments. Additional conformational information was obtained for these epimers by changing solvent polarity by the stepwise addition of methanol to the aqueous solution. The increasing populations of the excluded conformer for both RC-2 and SC-2 with decreasing solvent polarity was observed. Chiral distinction capability of these compounds in methanolic solution was also confirmed by the observation of the splitting of proton resonances of 3,5-DNB group of 3,5-DNB-PG.

Finally, monosubstituted **NEC-CDs** were successfully applied as chiral additives in **CZE** to study the chiral recognition mechanisms of these molecules towards several **3,5-DNB-AAs**. By comparing these results with those of native **β-CD** as **CMA**, it was found that the naphthyl substitutent decreases the interaction between analytes/CD in most cases (excluding **SC-6**). However, the modification of various hydroxyl groups resulted in unique enantio-selectivity. Although inclusion complex formation still seems to be the main reason for the observed chiral separation, the naphthyl group surely takes part in the overall chiral separation of **NEC-β-CDs**.

5.2 Suggestions for further experiments

Even though monosubstitution **NEC-β-CDs** have been regiospecifically synthesized and their chiral capability has been studied, more experiments are needed to correlate these findings to the actual mechanisms of **NEC-β-CD-CSPs**. Given that the average degree of substitution varies from 3 to 8, the chiral recognition mechanism of these phases may be too complicated to be represented by a monosubstituted model. However, the study on the monosubstitution product can serve as a good starting basis for further experiments.

Disubstituted products can provide informations which could not be obtained from singly substituted products. In a higher degree substitution product, an anchimeric assistance from the **NEC** group of another glucose could be imagined when it complexes with an analyte. Therefore, disubstitution products may be the next step to be taken for the better understanding of these stationary phases. Preliminary results on the disubstituted products suggest that the best solvent for NMR experiment may be water to characterize the substitution sites. However, disubstitution products have minimal solubility in water. Therefore, attachment of sulfate or phosphate group to the primary site may be necessary to increase solubility in water. Disubstituted products with sulfate or phosphate groups may also be directly applicable as **CMA** in **CZE**.

Another possible model for **NEC-β-CD-CSPs** may be obtained by derivatization of all seven C-2 hydroxyls. This may be synthesized by protecting all primary hydroxyl groups of **β-CD** followed by derivatization of C-2 hydroxyls with **NEIC**. Tertiary butyldimethyl silylchloride was successfully applied to protect only primary hydroxyls. Seven degree substitution products may also be of merit for the purpose of spectroscopic study because symmetry may be restored and NMR spectra may be simplified.

Finally, different kinds of derivatizing agents instead of **NEIC** may be worth explaining. From the present study, it is clear that even a small change in molecular structure results in remarkably different chiral separations as observed in the cases of **RC-2 vs. SC-2** and **RC-6 vs. SC-6** in **CZE**. One choice might be 3,5-dinitrobenzoyl derivative. This derivative is π acidic which is opposite to the **NEC** group used in the present study. This compound may separate π basic compounds.

REFERENCES

1. C&E News, March 19, 1990, 40.
2. E.J. Ariens, Anal. Proceedings, 1992, 29, 232-234.
3. D.E. Drayer, Clin. Pharmacol. Ther., 1986, 40, 125-133.
4. R.T. Coutts and G.B. Baker, Chirality, 1989, 1, 99-120.
5. J. Hartenstein and B. Wagner, "Cardiovascular Drugs", ed. by J.A. Bristol, John Wiley & Sons, Inc., New York, 1986, 305-415.
6. R.L. Lalonde, D.M. Tenero, B.S. Burlew, V.L. Herring and M.B. Bottorff, Clin. Pharmacol. Ther., 1990, 47, 447-455.
7. M. Zief and L.J. Crane, eds., "Chromatographic Chiral Separations", Marcel Dekker, 1988.
8. A.M. Krustulovic, "Chiral separations by HPLC", Ellis Horwood, Chichester, 1989.
9. W.G. Kuhr, Anal. Chem., 1990, 62, 403R-414R.
10. B.L. Karger, American Laboratory, October, 1993, 23-27.
11. P. Macaudiere, M. Lienne, M. Caude, and A. Tambute, "Pirkle-type and related chiral stationary phases for enantiomeric resolution", Chapter 14 of "Chiral separations by HPLC", ed. by A. M. Krustulovic, Ellis Horwood Limited, 1989, p399-445.
12. S. Allenmark, "Protein-bonded phases", Chapter 11 of " Chiral separations by HPLC", ed. by A.M. Krstulovic, Ellis

Horwood Limited, 1989, p287-315.

13. T. Ward and D.W. Armstrong, "Cyclodextrin-stationary phases", ed. by L.J. Crane and M. Zief, publisher, Marcel Dekker, New York, 1988, p131-163.

14. W.H. Pirkle and T.C. Pochapsky, J. Am. Chem. Soc., 1987, 109, 5975-5982.

15. W.H. Pirkle and D.W. House, J. Org. Chem., 1979, 44, 1957-1960.

16. W.H. Pirkle, D.W. House and J. M. Finn, J. Chromatogr., 1980, 192, 143-158.

17. W.H. Pirkle, T.C. Pochapsky, G.S. Mahler and R.E. Field, J. Chromatogr., 1985, 348, 89-96.

18. W.H. Pirkle and T.C. Pochapsky, J. Am. Chem. Soc., 1986, 108, 352-354.

19. W.H. Pirkle, T.C. Pochapsky, G.S. Mahler, D.E. Corey, D.S. Reno and D.M. Alessi, J. Org. Chem., 1986, 51, 4991-5000.

20. C.R. Lowe, "An Introduction to Affinity Chromatography", North-Holland Publishing comp., Oxford, 1979.

21. S. Allenmark, B. Bomgren, and H. Boren, J. Chromatogr., 1983, 264, 63-68.

22. J. Hermansson, J. Chromatogr., 1984, 298, 67-78.

23. T. Miwa, T. Miyakawa, M. Kayano, and Y. Miyake, J. Chromatogr., 1987, 408, 316-322.

24. M.L. Bender and M. Komiyama, "Cyclodextrin Chemistry", Springer-Verlag, New York, 1978.

25. D.W. Armstrong, " Cyclodextrins in analytical chemistry", Proceedings of the fourth international symposium on cyclodextrins, ed. by O. Huber and J. Szejtli, Kluwer Academic Publishers, 1988, p437-449.

26. W.L. Hinze, Separation and Purification Methods, 1981, 10, 159-237.

27. D.W. Armstrong, U.S. Patent No. 4,539,399 (1985).

28. K. Fugimura, T. Veda and T. Anodo, Anal. Chem., 1983, 55, 446-450.

29. Y. Kawaguchi, M. Tanaka, M. Nakae, K. Funazo, and T. Shono, Anal. Chem., 1983, 55, 1852-1857.

30. S.M. Han and D.W. Armstrong, "HPLC separation of enantiomers and other isomers with CD-bonded phases: rule for chiral recognition", Chapter 10 of "Chiral separations by HPLC", ed. by A.M. Krustulovic, Ellis Horwood Limited, 1989, p208-286.

31. A.M. Stalcup, S.C. Chang, D.W. Armstrong, and J. Pitha, J. Chromatogr., 1990, 513, 181-194.

32. T. Hargitai, and Y. Okamoto, J. Liquid Chromatogr., 1993, 16, 843-858.

33. C.N. Nakatsu and A.M. Stalcup, J. Liquid Chromatogr., 1993, 16, 209-223.

34. D.W. Armstrong, A.M. Stalcup, M.L. Hilton, J.D. Duncan, J.R. Faulkner and S.C. Chang, Anal. Chem., 1990, 62, 1610-1615.

35. D.W. Armstrong, M.L. Hilton, and L. Coffin, LC-GC, 1991, 9, 646-652.

36. M.L. Hilton, S.C. Chang, M.P. Gasper, M. Pawlowska, D.W. Armstrong and A.M. Stalcup, J. Liquid Chromatogr., 1993, 16, 127-147.

37. A.M. Stalcup, S.C. Chang, and D.W. Armstrong, J. Chromatogr., 1991, 540, 113-128.

38. D.W. Armstrong, C.D. Chang, S.H. Lee, J. Chromatogr., 1991, 539, 83-90.

39. S.H. Lee, A. Berthod, and D.W. Armstrong, J. Chromatogr., 1992, 603, 83-93.

40. J.W. Jorgenson, and K.D. Lukacs, Anal. Chem., 1981, 53, 1298-1302.

41. A.S. Cohen, A. Paulus, and B.L. Karger, Chromatographia, 1987, 24, 15-24.

42. M.A. Mosely, L.J. Deterding, K.B. Tomer, and J.W. Jorgenson, Anal. Chem., 1991, 63, 109-114.

43. Y.F. Cheng, and N.J. Dovichi, Science, 1988, 242, 562-564.

44. R.D. Smith, J.A. Loo, C.J. Barinaga, C.G. Edmonds, H.R. Udseth, J. Chromatogr., 1989, 480, 211-232.

45. T.J. Kasper, M. Melera, P. Gozel, and R.G. Brownlee, J. Chromatogr., 1988, 458, 303-312.

46. R.A. Wallingford, and A.G. Ewing, Anal. Chem., 1988, 60, 1972-1975.

47. C. Quang and M.G. Khaledi, Anal. Chem. 1993, 65, 3354-3358.

48. P. Gozel, E. Gassmann, H. Michelsen, and R.N. Zare, Anal. Chem., 1987, 59, 44-49.

49. E. Gassmann, J.E. Kuo, and R.N. Zare, Science, 1985, 230 813-814.

50. S. Terabe, K. Otsuka, K. Ichikawa, A. Tsuchiya and T. Ando, Anal. Chem., 1984, 56, 111-113.

51. S. Terabe, K. Otsuka, and T. Ando, Anal. Chem., 1985, 57, 834-841.

52. A. Dobashi, T. Ono, S. Hara, and J. Yamaguchi, J. Chromatogr., 1989, 480, 413-420.

53. S. Terabe, M. Shibata, and Y. Miyashita, J. Chromatogr., 1989, 480, 403-411.

54. E. Francotte, S. Cherkaoui and M. Faupel, Chirality, 1993, 5, 516-526.

55. K.D. Altria, R.C. Harden, M. Hart, J. Hevizi, P.A. Hailey, J.V. Makwana, and M.J. Portsmouth, J. Chromatogr., 1993, 641, 147-153.

56. M.J. Sepaniak, R.O. Cole, and B.K. Clark, J. Liquid Chromatogr., 1992, 15, 1023-1040.

57. H. Soini, M.L. Riekkola, and M.V. Novotny, J. Chromatogr., 1992, 608, 265-274.

58. J. Snopek, I. Jelinek, and E. Smolkova-Keulemansova, J. Chromatogr., 1988, 438, 211-218.

59. S. Fanali, J. Chromatogr., 1991, 545, 437-444.

60. J. Snopek, H. Soini, M. V. Novotny, E. Smolkova-Keulemansova, and I. Jelinek, J. Chromatogr., 1991, 559,

215-222.

61. M. Yoshinaga, S. Asano, M. Tanaka, and T. Shono, Anal. Science, 1991, 7, 257-260.

62. S. Fanali, J. Chromatogr., 1989, 474, 441-446.

63. J.L. Carpenter, P. Camilleri, D. Dhanak, and D. Goodall, J. Chem. Soc., Chem. Commun., 1992, 804-6.

64. A. Shibukawa, D.K. Lloyd, and I.W. Wainer, Chromatographia, 1993, 35, 419-429.

65. A. Guttman, A. Paulus, A.S. Cohen, N. Grinberg, and B.L. Karger, J. Chromatogr., 1988, 448, 41-53.

66. S.A.C. Wren, and R.C. Rowe, J. Chromatogr., 1992, 603, 235-241.

67. S.A.C. Wren, and R.C. Rowe, J. Chromatogr., 1992, 609, 363-367.

68. Y.Y. Rajee, D.U. Staerk, and G.J. Vigh, Chromatogr., 1993, 635, 291-306.

69. W.H. Pirkle and T.C. Pochapsky, J. Am. Chem. Soc., 1986, 108, 5627-5628.

70. G. Wenz and E. von der Bey, "Inclusion properties of hydrophobic derivatives of CDs", ed. by O. Huber and J. Szejtli, Proceedings of the Fourth International Symposium on Cyclodextrins, Kluwer Academic Publishers, 1988, p133-138.

71. R.L. VanEtten, J.F. Sebastian, G.A. Clowes and M.L., Bender, J. Am. Chem. Soc., 1967, 89, 3242-3253.

72. A. Ueno, I. Suzuki and T. Osa, Chem. Lett., 1989, 1059-1062.

73. A. Ueno, F. Moriwaki, T. Osa, F. Hamada and K. Murai, Bull. Chem. Soc. Jpn., 1986, 59, 465-470.

74. D. Parker, Chemical Reviews, 1991, 91, 1441-1457.

75. D.J. Wood, F.E. Hruska, and W. Saenger, J. Am. Chem. Soc., 1977, 99, 1735-1740.

76. P.V. Demarco, and A.L. Thakkar, Chem. Commun., 1970, 2-4.

77. D. Greatbanks and R. Pickford, Mag. Resonan. Chem., 1987, 25, 208-215.

78. A. Botsi, K. Yannakopoulou, E. Hadjoudis, and B. Perly, J. Chem. Soc., Chem. Commun., 1993, 1085-1086.

79. J.C. Marquez, M. Hernandez and F. G. Sanchez, Analyst, 1990, 115, 1003-1005.

80. H. Ikeda, Y. Nagano, Y. Du, T. Ikeda and F. Toda, Tetrahedron lett., 1990, 31, 5045-5048.

81. A. P. Croft and R. A. Bartsch, Tetrahedron, 1983, 39 1417-1474.

82. R. Breslow, A. W. Czarnik, M. Lauer, R. Leppkes, J. Winkler and S. Zimmerman, J. Am. Chem. Soc., 1986, 108, 1969-1979.

83. I. Tabushi and Y. Kuroda, J. Am. Chem. Soc., 1984, 106, 4580-4584.

84. S. Minato, T. Osa, M. Morita, A. Nakamura, H. Ikeda, F. Toda and A. Ueno, Photochem. Photobiol., 1991, 54, 593-597.

85. A. Ueno, S. Minato, I. Suzuki, M. Fukushima, M. Ohkubo, T. Osa, F. Hamada and K. Murai, Chem. Lett., 1990, 605-608.

86. A. Ueno, I. Suzuki and T. Osa, J. Am. Chem. Soc., 1989, 111, 6391-6397.

87. I. Ciucanu and F. Kerek, Carbohydr. Res., 1984, 131, 209-217.

88. M. N. Bereran-Santos, J. Canceill, J.-C. Brochon, L. Jullien, J. -M. Lehn, J. Pouget, P. Tauc and B. Valeur, J. Am. Chem. Soc., 1992, 114, 6427-6436.

89. K. Takeo, H. Mitoh and K. Uemura, Carbohydr. Res., 1989, 187, 203-221.

90. A. Ueno and R. Breslow, Tetrahedron Lett., 1982, 23, 3451-3454.

91. K. Takahashi, K. Hattori and F. Toda, Tetrahedron Lett., 1984, 3331-3334.

92. K. Fujita , T. Tahara, T. Imoto and T. Koga, J. Am. Chem. Soc., 1986, 108, 2030-2034.

93. P. Fugedi, Carbohydr. Res., 1989, 192, 366-369.

94. D. Rong and V.T. D'Souza, Tetrahedron Lett., 1990, 31, 4275-4278.

95. C.T. Rao and J. Pitha, Carbohydr. Res., 1991, 220, 209-213.

96. S.H. Smith, S.M. Forrest, D.C. Williams, Jr., M.F. Cabell, M.F. Acquavella and C.J. Abelt, Carbohydr. Res., 1992, 230, 289-297.

97. L.D. Melton and K.N. Slessor, Carbohydr. Res., 1971, 18, 29-37.

98. D. W. Armstrong and W. Li, Chromatogr. Forum, 1987, 2, 43-48.

99. W. Saenger, "Environmental Effects on Molecular Structure and Properties", ed. by B. Pullman, Reidel Publishing Company, Dordrecht-Holland, 1976, p265-305.

100. W. Saenger, Angew, Chem. Int. Ed. Engl., 1980, 19, 344-362.

101. G. Uccello-Barretta, C. Chiavacci, C. Bertucci, P. Salvadori, Carbohydr. Res., 1993, 243, 1-10.

102. S.E. Brown, J.H. Coates, P.A. Duckworth, S.F. Lincoln, C.J. Easton and B.L. May, J. Chem. Soc. Faraday Trans, 1993, 89, 1035-1040.

103. T.X. Lu, D.B. Zhang and S.J. Dong, J. Chem. Soc., Faraday Trans. 2, 1989, 85, 1439-1445.

104. M.J. Sherrod, "Theoretical Studies of Cyclodextrins and Their Inclusion Complexes", ed. by Davies, J.E.D. in "Spectroscopic and Computational Studies of Supramolecular Systems", Kluwer Academic Publishers, 1992, p187-205.

105. C. Jaime, J. Redondo, F. Sanchez-Ferrando and A. Virgili, J. Org. Chem., 1990, 55, 4772-4776.

106. J.J. Richards and M.L. Webb, Anal. Proceedings, 1992, 251-253.

107. M. Bernabe, J. Jimenez-Barbero, M. Martin-Lomas, S. Penades, and C. Vicent, Carbohydr. Res., 1990, 208, 255-259.

108. A.F. Casy and A.D. Mercer, Mag. Resonan. Chem., 1988, 26, 765-774.

109. K.B. Lipkowitz, J. Org. Chem., 1991, 56, 6357.

110. Y. Inoue, Y. Kanda, Y. Yamamoto, and S. Kobayashi, Carbohydr. Res., 1992, 226, 197-208.

111. G.A. Morris, and L.D. Hall, J. Am. Chem. Soc., 1981, 103, 4703-4711.

112. A. Bax and M.F. Summers, J. Am. Chem. Soc., 1986, 108, 2093-2094.

113. U.R. Desai, J.M. Wang, T.R. Kelly, and R.J. Linhardt, Carbohydr. Res., 1993, 241, 249-259.

114. M. Gruter, B.R. Leeflang, J. Kuiper, J.P. Kamerling, J.F.G. Vliegenthart, Carbohydr. Res., 1992, 231, 273-291.

115. U. Piantini, O.W. Sorensen, and R.R. Ernest, J. Am. Chem. Soc., 1982, 104, 6800-6801.

116. D.J. States, R.A. Haberkorn, and D.J. Ruben, J. Magn. Resonan., 1982, 48, 286-292.

117. L. Muller, J. Am. Chem. Soc., 1979, 101, 4481-4484.

118. A. Bax, and S. Subramanian, J. Magn. Resonan., 1986, 67, 565-569.

119. M.F. Summers, L.G. Marzilli, and A. Bax, J. Am. Chem. Soc., 1986, 108, 4285-4294.

120. A. Bothner-By, R.L. Stephens, J.M. Lee, C.D. Warren, and R.W. Jeanloz; J. Am. Chem. Soc., 1984, 106, 811-813.

121. H. Kessler, C. Griesinger, R. Kerssebaum, K. Wagner, and R.R. Ernst, J. Am. Chem. Soc., 1987, 109, 607-609.

122. A. Bax, and D,G. Davis, J. Magn. Resonan., 1985, 63, 207-213.

123. D.G. Davis, and A. Bax, J. Am. Chem. Soc., 1985, 107, 7197-7198.

124. D.G. Davis, and A. Bax, J. Am. Chem. Soc., 1985, 107, 2820-2821.

125. K. Linder, and W. Saenger, Carbohydr. Res., 1982, 99, 103-115.

126. "Spectrometric identification of organic compounds", Silverstein, R.M.; Bassler, G. C.; Morrill, T.C., 4th ed., John Wiley & Sons, 1981, p210.

127. W.H. Pirkle, K.A. Simmons, and C.W. Boeder, J. Org. Chem., 1979, 44, 4891-4896.

128. C.W. Demarest, E.A. Monnot-Chase, J. Jiu, and R. Weinberger, "Separation of small molecules by high-performance capillary electrophoresis", Chapter 11 of "Capillary electrophoresis", ed. by P.D. Grossman and J.C. Colburn, Academic Press, Inc., 1992, p301-341.

129. K.D. Altria, D.M. Goodall, and M.M. Rogan, Chromatographia, 1992, 34, 19-24.

130. D.W. Armstrong, W. DeMond, A. Alak, W.L. Hinze, T.E. Riehl, and K.H. Bui, Anal. Chem., 1985, 57, 234-237.

131. K.H. Gahm, W.Y. Yoshida, W.P. Niemczura and A.M. Stalcup, Carbohydr. Res., 1993, 248, 119-128.

132. R.E. Boehm, D.E. Martire, and D.W. Armstrong, Anal. Chem., 1988, 60, 522-528.